Models and Methods for Free Material Optimization

$$P = \tfrac{1}{2}\rho A v^3 C_p$$

Alemseged Gebrehiwot Weldeyesus
DTU Wind Energy PhD-0041 (EN)
August 2014

Models and Methods for Free Material Optimization

Alemseged Gebrehiwot Weldeyesus

Department of Wind Energy
Technical University of Denmark (DTU)

The thesis is submitted to the Danish Technical University in partial fulfillment of the requirements for the PhD degree.

Abstract

Free Material Optimization (FMO) is a powerful approach for structural optimization in which the design parametrization allows the entire elastic stiffness tensor to vary freely at each point of the design domain. The only requirement imposed on the stiffness tensor lies on its mild necessary conditions for physical attainability, in the context that, it has to be symmetric and positive semidefinite. FMO problems have been studied for the last two decades in many articles that led to the development of a wide range of models, methods, and theories.

As the design variables in FMO are the local material properties any results using coarse finite element discretization are not essentially predictive. Besides the variables are the entries of matrices at each point of the design domain. Thus, we face large-scale problems that are modeled as nonlinear and mostly non convex semidefinite programming. These problems are more difficult to solve and demand higher computational efforts than the standard optimization problems. The focus of today's development of solution methods for FMO problems is based on first-order methods that require a large number of iterations to obtain optimal solutions. The scope of the formulations in most of the studies is indeed limited to FMO models for two- and three-dimensional structures. To the best of our knowledge, such models are not proposed for general laminated shell structures which nowadays have extensive industrial applications.

This thesis has two main goals. The first goal is to propose an efficient optimization method for FMO that exploits the sparse structures arising from the many small matrix inequality constraints. It is developed by coupling second-order primal dual interior point solution techniques for the standard nonlinear optimization problems and linear semidefinite programs. The method has successfully obtained solutions to large-scale classical FMO problems of simultaneous analysis and design, nested and dual formulations. The second goal is to extend the method and the FMO problem formulations to general laminated shell structures.

The thesis additionally addresses FMO problem formulations with stress constraints. These problems are highly nonlinear and lead to the so-called singularity phenomenon. The method described in the thesis has successfully solved these problems. In the numerical experiments the stress constraints have been satisfied with high feasibility tolerances.

The thesis further includes some preliminary numerical progresses on solving FMO problems using iterative solvers.

Resumé (In Danish)

Fri Materiale Optimering (FMO) er en kraftfuld metode inden for strukturel optimering, hvori parametriseringen af designet tillader den fulde elastiske stivhedstensor at variere frit i ethvert punkt i designområdet. Det eneste krav til stivhedstensoren ligger i de svage betingelser om fysisk opnåelighed, hvilket vil sige, at den skal være symmetrisk og positiv semi-definit. Indenfor de seneste to årtier er problemer inden for FMO blevet studeret i en lang række artikler, hvilket har affødt en bred vifte af modeller, metoder og teorier.

Da design-parametrene i FMO er lokale egenskaber ved materialet, er ethvert designresultat baseret på en grov diskretisering med finite element metoden ikke prædiktivt. Hertil kommer det faktum at variablene er matrix-elementer i ethvert punkt i designdomænet. Vi har altså at gøre med stor-skala-problemer, som skal modelleres vha. ikke-lineær og primært ikke-konveks semi-definit programmering. Sådanne problemer er sværere at løse og mere beregningstunge end almindelige optimeringsproblemer. Udviklingen af metoder til problemer indenfor FMO fokuserer i dag på førsteordens metoder, som kræver et stort antal iterationer for at opnå optimale løsninger. Rammerne for formuleringerne i de fleste studier er begrænset til 2- og 3-dimensionale strukturer. Sådanne modeller er - efter vores bedste overbevisning - ikke fremsat for generelle laminerede skal-strukturer, som i dag finder bred anvendelse i industrien.

Denne afhandling har to hovedformål. Det første formål er fremsætte en effektiv optimeringsmetode inden for FMO, som udnytter den sparse struktur, der kommer fra de mange små matrix-uligheder som bibetingelser. Den er udviklet ved at koble andenordens *primal-dual interior point* løsningsteknikker for almindelige ikke-lineære optimeringsproblemer med lineære semi-definite programmer. Metoden er med succes blevet anvendt til at løse klassiske problemer indenfor FMO på stor skala med samtidig analyse og design, i både indlejret og dual formulering. Det andet mål er at udvide metoden og formuleringerne af problemerne inden for FMO til generelle laminerede skal-strukturer.

Afhandlingen behandler desuden problemformuleringer inden for FMO, som indeholder betingelser på stress. Disse problemer er stærkt ikke-lineære og giver anledning til såkaldte singularitetsfænomener. Metoden, som er beskrevet i denne afhandling, har med succes løst sådanne problemer. Stress-betingelserne er blevet opfyldt med en høj tolerance på gennemførligheden i de numeriske eksperimenter.

Afhandlingen indeholder desuden foreløbigt arbejde vedrørende løsning af problemer inden for FMO ved brug af iterative løsere.

Preface

This thesis was submitted in partial fulfillment of the requirements for obtaining the PhD degree at the Technical University of Denmark. The work was done at the Department of Mathematics from December 2010 to April 2011 and at the Wind Turbine Structures section of the Department of Wind Energy from May 2011 to August 2014. The period includes about six months of paternity leave. The PhD project was funded by the Danish Council for Strategic Research through the *Danish Center for Composite Structures and Materials* (DCCSM). Supervisor on the project was Senior Researcher Dr.Techn. Mathias Stolpe and co-supervisor was Professor Erik Lund.

First and foremost I would like to express my special gratitude and thanks to my supervisor for his guidance, support, and for always offering his time for discussions. My special thanks extend to my co-supervisor for his fruitful discussions on composites and valuable comments on my results. I am very much grateful to Dr. Stefanie Gaile for her discussions on Free Material Optimization problems and the development of finite element codes.

It was a pleasure for me to be part of the wonderful people in the Department of Mathematics and Department of Wind Energy.

A special thank to my friends and family. Thanks mom. Last but not the least, I would like to thank my wife Helen and my daughter Mia for all the love and encouragement.

<div align="right">

Roskilde, August 2014

Alemseged Gebrehiwot Weldeyesus

</div>

Contents

Part I

Background

Chapter 1

Introduction

There has been remarkable advancement in manufacturing techniques for composite structures in the recent decades. This has given a rise to the application of structural optimization in industries to produce a wide range of light weight structures. Structural optimization is a discipline that deals with the improvement of the mechanical performance of load carrying structures. The most common measures of structural performance are weight, stiffness, stresses, strains, critical loads, displacements and geometry. The optimization problems can thus be formulated by taking one or more of these measures as an objective function and some of the other measures as constraints. The choice of geometric features or the size of the set of admissible materials lead to several forms of structural optimization. *Topology optimization* introduced in [33] for truss structures and in [5] for continuum structures is one of the general forms that concerns with obtaining (almost) 0-1 optimal distribution of materials in a given design space. It is a class of structural optimization that has been extensively studied with extremely diversified approaches of problem formulations and solution methods, see e.g. [6]. *Discrete Material Optimization* introduced in [34], [35], and [25] concerns with optimal design of laminated composite structures by determining the best discrete material selection, stacking sequence, and thickness distribution. There are further studies treating problem formulations involving more design criteria such as eigenfrequencies in [26] and buckling loads in [24]. These articles use parametrization based on weighting functions for optimal material selection. In [10] new approach for parameterization based on shape functions is proposed. The set of admissible materials can be extended further avoiding any restriction to pre-existing materials and searching for more general material properties. This leads to the most general form the so-called *Free Material Optimization* (FMO) which deals with determining the optimal material distribution and the optimal

local material properties of structures through the stiffness tensors.

The development of an efficient solution techniques and new FMO models are the main goals of the thesis. One of the main motivations concerns the nature and size of FMO problems. As the design variables in FMO are the stiffness tensors at each point of the design domain it is important to work with relatively fine finite element discretizations to obtain essentially predictive solutions. The number of independent variables in each stiffness tensor is 6 for two-dimensional, 21 for three-dimensional, and 9 for problems on (thick) shells. Hence, we often face large-scale problems. Moreover, the problems are modeled as nonlinear (and non convex) SemiDefinite Programming (SDP) for which studies on theories and numerical methods are much more recent than linear SDP problems and standard optimization problems. Solving large-scale problems of this class lead to high computational complexity that often demands specialized solution techniques. For this reason researches on FMO problems are mostly accompanied with solution techniques, see Chapter 2. The focus of most of today's development of optimization methods for FMO problems is based on first-order methods that often leads to large number of iterations. Second-order methods are considered computationally too expensive. The thesis proposes a second-order interior point method that efficiently utilizes the structure that each of the many matrix inequalities in FMO is small giving sparse structures in the optimization process. It is developed by coupling existing primal-dual interior point method for standards nonlinear programming, see e.g. [13], [14], and [7], and the techniques for linear SDP, see e.g. [29]. The method is also inspired by the recent developments in interior point methods for general nonlinear SDP problems, see e.g. [42] and [41]. Another motivation is the scope of the available FMO models. Most of these deal with FMO problems for two- and three-dimensional structures. As far as to our knowledge, no FMO models have been proposed in the literature for general laminated structures which are nowadays used in many engineering applications. The thesis proposes new FMO models for laminated plates and shells by extending the formulations in [15].

The thesis is organized in two parts. In Part I the introduction to the course of the study is addressed. In Chapter 2 the review of the researches on FMO, the underlying FMO problem formulations for solids and laminated structures, and the overview of the method proposed in the thesis are described. The summary of the papers included in the thesis is presented in Chapter 3. The conclusions, contributions and proposed research areas of the thesis are presented in Chapter 4. Part II includes 4 papers listed below.

Chapter 5   Weldeyesus, A.G., Stolpe, M.: A primal-dual interior point method for largescale free material optimization. *Computational Optimization and Applications* (2014). DOI 10.1007/s10589-014-9720-6

Chapter 6   Weldeyesus, A.G., Stolpe, M.: Free Material Optimization for Laminated Plates and Shells. *Journal of Structural and Multidisciplinary Optimization.* Accepted in 2014 and in print.

Chapter 7   Weldeyesus, A.G.: Models and methods for Free Material Optimization with local stress constraints. Submitted to *Journal of Structural and Multidisciplinary Optimization* in 2014. In review.

Chapter 8   Stolpe, M., Weldeyesus, A.G.: On solving Free Material Optimization problems using iterative methods. Department of Wind Energy, Technical University of Denmark, 2014. To be submitted.

Chapter 2

Free Material Optimization

The design parametrization in Free Material Optimization (FMO) varies the entire stiffness tensor freely at each point of the design domain. We impose only certain requirements on the material tensor as necessary conditions on physical attainability. The stiffness tensors are forced to be symmetric and positive semidefinite. FMO obtains conceptual optimal structures characterized by optimal material distribution and optimal material properties which can be regarded as ultimately best structures among other possible elastic continua [43]. FMO thus can be used to generate benchmark solutions for other models and besides to propose novel ideas for new design situations. For instance, in [23] we can see conceptual optimal design of ribs in the leading edge of Airbus A380 that led to substantial weight reduction.

The basic FMO problem formulations of minimizing compliance dates back to the 1990s in [3], [4], and [32]. Recent FMO models more are advanced than these formulations taking in to account several engineering constraints. FMO models aiming at limiting high stresses, which often cause failures in engineering structures, are introduced and solved in [23], [22], and [21] for two-dimensional and in [16] for three-dimensional structures. The models are further extended to address certain prescribed deformation behaviors through displacement constraints in [23] and [16]. We find FMO formulations with eigenfrequency constraints in [38] that take in to account dynamic processes. In analogy to these multidisciplinary problem formulations, FMO models for shells and plates are proposed in [15] to get designs more suited for thin-walled structures.

Considering the size and structure of FMO problems it is crucial that special purpose methods are preferred to general methods. For similar arguments and details, see e.g. [37]. Small size FMO problems of slightly different matrix inequality constraints than recent FMO problems were solved in [32] with

an interior point method. A method based on penalty/barrier multipliers called PBM is developed and is used to solve FMO problems in [43]. A computer code PENNON based an augmented Lagrangian function method developed in [20] to solve convex nonlinear and SemiDefinite Programming (SDP) and further studied in [36] is used to solve multidisciplinary FMO problems in several articles, e.g. stress constrained problems in [21] and displacement and stress constrained problems in [23]. A method based on a sequential convex programming concept in which the subproblems are convex and separable SDPs is developed in [40, 39] and have been used to solve FMO problems in, e.g [16].

Theoretical treatments of FMO problems have been analyzed in several articles. The existence of optimal solution to FMO problems is shown in the early studies [2] and [43] and latter in [27] based on saddle-point point theory and in [27] based on duality theory. These theories are not applicable when the engineering constraints mentioned above are included in the problem formulations. In [16] a generic FMO problem intended to take in to account displacement and stress constraints is formulated for which existence of solution is shown using a mathematical tool described as H-convergence. The article indeed shows the convergence of the solution of the finite element discretized problems to the solution of the original problem.

There are studies focusing on the post processing of FMO results to approximate the conceptual designs with real materials suited for manufacturing process. In [18] the realization of FMO results by composite materials has been described. There are tools developed in [9] and [8] offering various possibilities and techniques of FMO data realization and visualization.

2.1 The underlying FMO problem formulations

In this section we present the underlining minimum compliance (maximum stiffness) FMO problem formulation for two- and three-dimensional solids and laminated plates and shells. In both cases we start with the discrete version of the problem formulation. The problem formulations and finite element discretization for solids closely follow, e.g. [40] and [23]. For the problems on laminated structures we refer the reader to [11] for details on the shell kinematics and to Chapter 7 for the FMO problem formulations in function spaces and the finite element discretization.

In the optimization problems we consider the material tensor is in general anisotropic, the loads are static and linear elasticity is assumed. From physical attainability point of view the stiffness tensor has to be symmetric and positive semidefinite. We follow the approach in most articles for choosing the trace of the stiffness tensor to measure material stiffnesses. We locally bound from above by $\bar{\rho}$ to avoid arbitrarily stiff materials and from below by $\bar{\rho}$ to limit softness. The

bounds are chosen to satisfy the relation $0 \leq \underline{\rho} < \bar{\rho} < \infty$. These constraints on the local stiffnesses do not depend on coordinate systems due to the invariance property of the trace under orthogonal transformations.

Let $f_\ell \in \mathbb{R}^n$, where $\ell \in L = \{1, \ldots, n_L\}$ and n is the number of finite element degrees of freedom be given external nodal load vectors with prescribed weights w_ℓ satisfying $\sum_\ell w_\ell = 1$ and $w_\ell > 0$ for each $\ell \in L$.

2.1.1 FMO for solid structures

Let the design domain Ω be partitioned in to m uniform finite elements Ω_i for $i = 1, \ldots, m$. We approximate the elastic stiffness tensor $E(x)$ by a piecewise constant function with its element values constituting the vector of block matrices $E = (E_1, \ldots, E_m)^T$. For a given load vectors f_ℓ the associated displacement vectors $u_\ell \in \mathbb{R}^n$ are determined by the linear elastic equilibrium equations

$$A(E)u_\ell = f_\ell, \; \ell \in L, \tag{2.1}$$

where the global stiffness matrix $A(E) \in \mathbb{R}^{n \times n}$ is given by

$$A(E) = \sum_{i=1}^{m} A_i(E), \;\; A_i(E) = \sum_{k=1}^{n_G} B_{i,k}^T E_i B_{i,k}. \tag{2.2}$$

The matrices $B_{i,k}$ are (scaled) strain-displacement matrices computed from the derivative of the shape functions and n_G is the number of Gaussian integration points, see e.g. [12]. We define the set of admissible materials $\tilde{\mathcal{E}}$ by

$$\tilde{\mathcal{E}} := \left\{ E \in (\mathbb{R}^{dm \times d}) | E_i = E_i^T \succeq 0, \underline{\rho} \leq Tr(E_i) \leq \bar{\rho}, i = 1, \ldots, m \right\} \tag{2.3}$$

and the amount of material to distribute in the structure by

$$v(E) := \sum_{i=1}^{m} Tr(E_i). \tag{2.4}$$

The exponent d in (2.3) takes the value 3 for two-dimensional problems and 6 for three-dimensional problems. The primal minimum compliance FMO problem for solid structures is formulated as

$$\begin{aligned}
\underset{u_\ell \in \mathbb{R}^n, E \in \tilde{\mathcal{E}}}{\text{minimize}} \quad & \sum_{\ell \in L} w_\ell f_\ell^T u_\ell \\
\text{subject to} \quad & A(E)u_\ell = f_\ell, \; \ell \in L, \\
& v(E) \leq V.
\end{aligned} \tag{2.5}$$

(a) (b)
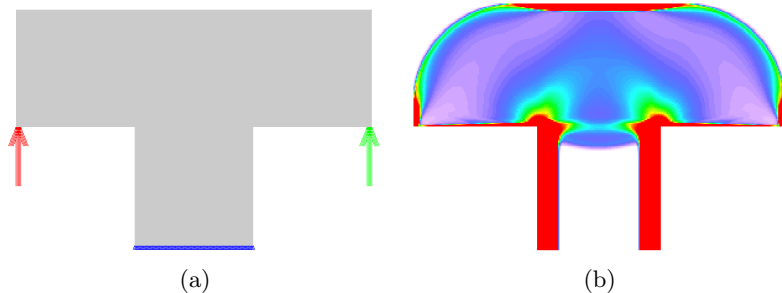
Figure 2.1: Two-dimensional T-shaped design domain, boundary conditions, and two external loads (a), optimal density distribution (b).

The volume fraction constant $V > 0$ is chosen to satisfy

$$\sum_{i=1}^{m} \underline{\rho} < V < \sum_{i=1}^{m} \overline{\rho}.$$

The minimum compliance problem (2.5) can be equivalently formulated as a linear problem or a nonlinear convex nested formulations. One can also derive the dual formation. All these formulations, various minimum weight problems, and relevant mathematical properties are briefly discussed in Chapter 5. Primal FMO problem formulations with constraints on local stresses are described and solved in Chapter 7.

The Figures 2.1 and 2.2 show examples of two- and three-dimensional optimal designs obtained by FMO.

2.1.2 FMO for laminated plates and shells

We consider a laminate of N layers with the midsurface ω partitioned in to m uniform finite elements ω_i for $i = 1, \ldots, m$. The plane-stress in-plane elastic stiffness tensor $C(x)$ and transverse tensor $D(x)$ are approximated by piecewise functions. Let C_{il} and D_{il} denote the constant approximations of $C(x)$ and $D(x)$ on the ith element and lth layer respectively. These values constitutes the vectors of block matrices

$$C = (C_{11}, \ldots, C_{1N}, \ldots, C_{m1} \ldots, C_{mN})^{T}$$

and

$$D = (D_{11}, \ldots, D_{1N}, \ldots, D_{m1} \ldots, D_{mN})^{T}.$$

<center>(a)   (b)</center>
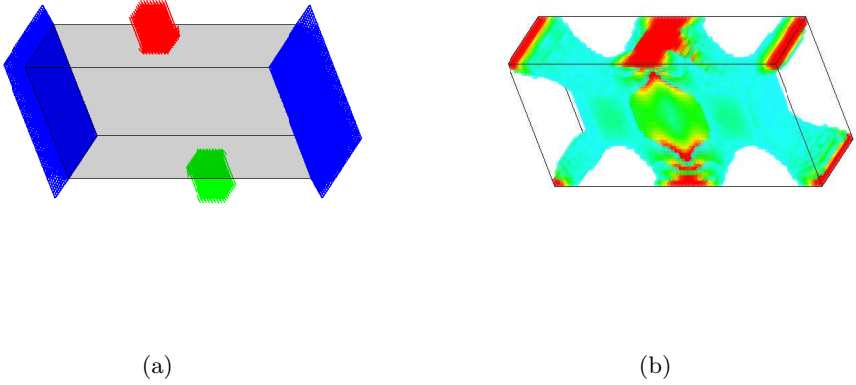
Figure 2.2: Three-dimensional design domain, boundary conditions, and two external loads (a), optimal density distribution (b).

For a given load vectors f_ℓ the associated displacement vectors $(u, \theta)_\ell$ (translational and rotational) are determined by the linear elastic equilibrium equations

$$K(C, D)(u, \theta)_\ell = f_\ell, \ \ell \in L, \tag{2.6}$$

where the global stiffness matrix $K(C, D)$ is given by

$$K(C, D) = \sum_{i=1}^{m}(K_i^\gamma(C) + K_i^{\gamma\chi}(C) + (K_i^{\gamma\chi}(C))^T + K_i^\chi(C) + K_i^\zeta(D)). \tag{2.7}$$

The element stiffness matrices in (2.7) are given by

$$K_i^\gamma(C) = \sum_{l,(j,k)\in n_i} \int_{\omega_i} t_{il}(B_{jl}^\gamma)^T C_{il} B_{kl}^\gamma dS \tag{2.8a}$$

$$K_i^{\gamma\chi}(C) = \sum_{l,(j,k)\in n_i} \int_{\omega_i} \tilde{t}_{il}(B_{jl}^\gamma)^T C_{il} B_{kl}^\chi dS \tag{2.8b}$$

$$K_i^\chi(C) = \sum_{l,(j,k)\in n_i}^{N} \int_{\omega_i} \tilde{\tilde{t}}_{il}(B_{jl}^\chi)^T C_{il} B_{kl}^\chi dS \tag{2.8c}$$

$$K_i^\zeta(D) = \kappa \sum_{l,(j,k)\in n_i} \int_{\omega_i} t_{il}(B_{jl}^\zeta)^T D_{il} B_{kl}^\zeta dS, \tag{2.8d}$$

<center>8</center>

where n_i is the index set of nodes associated with the element ω_i. The matrices B_{il}^γ, B_{il}^γ and $B_{i,l}^\zeta$ are the (scaled) strain-displacement matrices for membrane strains, for bending strains, and for shear strains, respectively, and are constructed from the derivatives of the shape functions. The factors t_{il}, $\tilde{t}_{il}$, and $\tilde{\tilde{t}}_{il}$ are the result of evaluating the volume integral over the thickness and are computed as

$$t_{il} = t_{il}^b - t_{il}^a, \ \ \tilde{t}_{il} = \frac{1}{2}((t_{il}^b)^2 - (t_{il}^a)^2), \ \ \tilde{\tilde{t}}_{il} = \frac{1}{3}((t_{il}^b)^3 - (t_{il}^a)^3), \qquad (2.9)$$

where t_{il}^b and t_{il}^a are the upper and lower transverse coordinates of the lth layer at the center of the element ω_i. The shear term (2.8d) is multiplied by a constant $\kappa < 1$ is to take into account the shell model often considered in applications.

For laminates we define the set of admissible material $\tilde{\mathcal{E}}$ by

$$\tilde{\mathcal{E}} = \left\{ (C,D) \in (\mathbb{R}^{3mN \times 3}) \times (\mathbb{R}^{2mN \times 2}) \middle| C_{il} = C_{il}^T \succeq 0, D_{il} = D_{il}^T \succeq 0, \right.$$

$$\left. \underline{\rho} \le t_{il} \left(\mathrm{Tr}(C_{il}) + \tfrac{1}{2}\mathrm{Tr}(D_{il}) \right) \le \bar{\rho}, \quad i = 1, \dots, m, l = 1, \dots, N \right\}, \quad (2.10)$$

and the amount of material to distribute in the structure by

$$v(C,D) := \sum_{i=1}^{m} \sum_{l=1}^{N} t_{il} \left(Tr(C_{il}) + \frac{1}{2} Tr(D_{il}) \right). \qquad (2.11)$$

The primal minimum compliance FMO problem for laminated plates and shells is then formulated as

$$\begin{aligned} \underset{(u,\theta)_\ell \in \mathbb{R}^n, (C,D) \in \tilde{\mathcal{E}}}{\text{minimize}} \quad & \sum_{\ell \in L} w_\ell (f_\ell)^T (u,\theta)_\ell \\ \text{subject to} \quad & K(C,D)(u,\theta)_\ell = f_\ell, \ \ell \in L, \\ & v(C,D) \le V. \end{aligned} \qquad (2.12)$$

The volume fraction constant $V > 0$ satisfies

$$\sum_{l=1}^{N} \sum_{i=1}^{m} \underline{\rho} < V < \sum_{l=1}^{N} \sum_{i=1}^{m} \bar{\rho}.$$

For the minimum weight problem, and stress constrained problem formulations, see Chapters 6 and 7.

In Figure 2.3 we present an optimal design obtained by FMO of an eight layer clamped plate under four transversal loads with volume fraction 50%.

(a)
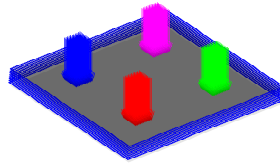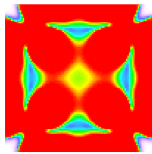
Layer=1   Layer=2   Layer=3   Layer=4
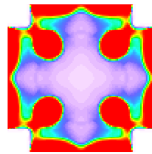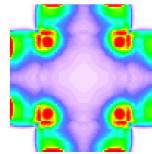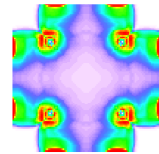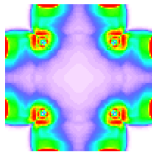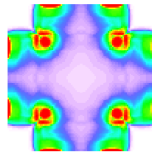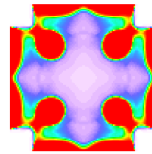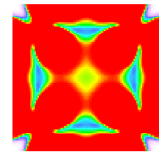
Layer=5   Layer=6   Layer=7   Layer=8

(b)

Figure 2.3: Design domain and boundary conditions of an eight layer clamped plate under four transversal loads (a), optimal density distribution(b), the layers are numbered from bottom to top in the thickness direction.

2.2 The primal-dual interior point method

The FMO problem formulations (2.5), (2.12) and those in Chapters (5)–(8) can be represented by the following nonlinear SDP

$$
\begin{aligned}
\underset{X \in \mathbb{S}, u \in \mathbb{R}^n}{\text{minimize}} \quad & f(X, u) \\
\text{subject to} \quad & g_j(X, u) \leq 0, \quad j = 1, \ldots, k, \\
& X_i \succeq 0, \qquad i = 1, \ldots m,
\end{aligned}
\tag{2.13}
$$

where

$$
\mathbb{S} = \mathbb{S}^{d_1} \times \mathbb{S}^{d_2} \times \cdots \times \mathbb{S}^{d_m} \text{ and } (d_1, d_2, \ldots, d_m) \in \mathbb{N}^m,
$$

and $\mathbb{S}^d$-space of symmetric $d \times d$ matrices. The functions $f, g_j : \mathbb{S} \times \mathbb{R}^n \to \mathbb{R}$, for $j = 1, \ldots, k$ are assumed to be sufficiently smooth. The outline of the proposed primal-dual interior method is briefly presented for problem (2.13) in Chapter (5). The state-of-the art is the combination of the standard interior point methods for nonlinear optimization problems and linear SDPs. It includes the introduction of slack variables for the inequality constraints, the formulation of the associated barrier problem, the derivations of optimality conditions, and the consequent large and reduced saddle-point systems. The most common search directions in SDPs, namely, the AHO direction [1], the HRVW/KSV/M direction [17, 19, 28], and the NT direction [30, 31] are computed. This chapter additionally includes the detail description of the correspondence of the generic formulation and the interior point systems to FMO problem formulations. The method is further extended in Chapter 7 to handle stress constrained FMO problems which are essentially non convex problems. In Chapter 8 some of the interior point saddle-point systems are solved using iterative solvers.

Chapter 3

Summary of the articles

We present the summary for each of the articles included in the thesis.

A Primal-Dual Interior Point Method for Large-Scale Free Material Optimization (Chapter 5)   This article concerns efficient solution method for FMO problems. A primal-dual interior point method which is special purpose for FMO is developed by coupling the solution techniques for linear semidefinite programmings and standard nonlinear problems. Its efficiency relies on exploiting the sparse structures that result from the many small matrix inequalities. Problem formulations of simultaneous analysis and design (SAND), nested and dual are considered. The article reports high quality solutions obtained within a modest number of iterations to the classical FMO problem formulations. The most common symmetrization schemes used in SDP which are AHO, HRVW/KSV/M and NT are numerically investigated for FMO problems. Performance profiles of the different problem formulations and the symmetrization schemes are reported using the number of iterations required and CPU time spent as measuring criteria. The problem formulations seem to perform more or less similar. The algorithm needs more number of iterations with HRVW/KSV/M directions than the other two directions. The sensitivity of the NT directions to algorithmic parameters is more robust than AHO.

Free Material Optimization for Laminated Plates and Shells (Chapter 6)   The focus of this article is on formulating FMO models for laminated plates and shells. The shell geometry and kinematics are briefly described. Existing FMO models for plates and shells are extended to laminated structures for the first time. The method proposed in Chapter 5 for FMO problems for two- and three-dimensional solid structures is generalized for the problems of this ar-

ticle. The proposed models and the extended method are supported by several numerical examples.

Models and methods for Free Material Optimization with local stress constraints (Chapter 7)   In this article we introduce stress constraints to FMO models for laminates proposed in Chapter 6. The formulations are based on the exiting stress constrained FMO models for solid structure. The resulting stress constrained problems are more difficult to solve than the classical problems in Chapters 5 and 6. The method described in Chapters 5 and 6 is further generalized in order to solve the stress constrained problems. A perturbation technique based on inertia controlling strategies already used in standard nonlinear optimization problems is employed to the method. The article includes several numerical experiments. The numerical experiments show that in FMO the change of material properties play primary role in high stresses reduction. The practice is different in other structural optimization approaches where the material properties are fixed.

On solving Free Material Optimization problems using iterative methods, (Chapter 8)   The goal of this article is to introduce iterative solvers to the method described in Chapter 5. The use of direct methods to solve saddle-point systems that appear in the optimization process of large-scale FMO problems has limitation due to memory issues. This is a barrier on the size of problems that can be solved and is usually tackled by replacing the direct methods with iterative methods. The main challenge in using iterative methods is developing cheap but effective preconditioners. This article includes some progresses on developing certain preconditioners to use iterative solvers in the method.

Chapter 4

Conclusions, contributions and future research areas

4.1 Conclusions and contributions

The thesis deals with various FMO models and an efficient solution method. Most of today's FMO studies focus on FMO models for solid structures. Nowadays, laminated structures are extensively used in engineering applications. We extend existing FMO models for shells to laminated structures. We propose new FMO problem formulations for laminates for the first time. These formulations include constraints on local stresses and are supported by numerical examples. The solutions to the FMO problems for laminated structures are in favour of sandwich-like structures when the laminate is subject to out-of-plane loads.

The problem formulations in FMO are modeled as nonlinear SemiDefinite Programming (SDP) which is relatively more recent class of optimization. In FMO the material properties at each point of the design domain are the design variables. Thus FMO problems are essentially large scale-problems and require specialized method and implementation suited to their structures. In this thesis we develop a special purpose primal-dual interior point method and solve robustly by far large classical FMO problems for solid and laminated structures. The number of iterations the method requires is modest and is almost independent of problem size. The thesis introduces some promising progresses on using iterative solvers for large-scale 3D FMO problems.

The thesis investigates the numerical behavior of certain equivalent classical FMO problem formulations and the most common symmetrization schemes in SDPs. The problems formulations are the nested and the simultaneous analysis and design formulations for the minimum weight problem and additionally the

dual problem for the minimum compliance problem. The computed search directions include the AHO direction, the HRVW/KSV/M direction and the NT direction. The performance profiles show that the problems of all formulations perform almost in the same way. Among the search directions we recommend the NT direction for its better robustness than the others. The HRVW/KSV/M direction result in more number of interior point iterations than NT and AHO directions. This is because the KKT error is always relatively large at the start of each inner interior point iteration.

The method is also generalized further to tackle the non convex problems with stress constraints. The algorithm treats the stress constraints keeping their original setting. This is unlike the practice in most existing studies where the stress constraints are included in the objective function using a penalty term and an approximation problem is formulated. This leads to several solves of the approximate problem to obtain more accurate solution. The generalized method has obtained solutions to stress constrained FMO problems for both solids and laminated structures. The stress constraints are satisfied with high accuracy. The solution to the problems reveal some typical behaviors FMO problems. In agreement to previous studies the high stresses are reduced in FMO predominantly by changing material properties which is not the case in other structural optimizations. Moreover, the extent of worsening the compliance is much smaller.

4.2 Future research areas

The method and the new proposed FMO models are mainly supported by numerical experiments. Theoretical treatments on convergence theory of the method and existence of optimal solution for the new FMO models must be further analyzed. The applicability of relevant available theories in the literature should be determined.

The stress constraints are defined over the entire domain in the problem formulations. However, these constraints are active only on certain regions and treating all of them in the algorithm is not numerically efficient. This can be improved by introducing active set strategy where inactive stress constraints are ignored in the optimization process.

The preliminary success in using iterative solvers for FMO problems could motivate for possible future researches to couple these solvers in the development of optimization methods for FMO.

The proposed FMO models for laminates are limited to only stress constraints. The scope of exiting FMO models for solid structures is wider considering more constraints on strains, displacements, and eigenfrequencies. These constraints could be introduced to the FMO models for laminates.

The available FMO problem formulations are in general formulated based

on linear model limited to deal with small deformation. The models could be generalized to deal with large deformations (geometric nonlinear modeling with small strains but large displacements) giving more reliable results for applications.

Fiber reinforced composite structures have been proposed as one of the favourite candidates for realization of FMO results. The relevance could be even higher for the results in this thesis obtained by solving the FMO models for laminates. The already available tools for realization and visualization of FMO data could be applied to evaluate the relevance.

The numerical examples in this thesis and most other studies consider design domains suited for academic purposes. The problems could be solved over more complex industrial structures such as wind turbine blades.

Bibliography

[1] F. Alizadeh, J. A. Haeberly, and M. L. Overton. Primal-dual interior-point methods for semidefinite programming: convergence rates, stability and numerical results. *SIAM Journal on Optimization*, 8(3):746–768, 2009.

[2] A. Ben-Tal and A. Nemirovski. Robust truss topology design via semidefinite programming. *SIAM Journal on Optimization*, 7(4):991–1016, 1997.

[3] M. P. Bendsøe and A. R. Díaz. Optimization of material properties for Mindlin plate design. *Structural Optimization*, 6:268–270, 1993.

[4] M. P. Bendsøe, J. M. Guedes, R. B. Haber, P. Pedersen, and J. E. Taylor. An analytical model to predict optimal material properties in the context of optimal structural design. *Journal of Applied Mechanics*, 61:930–937, 1994.

[5] M. P. Bendsøe and N. Kikuchi. Generating optimal topologies in structural design using a homogenization method. *Computer Methods in Applied Mechanics and Engineering*, 71(2):197–224, 1989.

[6] M. P. Bendsøe and O. Sigmund. *Topology Optimization - Theories, Methods and Applications*. Springer Verlag, Berlin Heidelberg, 2004.

[7] H. Y. Benson and D. F. Shanno. Interior-point methods for nonconvex nonlinear programming: regularization and warmstarts. *Computational Optimization and Applications*, 40:143–189, 2008.

[8] G. Bodnár. Efficient algorithms for visualising FMO results. Technical report, PLATO-N Public Report PU-R-5-2007, 2007. Available from http://www.plato-n.org/.

[9] G. Bodnár, P. Stadelmeyer, and M. Bogomolny. Methods for computer aided interpretation of FMO results. Technical report, PLATO-N Public Report PU-R-3-2008, 2008. Available from http://www.plato-n.org/.

[10] M. Bruyneel. SFP-a new parameterization based on shape functions for optimal material selection: application to conventional composite plies. *Structural and Multidisciplinary Optimization*, 43(1):17–27, 2011.

[11] D. Chapelle and K. J Bathe. *The Finite Element Analysis of Shells - Fundamentals.* Springer, Heidelberg, 2003.

[12] R. D. Cook, D. S. Malkus, M. E. Plesha, and R. J. Witt. *Concepts and Applications of Finite Element Analysis.* John Wiley and Sons, 4th edition, 2002.

[13] A. Forsgren and P. E. Gill. Primal-dual interior methods for nonconvex nonlinear programming. *SIAM Journal on Optimization*, 8(4):1132–1152, 1998.

[14] A. Forsgren, P. E. Gill, and M. H. Wright. Interior methods for nonlinear optimization. *SIAM Review*, 44(4):525–597, 2002.

[15] S. Gaile. *Free material optimization for shells and plates.* PhD thesis, Institute of Applied Mathematics II, Friedrich-Alexander University of Erlangen-Nuremberg, 2011.

[16] J. Haslinger, M. Kočvara, G. Leugering, and M. Stingl. Multidisciplinary free material optimization. *SIAM Journal on Applied Mathematics*, 70(7):2709–2728, 2010.

[17] C. Helmberg, F. Rendl, R. J. Vanderbei, and H. Wolkowicz. An interior-point method for semidefinite programming. *SIAM Journal on Optimization*, 6:342–361, 1996.

[18] H. R. E. M. Hörnlein, M. Kočvara, and R. Werner. Material optimization: Bridging the gap between conceptual and preliminary design. *Aerospace Science and Technology*, 5(8):541–554, 2001.

[19] M. Kojima, S. Shindoh, and S. Hara. Interior-point methods for the monotone semidefinite linear complementarity problem in symmetric matrices. *SIAM Journal on Optimization*, 7(1):86–125, 1997.

[20] M. Kočvara and M. Stingl. A code for convex nonlinear and semidefinite programming. *Optimization Methods and Software*, 18(3):317–333, 2003.

[21] M. Kočvara and M. Stingl. Free material optimization for stress constraints. *Structural and Multidisciplinary Optimization*, 33:323–355, 2007.

[22] M. Kočvara and M. Stingl. Mathematical models of FMO with stress constraints FMO. Technical report, PLATO-N Public Report PU-R-1-2008, 2009. Available from http://www.plato-n.org/.

[23] M. Kočvara, M. Stingl, and J. Zowe. Free material optimization: recent progress. *Optimization*, 57(1):79–100, 2008.

[24] E. Lund. Buckling topology optimization of laminated multi-material composite shell structures. *Composite Structures*, 91(2):158 – 167, 2009.

[25] E. Lund and J. Stegmann. On structural optimization of composite shell structures using a discrete constitutive parametrization. *Wind Energy*, 8:109–124, 2005.

[26] E. Lund and J. Stegmann. On structural optimization of composite shell structures using a discrete constitutive parametrization. *Wind Energy*, 8(1):109–124, 2005.

[27] J. Mack. Finite element analysis of free material optimization problem. *Applications of Mathematics*, 49(4):285–304, 2004.

[28] R. D. C. Monteiro. Primal-dual path-following algorithms for semidefinite programming. *SIAM Journal on Optimization*, 7(3):663–678, 1997.

[29] R. D. C. Monteiro. First- and second-order methods for semidefinite programming. *Mathematical Programming*, 97:209–224, 2003.

[30] Y. E. Nesterov and M. J. Todd. Self-scaled barriers and interior-point methods for convex programming. *Mathematics of Operations Research*, 22(1):1–42, 1997.

[31] Y. E. Nesterov and M. J. Todd. Primal-dual interior-point methods for self-scaled cones. *SIAM Journal on Optimization*, 8(2):324–364, 1998.

[32] U. T. Ringertz. On finding the optimal distribution of material properties. *Structural Optimization*, 5:265–267, 1993.

[33] W. S., R. E. Gomory Dorn, and H. J. Greenberg. Automatic design of optimal structures. *Journal de Mecanique*, 3:25–52, 1964.

[34] J. Stegmann. *Analysis and Optimization of Laminated Composite Shell Structures*. PhD thesis, Institute of Mechanical Engineering, Aalborg University, Aalborg, Denmark, 2004.

[35] J. Stegmann and E. Lund. Discrete material optimization of general composite shell structures. *International Journal for Numerical Methods in Engineering*, 62:2009–2007, 2005.

[36] M. Stingl. *On the Solution of Nonlinear Semidefinite Programs by Augmented Lagrangian Method.* PhD thesis, Institute of Applied Mathematics II, Friedrich-Alexander University of Erlangen-Nuremberg, 2006.

[37] M. Stingl, M. Kočvara, M., and G. Leugering. A new non-linear semidefinite programming algorithm with an application to multidisciplinary free material optimization. *International Series of Numerical Mathematics*, 158:275–295, 2009.

[38] M. Stingl, M. Kočvara, and G. Leugering. Free material optimization with fundamental eigenfrequency constraints. *SIAM Journal on Optimization*, 20(1):524–547, 2009.

[39] M. Stingl, M. Kočvara, and G. Leugering. A new non-linear semidefinite programming algorithm with an application to multidisciplinary free material optimization. *International Series of Numerical Mathematics*, 158:275–295, 2009.

[40] M. Stingl, M. Kočvara, and G. Leugering. A sequential convex semidefinite programming algorithm with an application to multiple-load free material optimization. *SIAM Journal on Optimization*, 20(1):130–155, 2009.

[41] C. H. Vogelbusch. *Numerical Treatment of Nonlinear Semidefinite Programs.* PhD thesis, Institut für Mathematik der Heinrich-Heine-Universität Düsseldorf, 2006.

[42] H. Yamashita, H. Yabe, and K. Harada. A primal-dual interior point method for nonlinear semidefinite programming. *Mathematical Programming*, 135:89–121, 2012.

[43] J. Zowe, M. Kočvara, and M. P. Bendsøe. Free material optimization via mathematical programming. *Mathematical Programming*, 79:445–466, 1997.

Part II

Articles

Chapter 5

A Primal-Dual Interior Point Method for Large-Scale Free Material Optimization

A Primal-Dual Interior Point Method for Large-Scale Free Material Optimization

Alemseged Gebrehiwot Weldeyesus[*] and Mathias Stolpe[†]

Abstract

Free Material Optimization (FMO) is a branch of structural optimization in which the design variable is the elastic material tensor that is allowed to vary over the design domain. The requirements are that the material tensor is symmetric positive semidefinite with bounded trace. The resulting optimization problem is a nonlinear semidefinite program with many small matrix inequalities for which a special-purpose optimization method should be developed. The objective of this article is to propose an efficient primal-dual interior point method for FMO that can robustly and accurately solve large-scale problems. Several equivalent formulations of FMO problems are discussed and recommendations on the best choice based on the results from our numerical experiments are presented. Furthermore, the choice of search direction is also investigated numerically and a recommendation is given. The number of iterations the interior point method requires is modest and increases only marginally with problem size. The computed optimal solutions obtain a higher precision than other available special-purpose methods for FMO. The efficiency and robustness of the method is demonstrated by numerical experiments on a set of large-scale FMO problems.

Mathematics Subject Classification 2010: 90C22, 90C90, 74P05, 74P15

Keywords: Structural optimization, free material optimization, semidefinite programming, interior point methods

---

[*]DTU Wind Energy, Technical University of Denmark, Frederiksborgvej 399, 4000 Roskilde, Denmark. E-mail: alwel@dtu.dk

[†]DTU Wind Energy, Technical University of Denmark, Frederiksborgvej 399, 4000 Roskilde, Denmark. E-mail: matst@dtu.dk

1 Introduction

The fundamental concept of Free Material Optimization (FMO) was introduced in the early 1990s in [6], [7], and [25]. Since then FMO has become one of the growing research areas within structural optimization. In FMO the design variable is the material tensor which can vary at each point of the design domain. Certain necessary conditions on the attainability are the only imposed requirements on the material tensor. The material tensors in FMO are forced to be symmetric positive semidefinite and have bounded trace. FMO thus yields optimal structures by describing not only the distribution of the amount of material but also the local material properties. Therefore, the optimal structure found by FMO can be considered as an ultimately best structure among all possible elastic continua [37]. However, the design is ideal as the manufacturing of structures with, generally anisotropic, material properties changing at each point of the design domain is difficult and expensive. Nevertheless, FMO can be used to generate benchmark solutions with which other models and methods can be compared and to propose novel ideas for new design situations.

The first models in FMO considered finding the stiffest (minimizing static compliance) structure by distributing limited resources of material. There has been significant progress in extending these basic models and multidisciplinary FMO problems have been proposed. FMO problems with constraints on local stresses and displacements are presented and solved in [20], [19], and [15]. FMO problems with constraints on fundamental eigenfrequencies are described and solved in [27]. FMO models for three dimensional structures are developed and analysed in [15] and for plates and shells in [13]. Theoretical aspects including proofs of existence of optimal solutions of FMO problems can be found in e.g. [34].

Due to the conditions imposed on the elasticity tensor in FMO, the resulting optimization problem is a nonlinear semidefinite programming (SDP), a nonstandard problem with many matrix inequalities for which special optimization methods have to be developed and implemented. Already in [25] an interior point method was used to solve small size FMO problems. The formulations in [25] have slightly different matrix inequalities compared to recent FMO models. A method based on penalty/barrier multipliers called PBM is used in [37] to solve FMO problems. A computer code PENNON which uses an augmented Lagrangian function method is also developed to solve convex nonlinear and semidefinte programming in [18] and is studied further in [26]. Several FMO problems are solved with this method, for example in [19] and [20]. The focus of today's development of optimization methods for FMO problems is based on first-order methods. Second-order methods are considered computationally too expensive. The most recent methods in [29, 28] are based on a sequential convex

programming concept in which the subproblems are convex and separable SDPs. The approach often leads to large number of iterations but can achieve relatively high accuracy.

The objective of this article is to propose an efficient primal-dual interior point method for the, by now, classical FMO formulations. The method is capable of efficiently and accurately solving large-scale FMO problems. The method and the implementation exploit the property that FMO problems have many but small matrix inequalities. The method computes accurate optimal solution within relatively few iterations. The numerical results indicate that the number of iterations furthermore only increases slowly, if at all, with problem size. The method is developed by extending existing robust and efficient primal-dual interior point method for nonlinear programming and coupling it with existing techniques for linear SDP. The method is also inspired by the developments in interior point methods for general nonlinear SDP problems, see e.g. [35] and [32]. For an overview of primal-dual interior point methods for nonlinear (and non convex) problems, see [11], [12], and [8]. Optimization methods for SDPs are listed in [22] and the references cited therein.

We consider two basic FMO problems which are the primal minimum compliance (maximum overall stiffness) problem and the primal minimum weight problem. For these problems different equivalent linear and nonlinear primal and dual formulations are available. Some of the important mathematical properties of the problems are listed. The primal-dual interior point method is then used to solve problem instances of all stated formulations. It is important that symmetry is maintained in the linearised first-order optimality conditions of SDP problems. There are different symmetrization schemes that are used to maintain the symmetry giving different search directions [30]. The most commonly used directions are the AHO direction [2], the HRVW/KSV/M direction [16, 17, 21], and the NT direction [23, 24]. All of these directions are implemented and a comparison of their computational complexity and effect on numerical convergence is reported.

The outline of this article is as follows. In Section 2 various FMO problem formulations with some of the useful mathematical properties are presented. In Section 3 the general outline of the proposed primal-dual interior point method is described for a generic nonlinear SDP. The algorithmic details of the method specialized to FMO problems are described in Section 4. The implementation of the method and the algorithmic parameters are described in Section 5. In Section 6 the numerical experiments, results and discussion are presented. The conclusions of this paper are given in Section 7.

2 FMO problem formulations

We start with the discrete version of the minimum compliance (maximum stiffness) and the minimum weight FMO formulations on two- or three-dimensional design domains. The problem formulations and the finite element discretization are exactly as proposed in published articles on FMO, see e.g. [29] and [20], without any alterations. Existence of optimal solutions to the problem formulations that we consider is shown in [15] under natural assumptions. The design domain Ω is partitioned in to m uniform finite elements Ω_i for $i = 1, \ldots, m$. The elastic stiffness tensor $E(x)$ is approximated by a function that is constant on each finite element. Let the element values constitute the vectors of block matrices $E = (E_1, \ldots, E_m)^T$. Given the external static nodal load vectors $f_\ell \in \mathbb{R}^n$ for $\ell \in L = \{1, \ldots, n_L\}$, where n is number of (finite element) degrees of freedom, the displacement u_ℓ must satisfy the linear elastic equilibrium equation

$$A(E)u_\ell = f_\ell, \ \ell \in L \tag{1}$$

where the stiffness matrix $A(E)$ is given by

$$A(E) = \sum_{i=1}^{m} A_i(E), \ \ A_i(E) = \sum_{k=1}^{n_G} B_{i,k}^T E_i B_{i,k}. \tag{2}$$

The (scaled) strain-displacement matrices $B_{i,k}$ are appropriately constructed from the derivative of the shape functions and n_G is the number of Gaussian integration points, see e.g. [9].

The two considered basic FMO formulations are the primal minimum compliance problem

$$
\begin{aligned}
\underset{u_1, \ldots, u_{n_L} \in \mathbb{R}^n, E \in \mathbb{E}}{\text{minimize}} \quad & \sum_{\ell \in L} w_\ell f_\ell^T u_\ell \\
\text{subject to} \quad & A(E)u_\ell = f_\ell, \ \forall \ell \in L, \\
& \sum_{i=1}^{m} Tr(E_i) \leq V,
\end{aligned}
\tag{3}
$$

and the primal minimum weight problem

$$
\begin{aligned}
\underset{u_1, \ldots, u_{n_L} \in \mathbb{R}^n, E \in \mathbb{E}}{\text{minimize}} \quad & \sum_{i=1}^{m} Tr(E_i) \\
\text{subject to} \quad & A(E)u_\ell = f_\ell, \ \forall \ell \in L, \\
& \sum_{\ell=1}^{L} w_\ell f_\ell^T u_\ell \leq \gamma,
\end{aligned}
\tag{4}
$$

where $\mathbb{E}$, denotes the set of admissible materials

$$\mathbb{E} := \left\{ E \in (\mathbb{S}_+^N)^m \mid \underline{\rho} \le Tr(E_i) \le \bar{\rho}, i = 1, \ldots, m \right\}.$$

Here, $\mathbb{S}_+^N$ is the cone of positive semidefinite matrices in the space $\mathbb{S}^N$ of symmetric $N \times N$ matrices. We say that $E_i \in \mathbb{S}_+^N$ if and only if $E_i = E_i^T$ and $E_i \succeq 0$. The given weights w_ℓ satisfy $\sum_\ell w_\ell = 1$, and $w_\ell > 0$ for each $\ell \in L$. For FMO problems on two-dimensional design domains N takes the value 3. For problems on three dimensional design domains $N = 6$. The positive semidefiniteness of E is a necessary condition on the physically attainability of the material. The $Tr(E_i)$ measures the stiffness of the material and is locally bounded from above by $\bar{\rho}$ to avoid locally arbitrarily stiff material. We also allow a lower trace bounds. Note that $0 \le \underline{\rho} < \bar{\rho} < \infty$. The constant $V > 0$ is an upper bound on the amount of resource material to distribute in the structure.

Both problems (3) and (4) have linear objective function with linear matrix inequalities and nonlinear (and nonconvex) vector constraints. Therefore, they are classified as nonconvex SDPs.

If we additionally assume that $E \succ 0$[1] and that, as a consequence, the stiffness matrix $A(E)$ is positive definite and so non-singular we can obtain a nested problem formulation, i.e. a formulation in the design variables E only. By solving for the displacement u_ℓ in the equilibrium equation (1), we get the reduced nested formulation of the minimum compliance problem (3)

$$
\begin{aligned}
&\underset{E \in \mathbb{E}}{\text{minimize}} && \sum_{\ell \in L} w_\ell f_\ell^T A^{-1}(E) f_\ell \\
&\text{subject to} && \sum_{i=1}^m Tr(E_i) \le V.
\end{aligned}
\tag{5}
$$

Similarly, a nested formulation of the minimum weight problem (4) is

$$
\begin{aligned}
&\underset{E \in \mathbb{E}}{\text{minimize}} && \sum_{i=1}^m Tr(E_i) \\
&\text{subject to} && \sum_{\ell \in L} w_\ell f_\ell^T A^{-1}(E) f_\ell \le \gamma.
\end{aligned}
\tag{6}
$$

In [29] it is shown that the function

$$c(E) = f_\ell^T A^{-1}(E) f_\ell$$

---

[1]This assumption is standard within structural optimization. In the implementation it is satisfied by forcing that $E_i \succeq \varepsilon I$ for some small $\varepsilon > 0$.

is convex and infinitely continuously differentiable. Therefore, both problems (5) and (6) are convex SDPs since all other constraints are linear. Using the Schur complement theorem it can also be shown that problem (3) is equivalent to

$$
\begin{aligned}
\underset{E \in \mathbb{E}, \varrho_\ell \geq 0}{\text{minimize}} \quad & \sum_{\ell \in L} w_\ell \varrho_\ell \\
\text{subject to} \quad & \sum_{i=1}^{m} Tr(E_i) \leq V, \\
& \begin{pmatrix} \varrho_\ell & f_\ell^T \\ f_\ell & A(E) \end{pmatrix} \succeq 0, \ \forall \ell \in L.
\end{aligned}
\tag{7}
$$

Problem formulations similar to (7) have also been proposed for truss topology optimization in a number of articles, see e.g. [4, 5]. Problem (7) has a linear objective function, and linear vector and matrix inequalities. Hence, it is a linear SDP. For its linearity this formulation leads to a nice mathematical structure but with additionally very large-scale matrix inequalities which are difficult to deal with in computations, see e.g. [20]. For this reason problem (7) is excluded from our numerical experiment.

The minimum compliance problem (3) has the following dual formulation. For the derivation, please see the Appendix A.

$$
\begin{aligned}
\underset{\substack{u_1,\ldots,u_{n_L} \in \mathbb{R}^n \\ \alpha \in \mathbb{R}, \bar{\beta} \in \mathbb{R}^m, \underline{\beta} \in \mathbb{R}^m}}{\text{maximize}} \quad & -\alpha \bar{V} + 2 \sum_{\ell \in L} w_\ell f_\ell^T u_\ell + \underline{\rho} \sum_{i=1}^{m} \underline{\beta}_i - \bar{\rho} \sum_{i=1}^{m} \bar{\beta}_i \\
\text{subject to} \quad & \sum_{\ell \in L} \sum_{k=1}^{n_G} w_\ell B_{i,k}^T u_\ell u_\ell^T B_{i,k} - (\alpha - \underline{\beta}_i + \bar{\beta}_i) I \preceq 0 \,, i = 1, \ldots, m \\
& \alpha \geq 0, \bar{\beta} \geq 0, \underline{\beta} \geq 0.
\end{aligned}
\tag{8}
$$

This is a problem with linear objective and convex quadratic constraints. Therefore, it is a convex problem. For this problem it can be verified that the Slater condition holds by choosing arbitrary $u_\ell \in \mathbb{R}^n$, $\underline{\beta} > 0$, $\bar{\beta} > 0$, and sufficiently large positive α. Since problem (3) can also be equivalently written as convex problems, for example problem (5), the duality gap is zero. Similar results for min-max problems can also be found in [27] and [3]. A solution to the primal problem (3) can be obtained by solving the dual problem (8). The primal variable E appears in the primal-dual system of (8) as a Lagrangian multiplier to the matrix inequality constraints. It is thus important that the dual problem is solved up to optimality to get a structure supporting the external loads.

Throughout this article we use the following assumptions on the problem data in the FMO problems. Similar assumptions are stated, implicitly or explicitly, in e.g. [3].

A1 The loads are non-zero, i.e. $f_\ell \neq 0$ for all $\ell \in L$.

A2 The trace bounds satisfy $0 \leq \underline{\rho} < \bar{\rho} < +\infty$ and the volume bound satisfies

$$\sum_{i=1}^{m} \underline{\rho} < V < \sum_{i=1}^{m} \bar{\rho}.$$

A3 The stiffness matrix $A(E)$ is positive definite for all $E \succ 0$.

A4 Given $\gamma > 0$ and weights $w_\ell > 0, \ell \in L$ there exists positive definite $E \in \mathbb{E}$ such that $\sum_{\ell \in L} w_\ell f_\ell^T A^{-1}(E) f_\ell \leq \gamma$.

Assumption (A1) is to exclude trivial cases. Combining the positive definiteness of the stiffness matrix $A(E)$ with assumption (A1) - (A4) imply that the feasible sets of problems (3), (4), and their equivalent problems are non-empty.

3 The primal-dual interior point method

In this section the primal-dual interior method is described in the setting of a general nonlinear SDP. The specializations to FMO problems are presented in Section 4. In line with the special structure of the FMO problems and motivated by the problem formulations in [29] we consider the nonlinear SDP

$$\begin{aligned}
\underset{X \in \mathbb{S}, u \in \mathbb{R}^n}{\text{minimize}} \quad & f(X, u) \\
\text{subject to} \quad & g_j(X, u) \leq 0, \quad j = 1, \ldots, k, \\
& X_i \succeq 0, \qquad i = 1, \ldots m,
\end{aligned} \tag{9}$$

with

$$\mathbb{S} = \mathbb{S}^{d_1} \times \mathbb{S}^{d_2} \times \cdots \times \mathbb{S}^{d_m} \text{ and } (d_1, d_2, \ldots, d_m) \in \mathbb{N}^m.$$

The functions $f, g_j : \mathbb{S} \times \mathbb{R}^n \to \mathbb{R}$, for $j = 1, \ldots, k$ are assumed to be sufficiently smooth. After introducing slack variables $s \in \mathbb{R}^k$ to problem (9) the associated barrier problem with barrier parameter $\mu > 0$ is

$$\begin{aligned}
\underset{X \in \mathbb{S}_+, u \in \mathbb{R}^n, s \in \mathbb{R}_+^k}{\text{minimize}} \quad & f(X, u) - \mu \sum_{i=1}^{m} \ln(\det(X_i)) - \mu \sum_{j=1}^{k} \ln(s_j) \\
\text{subject to} \quad & g_j(X, u) + s_j = 0, \quad j = 1, \ldots, k.
\end{aligned} \tag{10}$$

The central idea in interior point methods is that problem (10) is solved for a sequence of barrier parameter μ_k approaching zero and the barrier problem

approaches the original problem (9). With Lagrangian multiplier $\lambda \in \mathbb{R}_+^k$, the Lagrangian to problem (10) is

$$\mathcal{L}_\mu(X, u, s, \lambda) = f(X, u) - \mu \sum_{i=1}^{m} \ln(\det(X_i)) - \mu \sum_{j=1}^{k} \ln(s_j) + \lambda^T (g(X, u) + s).$$

The first-order optimality conditions of the barrier problem (10) are

$$\nabla_X \mathcal{L}_\mu(X, u, s, \lambda) = \nabla_X f(X, u) - \mu X^{-1} + \nabla_X (g(X, u)^T \lambda) = 0 \qquad \text{(11a)}$$
$$\nabla_u \mathcal{L}_\mu(X, u, s, \lambda) = \nabla_u f(X, u) + \nabla_u g(X, u)^T \lambda = 0 \qquad \text{(11b)}$$
$$\nabla_s \mathcal{L}_\mu(X, u, s, \lambda) = -\mu S^{-1} e + \lambda = 0 \qquad \text{(11c)}$$

together with the feasibility condition

$$g(X, u) + s = 0 \qquad \text{(12)}$$

and positive definiteness of X, positivity of the slack variables s and the dual variables λ. Following standard techniques for interior point methods for linear SDP, see for example [22], we introduce the additional matrix variable Z satisfying

$$Z := \mu X^{-1} \qquad \text{(13)}$$

in (11a) so that $XZ - \mu I = 0$. The optimality conditions in (11) are rewritten as

$$\begin{pmatrix} \nabla_X f(X, u) - Z + \nabla_X (g(X, u)^T \lambda) \\ \nabla_u f(X, u) + \nabla_u g(X, u)^T \lambda \\ S\Lambda e - \mu e \\ g(X, u) + s \\ XZ - \mu I \end{pmatrix} = \begin{pmatrix} 0 \\ 0 \\ 0 \\ 0 \\ 0 \end{pmatrix} \qquad \text{(14)}$$

where $S = \text{diag}(s)$, $\Lambda = \text{diag}(\lambda)$, and $e = (1, 1, \ldots, 1)^T$ is a vector of all ones of appropriate size.

It is important that symmetry is maintained during the linearization of the complementarity equation $XZ - \mu I = 0$ in order to apply Newton's method to the system in (14). This can be achieved by using the linear operator $H_P : \mathbb{R}^{n \times n} \to \mathbb{S}^n$, introduced in [36], and defined by

$$H_P(Q) := \frac{1}{2} \left(PQP^{-1} + (PQP^{-1})^T \right)$$

where $P \in \mathbb{R}^{n \times n}$ is some non-singular matrix. In [36], it is shown that

$$H_P(Q) = \mu I \Leftrightarrow Q = \mu I.$$

8

Therefore, the optimality conditions for (10) will be (14) with $XZ = \mu I$ replaced by

$$H_P(XZ) = H_P(\mu I) = \mu I. \tag{15}$$

Applying Newton's method to the system in (14) gives the search direction

$$(\Delta X, \Delta u, \Delta s, \Delta \lambda, \Delta Z) \in \mathbb{S} \times \mathbb{R}^n \times \mathbb{R}^k \times \mathbb{R}^k \times \mathbb{S}$$

as the solution of the system

$$
\begin{pmatrix}
\nabla^2_{XX}\mathcal{L}_\mu(X,u,s,\lambda) & \nabla^2_{Xu}\mathcal{L}_\mu(X,u,s,\lambda)^T & 0 & \nabla_X g(X,u)^T & -I \\
\nabla^2_{Xu}\mathcal{L}_\mu(X,u,s,\lambda) & \nabla^2_{uu}\mathcal{L}_\mu(X,u,s,\lambda) & 0 & \nabla_u g(X,u)^T & 0 \\
0 & 0 & \Lambda & S & 0 \\
\nabla_X g(X,u) & \nabla_u g(X,u) & I & 0 & 0 \\
\mathcal{E} & 0 & 0 & 0 & \mathcal{F}
\end{pmatrix}
\begin{pmatrix}
\Delta X \\ \Delta u \\ \Delta s \\ \Delta \lambda \\ \Delta Z
\end{pmatrix} =
$$
$$
- \begin{pmatrix}
\nabla_X f(X,u) - Z + \nabla_X(g(X,u)^T\lambda) \\
\nabla_u f(X,u) + \nabla_u g(X,u)^T\lambda \\
S\Lambda e - \mu e \\
g(X,u) + s \\
H_P(XZ) - \mu I
\end{pmatrix}. \tag{16}
$$

Remark 3.1. Some of the blocks in the coefficient matrix of the Newton's system (16) are tensors of order higher than two and the blocks in the right hand side and the search direction are combination of matrices and vectors. The violation of standard notation is intended to simplify the presentation. For the detailed meaning of the transposes and products, see Appendix B.

The block diagonal matrices $\mathcal{E} = \mathcal{E}(X,Z)$ and $\mathcal{F} = \mathcal{F}(X,Z)$ in (16) are the derivatives of $H_P(XZ)$ with respect to X and Z respectively and are given by

$$\mathcal{E} = P \odot P^{-T}Z \text{ and } \mathcal{F} = PX \odot P^{-1} \tag{17}$$

where the operator $P \odot Q : \mathbb{S}^n \to \mathbb{S}^n$ is defined by

$$(P \odot Q)K := \frac{1}{2}(PKQ^T + QKP^T).$$

By choosing among different matrices P in (17) we get different search directions. Directions obtained in this manner are called members of the Monteiro-Zhang (MZ) family [36]. In practice, the most used search directions are the AHO direction [2] obtained when $P = I$, the HRVW/KSH/M direction [16, 17, 21] when $P = Z^{1/2}$, the dual HRVW/KSH/M direction [17, 21] when $P = X^{-1/2}$, and the NT direction [23, 24] when $P = W^{-1/2}$ with $W = X^{1/2}(X^{1/2}ZX^{1/2})^{-1/2}X^{1/2}$. For the case of FMO problems such as (3) and (8), the matrices $\nabla^2_{XX}\mathcal{L}_\mu(X,u,s,\lambda)$,

$\mathcal{E}$ and $\mathcal{F}$ are block diagonal matrices where each block is small and relatively cheap to invert. Therefore, following the tradition in interior point methods for SDP, one can solve the reduced symmetric system

$$\begin{pmatrix} G & A \\ A^T & B \end{pmatrix} \begin{pmatrix} \Delta u \\ \Delta \lambda \end{pmatrix} = \begin{pmatrix} \tilde{r}_d \\ \tilde{r}_p \end{pmatrix} \tag{18}$$

where

$$\begin{aligned}
G =& \nabla^2_{uu} \mathcal{L}_\mu(X, u, s, \lambda) - \nabla^2_{Xu} \mathcal{L}_\mu(X, u, s, \lambda) \tilde{H}^{-1} \nabla^2_{Xu} \mathcal{L}_\mu(X, u, s, \lambda)^T \\
A =& \nabla_u g(X, u)^T - \nabla^2_{Xu} \mathcal{L}_\mu(X, u, s, \lambda) \tilde{H}^{-1} \nabla_X g(X, u)^T \\
B =& -\Lambda^{-1} S - \nabla_X g(X, u) \tilde{H}^{-1} \nabla_X g(X, u)^T,
\end{aligned}$$

and letting $(R_d, r_d, r_c, r_p, R_C)^T$ denote the right hand side of the system (16)

$$\begin{aligned}
\tilde{r}_d =& r_d - \nabla^2_{Xu} \mathcal{L}_\mu(X, u, s, \lambda) \tilde{H}^{-1} (R_d + \mathcal{F}^{-1} R_C) \\
\tilde{r}_p =& r_p - \Lambda^{-1} r_c - \nabla_X g(X, u) \tilde{H}^{-1} (R_d + \mathcal{F}^{-1} R_C)
\end{aligned}$$

with

$$\tilde{H} = \nabla^2_{XX} \mathcal{L}_\mu(X, u, s, \lambda) + \mathcal{F}^{-1} \mathcal{E}.$$

The other search directions $(\Delta X, \Delta s, \Delta Z)$ are then obtained from

$$\Delta X = \tilde{H}^{-1}(R_d + \mathcal{F}^{-1} R_C - \nabla^2_{Xu} \mathcal{L}_\mu(X, u, s, \lambda)^T \Delta u - \nabla_X g(X, u)^T \Delta \lambda) \tag{19a}$$

$$\Delta Z = \mathcal{F}^{-1}(R_C - \mathcal{E} \Delta X) \tag{19b}$$

$$\Delta s = \Lambda^{-1}(r_c - S \Delta \lambda). \tag{19c}$$

Given a current iterate (X, u, s, λ, Z) and a search direction $(\Delta X, \Delta u, \Delta s, \Delta \lambda, \Delta Z)$ the primal step length α_p and dual step length α_d are computed in two steps. First we compute the maximum possible step to the boundary of the feasible region by

$$\bar{\alpha}_p = \max\{\alpha \in (0, 1] : X + \alpha \Delta X \succeq (1 - \tau)X, s + \alpha \Delta s \geq (1 - \tau)s\} \tag{20a}$$

$$\bar{\alpha}_d = \max\{\alpha \in (0, 1] : Z + \alpha \Delta Z \succeq (1 - \tau)Z, \lambda + \alpha \Delta \lambda \geq (1 - \tau)\lambda\} \tag{20b}$$

where $\tau \in (0, 1)$ is the fraction to the boundary parameter. Next, a backtracking line search can be performed to compute the final step lengths

$$\alpha_p \in (0, \bar{\alpha}_p], \text{ and } \alpha_d \in (0, \bar{\alpha}_d]$$

to get sufficient decrease in a merit function ϕ. We use the norm of the optimality error given by

$$\begin{aligned}
\phi_\mu(X, u, s, \lambda, Z) :=& \|\nabla_X f(X, u) - Z + \nabla_X(g(X, u)^T \lambda)\|_F^2 + \|(S\Lambda - \mu I)e\|_2^2 \\
& + \|g(X, u) + s\|_2^2 + \|\nabla_u f(X, u) + \nabla_u g(X, u)^T \lambda\|_2^2 \\
& + \|H_P(XZ) - \mu I\|_F^2
\end{aligned} \tag{21}$$

as merit function. A search direction is said to sufficiently decrease the merit function if

$$\phi_\mu(X + \alpha_p \Delta X, u + \alpha_p \Delta u, s + \alpha_p \Delta_d s, \lambda + \alpha_d \Delta \lambda, Z + \alpha_d \Delta Z)$$
$$\leq (1 - \tau_0 \eta) \phi_\mu(X, u, s, \lambda, Z) \quad (22)$$

for a parameter $\eta \in (0,1)$ and for a constant $\tau_0 \in (0,1)$. The new iterate $(X^+, u^+, s^+, \lambda^+, Z^+)$ is then given by

$$(X^+, u^+, s^+) = (X, u, s) + \alpha_p(\Delta X, \Delta u, \Delta s) \quad (23a)$$
$$(\lambda^+, Z^+) = (\lambda, Z) + \alpha_d(\Delta \lambda, \Delta Z). \quad (23b)$$

The stopping criteria for the algorithm and the determination of the tolerances for the barrier problem (10) from the tolerances for the original problem (9) are motivated by [33]. Given that the optimality tolerance $\epsilon^o > 0$ and the feasibility tolerance $\epsilon^f > 0$ for the original problem (9) the interior point algorithm terminates when

$$\max \Big\{ \max_i \|\nabla_{X_i} f(X, u) - Z_i + \nabla_{X_i}(g(X, u)^T \lambda)\|_F,$$
$$\|\nabla_u f(X, u) + \nabla_u g(X, u)^T \lambda\|_\infty \Big\} \leq \epsilon^o$$
$$\max\{\max_i \|H_P(X_i Z_i)\|_F, \|S \Lambda e\|_\infty\} \leq \epsilon^o$$
$$\|g(X, u)_+\|_\infty \leq \epsilon^f \quad (24)$$

where $g_j(X, u)_+ = \max\{0, g_j(X, u)\}$. For the barrier problem (10) the tolerances are μ dependent since barrier problems with large barrier parameter are not solved to optimality. The inner iteration of the interior point method stops when

$$\max \Big\{ \max_i \|\nabla_{X_i} f(X, u) - Z_i + \nabla_{X_i}(g(X, u)^T \lambda)\|_F,$$
$$\|\nabla_u f(X, u) + \nabla_u g(X, u)^T \lambda\|_\infty \Big\} \leq \epsilon_\mu^o$$
$$\max\{\max_i \|H_P(X_i Z_i) - \mu I\|_F, \|S \Lambda e - \mu e\|_\infty \Big\} \leq \epsilon_\mu^o$$
$$\|g(X, u) + S\|_\infty \leq \epsilon_\mu^f. \quad (25)$$

In our numerical experiments we use

$$\epsilon_\mu^o = \max\{10\mu, \epsilon^o - \mu\} \quad \text{and} \quad \epsilon_\mu^f = \max\{10\mu, \epsilon^f\}. \quad (26)$$

It can be verified that determining the tolerances for the barrier problem as in (26) ensures that a point satisfying the inner stopping criteria for a small μ value also satisfies the stopping criteria for the outer iteration.

We use two strategies to update the barrier parameter μ. In the first strategy we estimate the μ value from a given (not necessarily feasible) point (X, u, s, λ, Z). By coupling results known from nonlinear programming and linear SDP, $Tr(X^T Z) + s^T \lambda$ measures the gap between the objective functions of primal and dual problems. Therefore we estimate the current μ value by

$$\mu = \sigma(\sum_i Tr(X_i^T Z_i)/d_i + s^T \lambda)/(m + k) \tag{27}$$

where $\sigma < 1$ is a prescribed centring parameter. In our numerical experiment it is observed that this update strategy gives a monotone decrease in μ for the problems we solve. The second strategy is a simple one. We initialize μ value and update it as

$$\mu^+ = \varepsilon_0 \mu, \quad \text{for } \varepsilon_0 < 1. \tag{28}$$

The over all description of the interior point method is given in Algorithm 1.

Remark 3.2. Our primary focus is to develop efficient methods for FMO problems. Since the FMO formulations in Section 2 such as (3) and (8) are all well-posed we do not include any techniques to detect infeasibility or unboundedness in the description of the primal-dual interior point method in Algorithm 1.

4 Algorithmic details for FMO problems

In this section we discuss the optimality conditions and the primal-dual systems for the interior point method specialized to the different FMO problem formulations in Section 2. The discussion in the rest of this section is for a single load case problem to simplify notations. The subscript ℓ in u_ℓ and f_ℓ is also dropped. Furthermore, we introduce the operators $\mathcal{T}_1 : \mathbb{S} \to \mathbb{R}^m$ defined by $(\mathcal{T}_1 E)_i = Tr(E_i)$ and $\mathcal{T}_2 : \mathbb{S} \to \mathbb{R}$ defined by $\mathcal{T}_2 E = \sum_i Tr(E_i)$ for every $E = (E_1, \ldots, E_m)^T \in \mathbb{S}$. The adjoints of these operators are $\mathcal{T}_1^* : \mathbb{R}^m \to \mathbb{S}$ defined by $(\mathcal{T}_1^* y)_i = y_i I$ for every $y \in \mathbb{R}^m$ and $\mathcal{T}_2^* : \mathbb{R} \to \mathbb{S}$ defined by $(\mathcal{T}_2^* \alpha)_i = \alpha I$ for every $\alpha \in \mathbb{R}$ where the identity matrix I in both cases has the same size as E_i.

Introducing the slack variables $(\bar{r}, \underline{r}, s) \in \mathbb{R}_+^m \times \mathbb{R}_+^m \times \mathbb{R}_+$ to the minimum

Algorithm 1 A primal-dual interior point algorithm for nonlinear SDP problems.

Choose $w_p^0 = (X^0, u^0, s^0)$, $w_d^0 = (\lambda, Z)$, and (μ_0 or use (27)).
Set the outer iteration counter $k \leftarrow 0$.
while stopping criteria (24) for problem (9) is not satisfied and $k < k_{max}$ **do**
  Set the inner iteration counter $i \leftarrow 0$
  while stopping criteria (25) for problem (10) is not satisfied and $i < i_{max}$
  do
    Compute the search direction $\Delta w_p^{k,i}$ and $\Delta w_d^{k,i}$ by solving system (18) and
    (19).
    Compute $\bar{\alpha}_p$ and $\bar{\alpha}_d$ as in (20).
    Set the line search iteration counter $l \leftarrow 0$.
    Set `LineSearch` $\leftarrow$ `False`
    while `LineSearch = False` and $l < l_{max}$ **do**
      $\alpha_p \leftarrow \eta^l \bar{\alpha}_p$ and $\alpha_d \leftarrow \eta^l \bar{\alpha}_d$
      if $\phi_\mu(w_p^{k,i} + \alpha_p \Delta w_d^{k,i}, w_d^{k,i} + \alpha_d \Delta w_d^{k,i}) \leq (1 - \tau_0 \eta^l)\phi_\mu(w_p^{k,i}, w_d^{k,i})$ **then**
        Set the new iterate $(w_p^{k,i+1}, w_d^{k,i+1})$ as in (23).
        `LineSearch` $\leftarrow$ `True`
      else
        $l \leftarrow l + 1$.
      end if
    end while
    $i \leftarrow i + 1$.
  end while
  Update μ_{k+1} as in (27) or (28).
  $k \leftarrow k + 1$.
end while

---

compliance problem (3), the associated barrier problem is given by

$$
\begin{aligned}
\underset{u \in \mathbb{R}^n, E \in \mathbb{E}, \bar{r}, \underline{r}, s}{\text{minimize}} \quad & f^T u - \mu \sum_{i=1}^m \ln(\det(E_i)) - \mu \sum_{i=1}^m \ln(\bar{r}_i) - \mu \sum_{i=1}^m \ln(\underline{r}_i) - \mu \ln(s) \\
\text{subject to} \quad & A(E)u - f = 0, \\
& \mathcal{T}_1 E + \bar{r} - \bar{\rho}e = 0, \\
& \rho e - \mathcal{T}_1 E + \underline{r} = 0, \\
& \mathcal{T}_2 E + s - V = 0,
\end{aligned}
\tag{29}
$$

where $\mu > 0$ is barrier parameter. The slack variables are implicitly kept strictly

positive. Then problem (29) has the following Lagrange function

$$
\begin{aligned}
\mathcal{L}(x) = & f^T u - \mu \sum_{i=1}^{m} \ln(\det(E_i)) - \mu \sum_{i=1}^{m} \ln(\bar{r}_i) - \mu \sum_{i=1}^{m} \ln(\underline{r}_i) - \mu \ln(s) \\
& + \lambda^T (A(E)u - f) + \bar{\beta}^T (\mathcal{T}_1 E + \bar{r} - \bar{\rho}e)
\end{aligned}
\tag{30}
$$

$$
+ \underline{\beta}^T (\underline{\rho}e - \mathcal{T}_1 E + \underline{r}) + \alpha(\mathcal{T}_2 E + s - V),
$$

where $x = (E, u, \bar{r}, \underline{r}, s, \lambda, \bar{\beta}, \underline{\beta}, \alpha)$ with $(\lambda, \bar{\beta}, \underline{\beta}, \alpha) \in \mathbb{R}^n \times \mathbb{R}_+^m \times \mathbb{R}_+^m \times \mathbb{R}_+$ Lagrange multipliers. With the technique in (13) the optimality conditions to problem (29) are

$$
\lambda^T F(u) - Z + \mathcal{T}_1^* \bar{\beta} - \mathcal{T}_1^* \underline{\beta} + \mathcal{T}_2^* \alpha = 0
\tag{31a}
$$

$$
A(E)\lambda + f = 0
\tag{31b}
$$

$$
A(E)u - f = 0
\tag{31c}
$$

$$
\mathcal{T}_1 E + \bar{r} - \bar{\rho}e = 0
\tag{31d}
$$

$$
\underline{\rho}e - \mathcal{T}_1 E + \underline{r} = 0
\tag{31e}
$$

$$
\mathcal{T}_2 E + s - V = 0
\tag{31f}
$$

$$
\bar{R}\bar{B} - \mu e = 0
\tag{31g}
$$

$$
\underline{R}\,\underline{B} - \mu e = 0
\tag{31h}
$$

$$
s\alpha - \mu = 0
\tag{31i}
$$

$$
H_P(E, Z) - \mu I = 0
\tag{31j}
$$

where
$$
\bar{B} = \mathrm{diag}(\bar{\beta}), \ \underline{B} = \mathrm{diag}(\underline{\beta}), \ \bar{R} = \mathrm{diag}(\bar{r}), \ \underline{R} = \mathrm{diag}(\underline{r}),
$$

and $F(u) = (A_1(E)^{j,k}u, \ldots, A_m(E)^{j,k}u)$ with $A_i(E)^{j,k} = \frac{\partial A_i(E)}{\partial (E_i)_{j,k}}$ and the multiplication $\lambda^T F(u)$ defined such that $(\lambda^T F(u))_i = \lambda^T A_i(E)^{j,k}u$ for each j and k in the set of indices of E_i. Under the assumption $E_i \succ 0$ for all i, the matrix $A(E)$ is positive definite. Therefore, the equation $A(E)\lambda + f = 0$ uniquely determines the Lagrange multiplier λ. By setting $\lambda = -u$ we get a reduced set of optimality conditions consisting of the primal residuals (31c)-(31f), the perturbed complementary conditions (31g)-(31j) and

$$
-u^T F(u) - Z + \mathcal{T}_1^* \bar{\beta} - \mathcal{T}_1^* \underline{\beta} + \mathcal{T}_2^* \alpha = 0.
\tag{32}
$$

We denote by R_d the negative of the left hand sides of (32), by $(r_{p_1}, \ldots, r_{p_4})$ the negative of the primal residuals and by $(r_{c_1}, \ldots, r_{c_3}, R_{c_4})$ the negative of perturbed complementary residuals. Applying Newton's method to the reduced

14

system and eliminating the search directions $\Delta\bar{\beta}$, $\Delta\underline{\beta}$, $\Delta\bar{r}$, $\Delta\underline{r}$, and Δs as in (36) results in the saddle point system

$$
\begin{pmatrix} -\frac{1}{2}A(E) & F(u) & 0 \\ F(u)^T & D & \mathcal{T}_2^* \\ 0 & \mathcal{T}_2 & -s/\alpha \end{pmatrix} \begin{pmatrix} \Delta\tilde{u} \\ \Delta E \\ \Delta\alpha \end{pmatrix} = \begin{pmatrix} f - A(E)u \\ R_1 \\ r_1 \end{pmatrix} \tag{33}
$$

where the block diagonal matrix D is given by

$$
D = \mathcal{F}^{-1}\mathcal{E} + \mathcal{T}_1^*(\bar{R}^{-1}\bar{B} + \underline{R}^{-1}\underline{B})\mathcal{T}_1.
$$

Note that $F(u)\Delta E = \sum_i \sum_{j,k}(A_i(E)^{j,k}u)(\Delta E_i)_{j,k}$ with j and k in the set of indices of E_i.

The residuals R_1 and r_1 are given by

$$
R_1 = R_d + \mathcal{F}^{-1}R_{c_4} - \mathcal{T}_1^*\bar{R}^{-1}(r_{c_1} - \bar{B}r_{p_2}) + \mathcal{T}_1^*\underline{R}^{-1}(r_{c_2} - \underline{B}r_{p_3}) \tag{34}
$$

$$
r_1 = r_{p_4} - \frac{1}{\alpha}r_{c_3}. \tag{35}
$$

The other search directions are then computed as

$$
\Delta u = -\Delta\tilde{u} \tag{36a}
$$

$$
\Delta Z = \mathcal{F}^{-1}(R_{c_4} - \Delta E) \tag{36b}
$$

$$
\Delta\bar{r} = r_{p_2} - \mathcal{T}_1\Delta E \tag{36c}
$$

$$
\Delta\underline{r} = r_{p_3} + \mathcal{T}_1\Delta E \tag{36d}
$$

$$
\Delta\bar{\beta} = \bar{R}^{-1}(r_{c_1} + \bar{B}(-r_{p_2} + \mathcal{T}_1\Delta E)) \tag{36e}
$$

$$
\Delta\underline{\beta} = \underline{R}^{-1}(r_{c_2} + \underline{B}(-r_{p_3} - \mathcal{T}_1\Delta E)) \tag{36f}
$$

$$
\Delta s = \frac{1}{\alpha}(r_{c_3} - s\Delta\alpha). \tag{36g}
$$

The change of variables in (36a) is introduced to make the coefficient matrix in the saddle point system (33) symmetric. Next we present the saddle point system to the nested minimum compliance problem (5). The compliance $c(E) = f^T A^{-1}(E)f$ has the completely dense Hessian

$$
\nabla^2 c(E) = 2F(u(E))^T A^{-1}(E)F(u(E)), \text{ where } u(E) = A^{-1}(E)f \tag{37}
$$

see e.g. [29]. Following a similar procedure as above, problem (5) results in the saddle point system

$$
\begin{pmatrix} 2F(u(E))^T A^{-1}(E)F(u(E)) + D & \mathcal{T}_2^* \\ \mathcal{T}_2 & -s/\alpha \end{pmatrix} \begin{pmatrix} \Delta E \\ \Delta\alpha \end{pmatrix} = \begin{pmatrix} R_1 \\ r_1 \end{pmatrix}. \tag{38}
$$

We can formulate an equivalent but sparse system to (38). We introduce a dummy variable $\Delta\tilde{u}$ such that

$$2A^{-1}(E)F(u(E))\Delta E = \Delta\tilde{u}$$

and get a larger but sparse system

$$\begin{pmatrix} -\frac{1}{2}A(E) & F(u(E)) & 0 \\ F(u(E))^T & D & \mathcal{T}_2^* \\ 0 & \mathcal{T}_2 & -s/\alpha \end{pmatrix} \begin{pmatrix} \Delta\tilde{u} \\ \Delta E \\ \Delta\alpha \end{pmatrix} = \begin{pmatrix} 0 \\ R_1 \\ r_1 \end{pmatrix}. \tag{39}$$

In FMO problems the systems (38) and (33) are large-scale due to the large size of the design variable E and the number of degrees of freedom. Since each block matrices in the block diagonal matrix D is also relatively small and cheap to invert we further eliminate ΔE from the systems and solve a smaller system with coefficient matrix

$$\begin{pmatrix} -\frac{1}{2}A(E) - F(u)D^{-1}F(u)^T & -F(u)D^{-1}\mathcal{T}_2^* \\ -\mathcal{T}_2 D^{-1}F(u)^T & -s/\alpha - \mathcal{T}_2 D^{-1}\mathcal{T}_2^* \end{pmatrix} \tag{40}$$

in the variables $(\Delta\tilde{u}, \Delta\alpha)$ and with updated right hand side. Our numerical experiments show that for larger problems it is even more efficient to eliminate again $\Delta\alpha$ from (40) and solve the system with coefficient matrix

$$-\frac{1}{2}A(E) - F(u)D^{-1}F(u)^T - F(u)D^{-1}\mathcal{T}_2^*(-s/\alpha - \mathcal{T}_2 D^{-1}\mathcal{T}_2^*)^{-1}(\mathcal{T}_2 D^{-1}F(u)^T) \tag{41}$$

in $\Delta\tilde{u}$ and then use the Sherman-Morrison formula [14] in which we only factorize the sparse matrix

$$-\frac{1}{2}A(E) - F(u)D^{-1}F(u)^T. \tag{42}$$

Remark 4.1. The reduction of the system by setting λ to some scalar multiple of u is limited to the classical FMO problems considered in this article. This reduction may not be possible if other problem formulations are considered, for example, problems that include local stress constraints, see [19].

Remark 4.2. The difference in sparsity pattern of the matrices $A(E)$ and $F(u)D^{-1}F(u)^T$ is more visible for multiple load problems with the second matrix being much more dense than the first matrix.

Remark 4.3. For problems (4), (6), and (8) similar saddle point systems to either (33) or (39) in size and structure can be formulated.

Remark 4.4. For the minimum weight problem in the simultaneous analysis and design approach (4) we set $\lambda = -\alpha u$, where λ and α are Lagrange multipliers, to the elastic equilibrium equation $A(E)u - f = 0$ and to $f^T u + s - \gamma = 0$ respectively to get reduced optimality conditions.

Remark 4.5. Since the matrix variables (E, Z) and hence the search directions $(\Delta E, \Delta Z)$ are symmetric, the computations are performed with the entries only in the lower triangular parts of these matrices.

5 Implementation, algorithmic parameters, and problem data

The interior point method and the finite element routines are implemented entirely in MATLAB Version 7.7 (R2008b). All numerical experiments are run on Intel Xeon X5650 six-core CPUs running at 2.66 GHz with 4GB of memory per core (only a single core is used per problem). The finite elements used are standard four node bilinear elements obtained by full Gaussian integration, see e.g. [9].

The saddle point systems (40) and (42) and the elastic equilibrium equation in the case of the nested problem formulations (5) and (6) are solved using the LU factorization routines which are built into MATLAB. As described in Section 3 different choices of the matrix P in (17) result in different search directions. Table 1 shows how the block diagonal matrices $\mathcal{E}$, $\mathcal{F}$, and the right hand side R_{c_4} of the linearised equation of the complementarity equation (31j) for the AHO, the HRVW/KSV/M and the NT directions are computed. Computation of the NT direction follows from [31]. The matrix G in Table 1 is determined by first performing a Cholesky factorization on E and Z, namely,

$$E = LL^T \text{ and } Z = RR^T$$

and then singular value decomposition on $R^T L$, say $UDV^T = R^T L$. Then we have

$$G = LVD^{-1/2}.$$

Table 1: Computation of $\mathcal{E}$, $\mathcal{F}$ and the right hand side R_{c_4}.

	AHO ($P = I$)	HRVW/KSV/M ($P = Z^{1/2}$) and pre- and post-multiplying by $Z^{-1/2}$	NT ($P = W^{-1/2}$ $= G^{-1}$)
$\mathcal{E}$	$I \odot Z$	$I \odot I$	$G^{-1} \odot G^T Z$
$\mathcal{F}$	$E \odot I$	$E \odot Z^{-1}$	$G^{-1} E \odot G^T$
R_{c_4}	$\sigma\mu I - \frac{1}{2}(EZ + ZE)$	$\sigma\mu Z^{-1} - E$	$\sigma\mu - D^2$

The optimality tolerance is set to $\epsilon^o = 10^{-7}$ while the feasibility tolerance is $\epsilon^f = 10^{-8}$ for all problems. The optimality and feasibility tolerances for the

17

barrier problems are computed as in (26). We say that the current iterate is a solution if it satisfies the stopping criteria for the inner and outer iterations as outlined in (25) and (24). The minimum barrier parameter value $\mu_{\min}$ is set to 10^{-9}. The boundary to the fraction parameter τ is set to 0.9. The parameters used in the backtracking line search are set as $\eta = 0.5$ and $\tau_0 = 10^{-5}$, respectively. For all problems we observe that the algorithm converges without performing any line search. This could be because the treated problems are either convex or can be equivalently written as a convex problem. For this reason the line search part of the algorithm was not activated in the numerical experiments. Both barrier update strategies given in (27) and (28) are implemented. In the numerical experiments we use (27) with $\sigma = 0.4$ since the μ values in this case are proportional to the duality gap.

The primal design variables are initially set to $E_i = 0.1\bar{\rho}I$ for all i, while the primal displacement variables are set to zero, i.e. $u_\ell = 0$ for all ℓ. All slack variables are all set to ones and that Lagrange multipliers for equality constraints are set to zero. Lagrange multipliers for scalar (or matrix) inequalities are otherwise set to ones (or identity matrices). When solving minimum compliance problems the total weight fraction is set to 33.3% of the maximum weight, i.e. $V = (m/3)\bar{\rho}$. When solving the minimum weight problems the bound on the compliance is set to 25% of the compliance evaluated at the initial point. The local bounds on the $Tr(E_i)$ are scaled in such away that $\bar{\rho}/\underline{\rho} = 10^4$.

6 Numerical experiments

The numerical experiments have three objectives. The first goal is to compare the performance of the interior point method when applied to the different FMO formulations presented in Section 2 and determine the best choice of formulation. The second goal is to investigate the numerical behaviour of the AHO, the HRVW/KSV/M, and the NT search directions and give recommendations. We use performance profiles as introduced in [10] to evaluate the numerical performances. The number of iterations and CPU time of the method required to obtain a solution are used as measures of the performances. The third goal is to show the efficiency of the method. This is achieved first by reporting solutions to a set of large-scale FMO problems. Second, by solving benchmark problems and making comparison to the recent numerical results presented in [29]. The results in [29] are obtained using a state-of-the-art special purpose method for FMO problems.

Throughout the article we use the colour bar in Figure 1 to show the optimal density distribution, that is, the trace of the stiffness tensor of the optimal designs.

$\underline{\rho}$ $\bar{\rho}$

Figure 1: Colour bar for the optimal density distribution.

6.1   Performance

We consider a set of FMO problem instances over 2D design domains to compare the performance of the formulations and search directions. Four two-dimensional benchmark problems from [37], [7], and [19] are considered. The design domains, boundary conditions, and loads for these problems are shown in Figure 2. The first one is a single load Cantilever beam problem with design domain dimensions 2×1. The second problem is a single load Michell beam problem with design domain dimensions 2×1. In the third problem we consider an L-shaped design domain with dimension 1×1 with a quarter square removed from one corner. The last benchmark is a two load problem with a rectangular design domain of dimension 2×1. In all cases we apply a load over a segment of length 0.04. For each design domain there are four level of finite element discretizations with the finer mesh obtained from the coarser by refining each element into four elements. Details of the problem instances are given in Table 2.

6.1.1   Performance of the formulations

Considering the minimum compliance problem we solve the three formulations, namely, the simultaneous analysis and design approach (3), the dual formulation (8), and the nested approach (5) for all problem instances in Table 2. It is shown in Figure 5 that the performance profiles are similar. The identical profiles of the dual and SAND formulations in Figure 5a is the result of the similarity (up to a scaling) of the optimality conditions (once λ is eliminated from the optimality condition of the SAND formulation to get (32)). While solving the nested formulation the additional computational effort of solving the elastic equilibrium equations as in the second part of (37) at each interior point iteration is almost not visible in the performance profiles. It is slightly more noticeable for the multiple load case problems. For example, for solving the minimum weight problem on the "Two Loads Case IV" in Table 2, the average CPU time spent on one interior point iteration was 453 seconds for solving the problem of SAND formulation and 465 seconds for the problem of nest formulation. We expect higher computational efforts if we solve much larger problems or problems over 3D design domains. For the minimum weight problem we solve the simultaneous

19
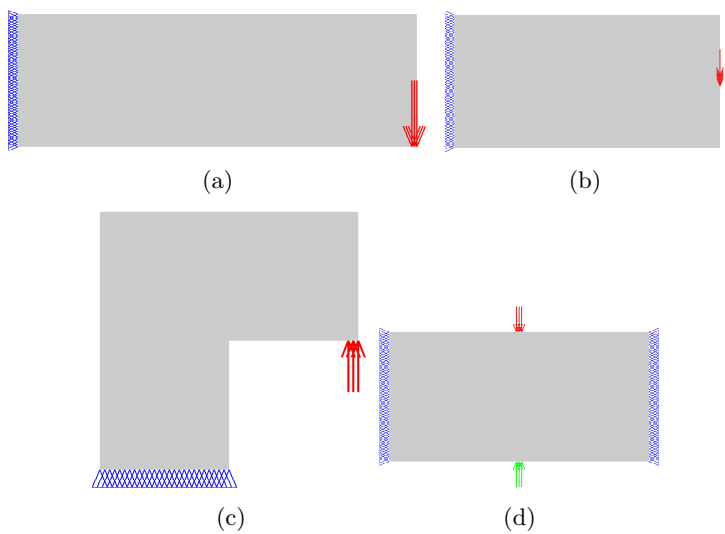
Figure 2: Design domains, boundary conditions, and external loads for the Cantilever benchmark problem (a), the Michell beam problem (b), the L-shape problem (c), and the two load case problem (d).

(a)   (b)

(c)   (d)
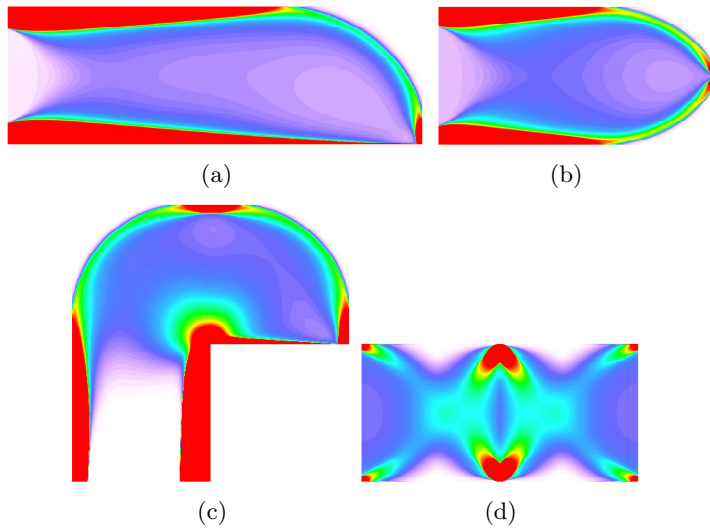
Figure 3: Optimal density distribution obtained by solving the minimum compliance problem (3) for the Cantilever IV benchmark problem (a), the Michell IV beam problem (b), the L-shape IV problem (c), and the two load case IV problem (d).

(a)   (b)
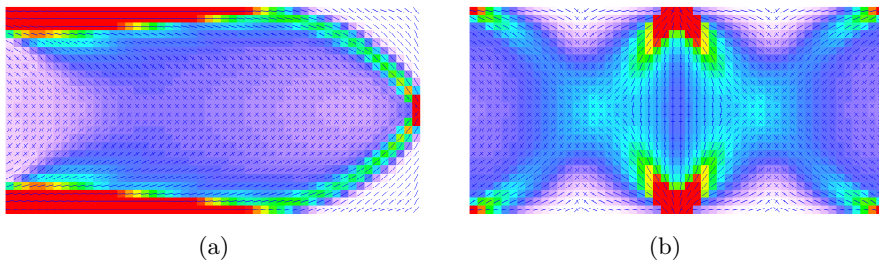
Figure 4: Principal material directions for the optimal designs for the Michell beam problem (a), and the two load case problem (b).

Table 2: Problem instances.

Problems	No. of finite elements	No. of design variables	No. of non-fixed state variables
Cantilever I	7500	45000	15300
Cantilever II	30000	180000	60600
Cantilever III	120000	720000	241200
Cantilever IV	480000	2880000	962400
Michell I	5000	30000	10200
Michell II	20000	120000	40400
Michell III	80000	480000	160800
Michell IV	320000	1920000	641600
L-shape I	1875	11250	3900
L-shape II	7500	45000	15300
L-shape III	30000	180000	60600
L-shape IV	120000	720000	241200
Two Loads case I	5000	30000	10098
Two Loads case II	20000	120000	40198
Two Loads case III	80000	480000	160398
Two Loads case IV	320000	1920000	640798

analysis and design problem (4) and the nested formulation (6) for all problem instances in Table 2. Figure 6 suggests similar results as to the minimum weight problems.

6.1.2 Performance of the search directions

We compare the numerical performance of the AHO, the HRVW/KSV/M, and the NT search directions. We solve the problem formulation in (3) for all problem instances in Table 2 using all search directions. Figure 7a shows that the number of iterations is fewer when using the AHO and NT directions compared to the HRVW/KSV/M direction. In our numerical experiments we generally get larger optimality error in each first inner iteration for HRVW/KSV/M direction than for the other two directions. As a result the method requires more inner iterations per outer iteration when the HRVW/KSV/M direction is used. It seems that this issue can be resolved by choosing a more aggressive barrier update strategy, for example, as in (28) with $\varepsilon_0 = 0.1$. However, this results in numerical instabilities for some of the problems as the iterates are close to the optimal solution. We also experience that the AHO direction is more sensitive than the NT direction to changes in algorithmic parameters and barrier update strategies. The plot in Figure 7b suggests that the CPU time for using the NT direction is in between the
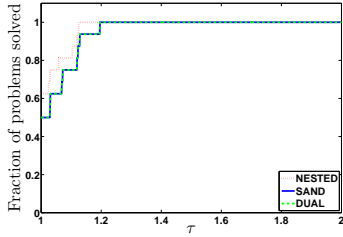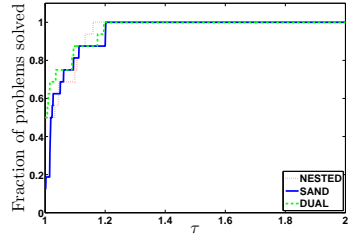
Figure 5: Performance profiles for the formulations of the minimum compliance problem. Number of iterations as performance measure (a), CPU time as performance measure (b).
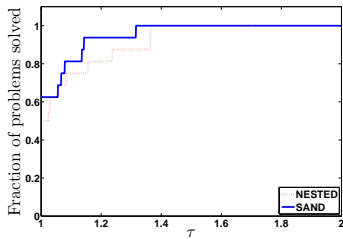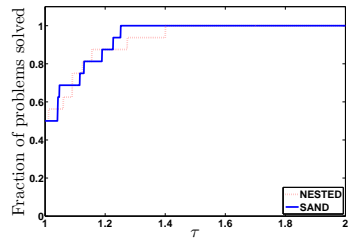
Figure 6: Performance profiles for the formulations of the minimum weight problem. Number of iterations as performance measure (a), CPU time as performance measure (b).
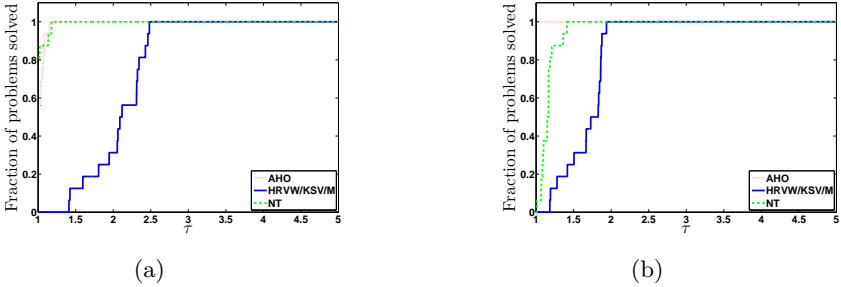
Figure 7: Performance profiles for the search directions. Number of iterations as performance measure (a), CPU time as performance measure (b).

AHO and the HRVW/KSV/M directions. This is because we perform Cholesky factorizations of each E_i and Z_i for $i = 1, \ldots, m$ and the additionally the Singular Value Decompositions of a matrix computed from the Cholesky factorizations.

The plots for the optimal density distribution of each design domain is given in Figure 3. The principal material directions of optimal designs for the Michell beam and the two load case problems are shown in Figure 4. The directions are computed based on the principal eigenvectors associated to the Voigt-stiffness tensor. The numerical result for solving problem (3) for each problem instances in Table 2 is given in Table 3.

6.2 Efficiency compared to alternative methods

The problems listed in Table 3 are, by far, the largest FMO problems reported to date. The proposed primal-dual interior point method requires a modest number of iterations. All problem instances reported in Table 3 are solved within 25-55 iterations. Table 3 illustrates that there is a mild increase in number of iterations with increasing problem size. We also notice that when solving the largest problems the memory requirements and the computational expense of the method are largely dominated by the solution of the saddle point system (42) and additionally of the elastic equilibrium equation for the nested formulations.

We also make comparisons with the FMO results presented in [29]. The problems in [29] are solved by the code PENSCP. At present the comparison is limited only to problems considered in this article. The comparison is indeed merely in a sense that we solve a multiple load case of problem formulation (5) while in [29] an alternative worst-case multiple problem is solved. Moreover, the loading and the size of fixed boundary regions could differ up to scaling. Comparison on CPU time also have discrepancy for the fact that the programming languages

Table 3: Numerical results for the problem instances in Table 2 and the minimum compliance problem (3).

Problems	No. of iterations	CPU time (s)	Compliance
Cantilever I	34	213	5.0816
Cantilever II	44	1128	5.0802
Cantilever III	40	4257	5.0826
Cantilever IV	40	17713	5.0925
Michell I	34	142	1.8331
Michell II	48	819	1.8349
Michell III	55	3809	1.8362
Michell IV	49	13787	1.8391
L-shape I	29	47	2.1780
L-shape II	35	215	2.1814
L-shape III	35	896	2.1845
L-shape IV	34	3518	2.1885
Two Loads case I	25	134	0.4220
Two Loads case II	28	622	0.4253
Two Loads case III	30	2941	0.4263
Two Loads case IV	31	14441	0.4272

and the machines used to perform numerical experiments are different. However, the reported results are still interesting since the efficiency both in CPU time and number of iterations required to get even a higher quality solution is significant. The design domain, boundary conditions, and loads are depicted in Figure 8. In Table 4 we report the numerical results for a four load case with three different discretizations. In the first column we list the number of finite elements, in the second column the number of iterations, in the third column the achieved optimality and feasibility tolerances, and in the fourth column the CPU time. In the fifth and sixth columns we include the number of iterations and the CPU time from [29] required by Penscp to solve the problem. Note that the CPU times reported include the entire computation process, i.e, starting from mesh and finite element generations to the end of the optimization process. When we compare the obtained results to the results in Table 7.1 in [29], we notice that the efficiency of the proposed interior point method both in time and number of iteration. The solutions obtained with the interior point method are also more accurate. In [29] one of the stopping criteria used is a measure of the optimality error that is set to lower tolerance than used in our numerical experiment. We also solve another problem with 5000 elements for three different load cases. The numerical result is presented in Table 5. In this table the first column contains the load cases and the other columns are similar to those of Table 4. This table
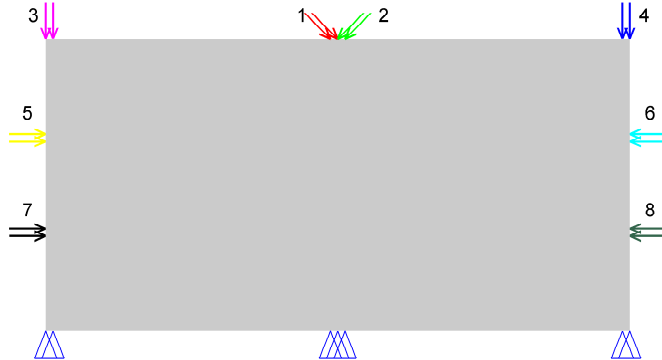
Figure 8: Design domain, boundary conditions, and external loads for the problem instances listed in Tables 4 and 5.

also shows the efficiency of the interior point method and accuracy of solutions when we compare to the results in Table 7.2 in [29].

We are also able to obtain a solution for 80000 finite elements and 8 load cases within 36 iterations and 81420 seconds. The optimal design is shown in Figure 9b.

Table 4: Numerical results for solving problem (5) with 4 load case. The two last columns in the table are from [29].

FEs	iter	opt/feas	CPU time (s)	iter PENSCP	CPU time (s), PENSCP
1250	26	0.0000e+00/6.7531e-08	56	622	256
5000	27	0.0000e+00/6.0402e-08	254	482	1027
20000	29	0.0000e+00/5.3046e-08	1298	522	7878

7   Conclusions

We propose an efficient primal-dual interior point method for several classical formulations of FMO. The number of iterations the method requires is appealing and increases only slowly with increases in problem size. With the interior point method we solve, by far, the largest FMO problem reported to date. The

(a)   (b)
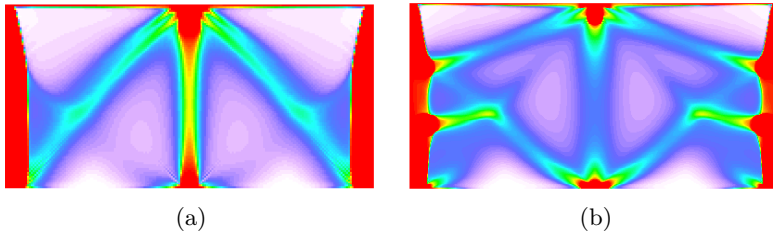
Figure 9: Optimal density distribution for the multiple load problem in Figure 8. Problem with 20000 finite elements and 4 load cases as described in Tables 4 and 5 (a), problem with 80000 finite elements and 8 load cases (b).

Table 5: Numerical results for solving problem (5). The design domain is partitioned into 5000 finite elements. The two last columns in the table are from [29].

Lc	iter	opt/feas	CPU time (s)	iter PENSCP	CPU time (s) PENSCP
2	31	0.0000e+00/1.2200e-08	166	543	585
4	27	0.0000e+00/6.0402e-08	245	489	1027
8	28	0.0000e+00/2.7303e-08	738	370	1319

obtained accuracy of the computed optimal solutions is higher compared to solutions obtained by other methods developed for FMO. For large-scale problems the memory requirements and the computation time of the method are dominated by the direct solution of the saddle point systems for computing the search direction. Future research will be directed towards developments of efficient preconditioner for iterative methods for the saddle-point systems with the aim to solve very large-scale 3D problems.

The number of iterations of the method is similar when solving either of the simultaneous analysis and design or the nested problem formulations. For solving the nested problem formulation the additional expected computational effort of solving the elastic equilibrium equations at each interior point iteration is almost not visible for the problems sizes considered. However, the differences that can be seen when solving multiple load problems could indicate higher computational efforts if we solve much larger problems or problems over 3D design domains. The dual formulation (8) also works well. However, there are no dual reformulations like (8) if other constraints, such as stress constraints, are included in the problem

formulations.

Our numerical experiments indicate that the NT and AHO directions are more efficient than the HRVW/KSV/M direction as they require fewer inner iterations per outer iteration. Comparing the AHO and NT directions we experience that the NT directions are less sensitive to changes in algorithmic parameters and speed of updating the barrier parameter. Therefore, the NT direction is our preferred choice.

The results in this article are exclusively supported by numerical experiments. Theoretical treatment of convergence theory of the interior point method must be further analysed. The applicability of relevant available theories in the literature should be investigated and potentially applied to show global convergence.

8   Acknowledgements

References

[1] Achtziger, W., Bendsøe, M., Ben-Tal, A., Zowe, J.: Equivalent displacement based formulations for maximum strength truss topology design. Impact of Computing in Science and Engineering **4**, 315–345 (1992)

[2] Alizadeh, F., Haeberly, J., Overton, M.: Primal-dual interior-point methods for semidefinite programming: convergence rates, stability and numerical results. SIAM Journal on Optimization **8**(3), 746–768 (2009)

[3] Ben-Tal, A., Kočvara, M., Nemirovski, A., Zowe, J.: Free material design via semidefinite programming: The multiload case with contact conditions. SIAM Journal on Optimization **9**(4), 813–832 (1999)

[4] Ben-Tal, A., Nemirovski, A.: Robust truss topology design via semidefinite programming. SIAM Journal on Optimization **7**(4), 991–1016 (1997)

[5] Ben-Tal, A., Nemirovski, A.: Handbook of semidefinite programming, chap. Structural Design, pp. 443–467. Kluwer Academic Publishers (2000)

[6] Bendsøe, M., Díaz, A.: Optimization of material properties for Mindlin plate design. Structural Optimization **6**, 268–270 (1993)

[7] Bendsøe, M., Guedes, J., Haber, R., Pedersen, P., Taylor, J.: An analytical model to predict optimal material properties in the context of optimal structural design. Journal of Applied Mechanics **61**, 930–937 (1994)

[8] Benson, H., Shanno, D.: Interior-point methods for nonconvex nonlinear programming: regularization and warmstarts. Computational Optimization and Applications **40**, 143–189 (2008)

[9] Cook, R., Malkus, D., Plesha, M., Witt, R.: Concepts and Applications of Finite Element Analysis, 4th edn. John Wiley and Sons (2002)

[10] Dolan, E., Moré, J.: Benchmarking optimization software with performance profiles. Mathematical Programming **97**(A), 201–213 (2002)

[11] Forsgren, A., Gill, P.: Primal-dual interior methods for nonconvex nonlinear programming. SIAM Journal on Optimization **8**(4), 1132–1152 (1998)

[12] Forsgren, A., Gill, P., Wright, M.: Interior methods for nonlinear optimization. SIAM Review **44**(4), 525–597 (2002)

[13] Gaile, S.: Free material optimization for shells and plates. Ph.D. thesis, Institute of Applied Mathematics II, Friedrich-Alexander University of Erlangen-Nuremberg (2011)

[14] Golub, G., van Loan, C.: Matrix Computations, 3rd edn. Johns Hopkins University Press (1996)

[15] Haslinger, J., Kočvara, M., Leugering, G., Stingl, M.: Multidisciplinary free material optimization. SIAM Journal on Applied Mathematics **70**(7), 2709–2728 (2010)

[16] Helmberg, C., Rendl, F., Vanderbei, R., Wolkowicz, H.: An interior-point method for semidefinite programming. SIAM Journal on Optimization **6**, 342–361 (1996)

[17] Kojima, M., Shindoh, S., Hara, S.: Interior-point methods for the monotone semidefinite linear complementarity problem in symmetric matrices. SIAM Journal on Optimization **7**(1), 86–125 (1997)

[18] Kočvara, M., Stingl, M.: PENNON A code for convex nonlinear and semidefinite programming. Optimization Methods and Software **18**(3), 317–333 (2003)

[19] Kočvara, M., Stingl, M.: Free material optimization for stress constraints. Structural and Multidisciplinary Optimization **33**, 323–335 (2007)

[20] Kočvara, M., Stingl, M., Zowe, J.: Free material optimization: recent progress. Optimization **57**(1), 79–100 (2008)

[21] Monteiro, R.: Primal-dual path-following algorithms for semidefinite programming. SIAM Journal on Optimization **7**(3), 663–678 (1997)

[22] Monteiro, R.: First- and second-order methods for semidefinite programming. Mathematical Programming **97**, 209–244 (2003)

[23] Nesterov, Y., Todd, M.: Self-scaled barriers and interior-point methods for convex programming. Mathematics of Operations Research **22**(1), 1–42 (1997)

[24] Nesterov, Y., Todd, M.: Primal-dual interior-point methods for self-scaled cones. SIAM Journal on Optimization **8**(2), 324–364 (1998)

[25] Ringertz, U.: On finding the optimal distribution of material properties. Structural Optimization **5**, 265–267 (1993)

[26] Stingl, M.: On the solution of nonlinear semidefinite programs by augmented Lagrangian method. Ph.D. thesis, Institute of Applied Mathematics II, Friedrich-Alexander University of Erlangen-Nuremberg (2006)

[27] Stingl, M., Kočvara, M., Leugering, G.: Free material optimization with fundamental eigenfrequency constraints. SIAM Journal on Optimization **20**(1), 524–547 (2009)

[28] Stingl, M., Kočvara, M., Leugering, G.: A new non-linear semidefinite programming algorithm with an application to multidisciplinary free material optimization. International Series of Numerical Mathematics **158**, 275–295 (2009)

[29] Stingl, M., Kočvara, M., Leugering, G.: A sequential convex semidefinite programming algorithm with an application to multiple-load free material optimization. SIAM Journal on Optimization **20**(1), 130–155 (2009)

[30] Todd, M.: A study of search directions in primal-dual interior-point methods for semidefinite programming. Optmization Methods and Software **11**, 1–46 (1999)

[31] Todd, Y., Toh, K., Tütüncü, R.: On the Nesterov-Todd direction in semidefinite programming. SIAM Journal on Optimization **8**(3), 769–796 (1998)

[32] Vogelbusch, C.H.: Numerical treatment of nonlinear semidefinite pro-
grams. Ph.D. thesis, Institut für Mathematik der Heinrich-Heine-Universität
Düsseldorf (2006)

[33] Waltz, R., Morales, J., Nocedal, J., Orban, D.: An interior algorithm for
nonlinear optimization that combines line search and trust region steps.
Mathematical Programming **107**, 391–408 (2006)

[34] Werner, R.: Free material optimization-mathematical analysis and numer-
ical solution. Ph.D. thesis, Institute of Applied Mathematics II, Friedrich-
Alexander University of Erlangen-Nuremberg (2001)

[35] Yamashita, H., Yabe, H., Harada, K.: A primal-dual interior point method
for nonlinear semidefinite programming. Mathematical Programming **135**,
89–121 (2012)

[36] Zhang, Y.: On extending some primal-dual interior-point algorithms from
linear programming to semidefinite programming. SIAM Journal on Opti-
mization **8**(2), 365–386 (1998)

[37] Zowe, J., Kočvara, M., Bendsøe, M.: Free material optimization via mathe-
matical programming. Mathematical Programming **79**, 445–466 (1997)

Appendix A

In this Appendix we derive the dual formulation (8) of the minimum weighted
compliance problem (3). Similar result for minimax problems can be found in
[3]. Analogous all-quadratic formulations of minimum compliance truss topology
optimization problems are described, for example, in [1]. The linear elasticity
static structural analysis problem can be written as

$$\sup_{u_\ell} \left\{ 2f_\ell^T u_\ell - u_\ell^T A(E) u_\ell \right\}$$

which is a quadratic problem with negative definite Hessian and hence a concave
maximization problem. The optimality condition is $A(E)u_\ell = f_\ell$ and the optimal
value is $f_\ell^T u_\ell$ if $f_\ell \in \mathcal{R}(A(E))$ and $-\infty$ otherwise. Due to the stated assumptions
we replace the sup with max in the following. Therefore, the minimum compliance

problem (3) is equivalent to

$$
\begin{aligned}
&\underset{E_1,\dots,E_m \succeq 0}{\text{minimize}} && \sum_{\ell \in L} w_\ell \max_{u_\ell} \left\{ 2 f_\ell^T u_\ell - u_\ell^T A(E) u_\ell \right\} \\
&\text{subject to} && \underline{\rho} \leq Tr(E_i) \leq \bar{\rho}\,,\, i = 1,\dots,m, \\
& && \sum_{i=1}^m Tr(E_i) \leq \bar{V}.
\end{aligned} \tag{43}
$$

The Lagrangian $\mathcal{L}$ associated with (43) is

$$
\begin{aligned}
\mathcal{L}(E, u_\ell, \alpha, \bar{\beta}, \underline{\beta}) &= \sum_{\ell \in L} w_\ell \max_{u_\ell} \left\{ 2 f_\ell^T u_\ell - u_\ell^T A(E) u_\ell \right\} + \sum_{i=1}^m \underline{\beta}_i (-Tr(E_i) + \underline{\rho}) \\
&\quad + \sum_{i=1}^m \bar{\beta}_i (Tr(E_i) - \bar{\rho}) + \alpha \big(\sum_{i=1}^m Tr(E_i) - \bar{V} \big) \\
&= \max_{u_1,\dots,u_{n_L}} \sum_{\ell \in L} w_\ell (2 f_\ell^T u_\ell - u_\ell^T A(E) u_\ell) + \sum_{i=1}^m \underline{\beta}_i (-Tr(E_i) + \underline{\rho}) \\
&\quad + \sum_{i=1}^m \bar{\beta}_i (Tr(E_i) - \bar{\rho}) + \alpha \big(\sum_{i=1}^m Tr(E_i) - \bar{V} \big) \\
&= \max_{u_1,\dots,u_{n_L}} \big(\sum_{\ell \in L} w_\ell (2 f_\ell^T u_\ell - u_\ell^T A(E) u_\ell) + \sum_{i=1}^m \underline{\beta}_i (-Tr(E_i) + \underline{\rho}) \\
&\quad + \sum_{i=1}^m \bar{\beta}_i (Tr(E_i) - \bar{\rho}) + \alpha \big(\sum_{i=1}^m Tr(E_i) - \bar{V} \big) \big) \\
&= \max_{u_1,\dots,u_{n_L}} \big(\sum_{\ell \in L} 2 w_\ell f_\ell^T u_\ell - \alpha \bar{V} + \underline{\rho} \sum_{i=1}^m \underline{\beta}_i - \bar{\rho} \sum_{i=1}^m \bar{\beta}_i \\
&\quad + \sum_{i=1}^m \left\langle E_i, (\alpha - \underline{\beta}_i + \bar{\beta}_i) I - \sum_{\ell \in L} \sum_{k=1}^{n_G} w_\ell B_{i,k}^T u_\ell u_\ell^T B_{i,k} \right\rangle \big).
\end{aligned}
$$

32

The corresponding dual function is

$$g(u_1, \ldots, u_{n_L}, \bar{\beta}, \underline{\beta}, \alpha)$$

$$= \underset{E_1,\ldots,E_m \succeq 0}{\text{minimize}} \; \underset{u_1,\ldots,u_{n_L}}{\max} \; \Big(\sum_{\ell \in L} 2w_\ell f_\ell^T u_\ell - \alpha \bar{V} + \rho \sum_{i=1}^m \underline{\beta}_i - \bar{\rho} \sum_{i=1}^m \bar{\beta}_i$$

$$+ \sum_{i=1}^m \Big\langle E_i, (\alpha - \underline{\beta}_i + \bar{\beta}_i)I - \sum_{\ell \in L}\sum_{k=1}^{n_G} w_\ell B_{i,k}^T u_\ell u_\ell^T B_{i,k} \Big\rangle \Big)$$

$$= \begin{cases} \underset{u_1,\ldots,u_{n_L}}{\max} \; (\sum_{\ell \in L} 2w_\ell f_\ell^T u_\ell - \alpha \bar{V} + \rho \sum_{i=1}^m \underline{\beta}_i - \bar{\rho}\sum_{i=1}^m \bar{\beta}_i) & \text{if (44) holds} \\ -\infty & \text{otherwise.} \end{cases}$$

Below is the condition that the dual function g attains its minimum value.

$$\sum_{\ell \in L}\sum_{k=1}^{n_G} w_\ell B_{i,k}^T u_\ell u_\ell^T B_{i,k} \preceq (\alpha - \underline{\beta}_i + \bar{\beta}_i)I, \; i = 1, \ldots, m. \qquad (44)$$

The dual formulation of the minimum compliance problem (3) becomes

$$\underset{u_1,\ldots,u_{n_L},\alpha\geq 0,\bar{\beta}\geq 0,\underline{\beta}\geq 0}{\sup} \quad -\alpha\bar{V} + 2\sum_{\ell \in L} w_\ell f_\ell^T u_\ell + \rho\sum_{i=1}^m \underline{\beta}_i - \bar{\rho}\sum_{i=1}^m \bar{\beta}_i$$

$$\text{subject to} \qquad \sum_{\ell \in L}\sum_{k=1}^{n_G} w_\ell B_{i,k}^T u_\ell u_\ell^T B_{i,k} - (\alpha - \underline{\beta}_i + \bar{\beta}_i)I \preceq 0, \, i = 1, \ldots, m.$$

Appendix B

The following products are in tensor notation.

1. $(\nabla^2_{X_r X_s}\mathcal{L}_\mu(X, u, s, \lambda)\Delta X_s)_{ij} = (\nabla^2_{X_r X_s}\mathcal{L}_\mu(X, u, s, \lambda))_{ijpq}(\Delta X_s)_{pq}$, for $r, s = 1, .., m$, for $i, j = 1, ..., d_r$, and for $p, q = 1, ..., d_s$.

2. $(\nabla^2_{X_r u}\mathcal{L}_\mu(X, u, s, \lambda)\Delta X_r)_i = (\nabla^2_{uX_r}\mathcal{L}_\mu(X, u, s, \lambda))_{ipq}(\Delta X_r)_{pq}$, for $r = 1, .., m$, for $p, q = 1, ..., d_r$, and for $i = 1, ..., n$.

3. $(\nabla^2_{X_r u}\mathcal{L}_\mu(X, u, s, \lambda)^T\Delta u)_{ij} = (\nabla^2_{X_r u}\mathcal{L}_\mu(X, u, s, \lambda))_{ijp}(\Delta u)_p$, for $r = 1, .., m$, for $i, j = 1, ..., d_r$, and for $p = 1, ..., n$.

4. $(\nabla_{X_r}g(X, u)^T\Delta\lambda)_{ij} = (\nabla_{X_r}(g(X, u)^T\Delta\lambda))_{ij}$, for $r = 1, .., m$, and for $i, j = 1, ..., d_r$.

5. $(\nabla_{X_r}g(X, u)\Delta X_r)_i = (\nabla_{X_r}g_i(X, u))_{pq}(\Delta X_r)_{pq}$, for $r = 1, .., m$, for $p, q = 1, ..., d_r$, and for $i = 1, ..., k$.

Chapter 6

Free Material Optimization for Laminated Plates and Shells

Free Material Optimization for Laminated Plates and Shells

Alemseged Gebrehiwot Weldeyesus* and Mathias Stolpe†

Abstract

Free Material Optimization (FMO) is a powerful approach for conceptual optimal design of composite structures. The design variable in FMO is the entire elastic material tensor which is allowed to vary almost freely over the design domain. The imposed requirements on the tensor are that it is symmetric and positive semidefinite. Most of today's studies on FMO focus on models for two- and three-dimensional structures. The objective of this article is to extend existing FMO models and methods to laminated plate and shell structures, which are used in many engineering applications. In FMO, the resulting optimization problem is generally a non convex semidefinite program with many small matrix inequalities which requires special-purpose optimization methods. The FMO problems are efficiently solved by a primal-dual interior point method developed and implemented by the authors. The quality of the proposed FMO models and the method are supported by several large-scale numerical experiments.

Mathematics Subject Classification 2010: 90C22, 90C90, 74P05, 74P15

Keywords: Structural optimization, free material optimization, nonlinear semidefinite optimization, laminated shells

*DTU Wind Energy, Technical University of Denmark, Frederiksborgvej 399, 4000 Roskilde, Denmark. E-mail: alwel@dtu.dk

†DTU Wind Energy, Technical University of Denmark, Frederiksborgvej 399, 4000 Roskilde, Denmark. E-mail: matst@dtu.dk

1 Introduction

In Free Material Optimization (FMO) the design parametrization allows complete control over the entire material tensor. It is allowed vary freely at each point of the design domain with the only requirement that it has to satisfy mild necessary conditions for physical attainability. Therefore, in optimal structures obtained by FMO both the distribution of the amount of material and the optimal local material properties are determined.

The basic concept of FMO was introduced in the early 1990s in [3], [4], and [22]. Since then, several studies led to the development of models, theories, and numerical methods for FMO problems. In the recently proposed FMO problems several types of constraints have been introduced. For example in [15], [14], and [10] problems with constraints on local stresses and displacements and in [26] problems with constraints on fundamental eigenfrequencies are presented and solved. Some of the studies not only emphasize on extending the formulations to multidisciplinary problems but also on development of new optimization methods. The methods include a method based on penalty/barrier multipliers (PBM) in [33] and a method based an augmented Lagrangian function in [13] and [25]. Recently a method based on a sequential convex programming concept [28, 27] and a method based on interior point methods [29] were proposed for FMO. Moreover, detailed theory covering choice of problem formulations and the existence of solutions can be found in [30].

Most of today's FMO studies focus on two- and three-dimensional design domains. In this article we focus on laminated plates and shells which nowadays are used in many engineering applications. There are several approaches to material optimization of such structures. One of them is Discrete Material Optimization (DMO) which was introduced in [23], [24], and [17]. DMO determines the best discrete material selection, stacking sequence, and thickness distribution. An FMO model for Mindlin plate design is introduced in [3]. Later in [9] FMO formulations, analogous to the recent FMO formulations for two- and three-dimensional structures, are proposed for single layer plates and shells. As far as to our knowledge, no FMO models have been proposed for general laminated shell structures. Therefore, we propose new FMO models for laminated plates and shells by extending the formulations in [9].

The requirement of physical attainability of the elastic stiffness tensor leads to a mathematical interpretation that the stiffness tensor must be symmetric positive semidefinite. For this reason, FMO problems result in an optimization problem that belongs to the class of nonlinear semidefinite programming (SDP). We generalize the primal-dual interior point method proposed by the authors in [29] which is especially developed for FMO problems. The method and its implementation exploit the property that FMO problems have many matrix in-

equalities with each inequality involving a small size matrix to efficiently solve large-scale problems. It obtains high quality solutions to large-scale FMO problems within a modest number of iterations.

This article has six sections. In section 2 the shell geometry and kinematics are first described. Then the existing FMO problem formulations for plates and shells are extended to laminated structures. In section 3 the primal-dual interior point method, initially proposed in [29] for two- and some three-dimensional FMO problems, is outlined. Then follows section 4 discussing the implementation of the method and the algorithmic parameters. The numerical experiments, results and discussions are presented in section 5. The conclusions and future research work are in section 6.

2 FMO problem formulations

In this section we first describe the geometry of a shell and then specialize solid kinematics to shell kinematics. We follow the approach in [7] and all details can be found therein. At the end of the section, we propose two FMO problem formulations for laminated plates and shells.

2.1 Shell kinematics

We refer a shell to a three dimensional structure that has curved inner and outer surfaces with a thickness in the middle of small size compared to other dimensions. Geometrically, a shell is characterized by its midsurface, say $\mathcal{S} = \phi(\bar{\omega})$, where ϕ is a smooth injective mapping called a chart from $\bar{\omega}$, the closure of the bounded open $\omega \subset \mathbb{R}^2$, into $\mathbb{R}^3$. The physical three dimensional space occupied by the shell is defined by the chart Φ given by

$$\Phi(\xi^1, \xi^2, \xi^3) = \phi(\xi^1, \xi^2) + \xi^3 a_3(\xi^1, \xi^2), \ (\xi^1, \xi^2, \xi^3) \in \Omega \tag{1}$$

where Ω is the 3D reference domain defined by

$$\Omega = \left\{ (\xi^1, \xi^2, \xi^3) \in \mathbb{R}^3 | (\xi^1, \xi^2) \in \omega, |\xi^3| < \frac{t(\xi^1, \xi^2)}{2} \right\} \tag{2}$$

with $t(\xi^1, \xi^2)$ the thickness of the shell at the point (ξ^1, ξ^2).

Throughout this section Greek indices and exponents take values in the set $\{1, 2\}$ while Latin indices and exponents are in the set $\{1, 2, 3\}$ with the assumption of Einstein summation convention. The local covariant basis vectors that form a basis to the plane tangent to the midsurface are $a_\alpha = \partial_\alpha \phi$, and the unit normal basis vector is $a_3 = (a_1 \times a_2)/\|a_1 \times a_2\|$. The contravariant local basis vectors a^i are defined such that they satisfy the relation $a_i \cdot a^j = \delta_i^j$ where δ_i^j is

the Kronecker symbol. The first fundamental form is given by $a_{\alpha\beta} = a_\alpha \cdot a_\beta$ in covariant form and $a^{\alpha\beta} = a^\alpha \cdot a^\beta$ in contravariant form. Note that the infinitesimal areas dS and $d\xi^1 d\xi^2$ are related as $dS = \sqrt{a}d\xi^1 d\xi^2$, where $a = a_{11}a_{22} - (a_{12})^2$. The second fundamental form of the surface is defined by $b_{\alpha\beta} = -a_\alpha \cdot \frac{\partial a_3}{\partial \xi^\beta}$ (and $b^\alpha_\beta = -a^\alpha \cdot \frac{\partial a_3}{\partial \xi^\beta}$). The third fundamental form is given by $c_{\alpha\beta} = b^\lambda_\alpha b_{\lambda\beta}$. The surface Christoffel symbols are $\Gamma^\lambda_{\beta\alpha} = a^\lambda \cdot \frac{\partial a_\beta}{\partial \xi^\alpha}$. The surface covariant derivative of a vector u_β is defined by $u_{\beta|\alpha} = \frac{\partial u_\beta}{\partial \xi^\alpha} - \Gamma^\lambda_{\beta\alpha} u_\lambda$.

Next, we describe the displacement field of the shell through its thickness. This is done by introducing a material line in the direction of a_3, orthogonal to the midsurface. These material lines are assumed to remain straight and do not experience any elongation in the deformed configuration. Then the displacements of the points located in the material line are

$$U(\xi^1, \xi^2, \xi^3) = u(\xi_1, \xi_2) + \xi^3 \theta_\lambda(\xi_1, \xi_2) a^\lambda(\xi_1, \xi_2) \tag{3}$$

where $u(\xi_1, \xi_2)$ is the translational displacement of the midsurface. The rotations θ_1 and θ_2 of the material line contribute to the displacement $\xi^3 \theta_\lambda(\xi_1, \xi_2) a^\lambda(\xi_1, \xi_2)$. For details we again refer the reader to [7]. The above assumption is known as *Reissner-Mindlin kinematical assumption.*

We present the shell model by specializing solid kinematics to shell kinematics as described in [7]. The linear Hooke's law for solid structures reads as

$$\sigma^{ij}(x) = E^{ijkl}(x)e_{kl}(x) \tag{4}$$

where E, σ and e are stiffness, stress and strain tensors, respectively. Referring to the structure of a (single layer) shell that the thickness is small compared to the other dimensions, the material properties are assumed to remain unchanged in the direction normal to the midsurface. Therefore, we assume the midsurface as the surface of symmetry making the shell monoclinic. This leads to some decoupling, see [21], and to the following assumptions on the stiffness tensor for solid structures.

$$E^{\alpha\beta\gamma3}(= E^{\alpha\beta3\gamma} = E^{\alpha3\beta\gamma} = E^{3\alpha\beta\gamma}) = 0, \text{ and}$$
$$E^{\alpha333}(= E^{3\alpha33} = E^{33\alpha3} = E^{333\alpha}) = 0. \tag{5}$$

Using (5) and under the additional assumption that $\sigma^{33} = 0$ the constitutive equations (4) are modified to

$$\sigma^{\alpha\beta} = C^{\alpha\beta\lambda\mu}e_{\lambda\mu} \text{ and } \sigma^{\alpha3} = \frac{1}{2}D^{\alpha\lambda}e_{\lambda3} \tag{6}$$

where

$$C^{\alpha\beta\lambda\mu} = E^{\alpha\beta\lambda\mu} - \frac{E^{\alpha\beta33}E^{\lambda\mu33}}{E^{3333}} \text{ and } D^{\alpha\lambda} = 4E^{\alpha3\lambda3}. \tag{7}$$

Let F be an external 3D loading that is applied to the shell structure. The basic shell model is then governed by the variational formulation

$$\int_{\Omega} (C^{\alpha\beta\lambda\mu} e_{\alpha\beta}(U) e_{\lambda\mu}(V) + D^{\alpha\lambda} e_{\alpha3}(U) e_{\lambda3}(V)) dV$$

$$= \int_{\Omega} F \cdot V dV \qquad (8)$$

where the unknown U is of the form (3) satisfying boundary conditions, and V is a test function fulfilling similar kinematic assumptions and the proper boundary conditions. The displacements in (3) lead to the following expression of the strains in (8),

$$e_{\alpha\beta} = \gamma_{\alpha\beta} + \xi^3 \chi_{\alpha\beta}, \text{ and } e_{\alpha3} = \zeta_\alpha. \qquad (9)$$

where $\gamma_{\alpha\beta}$, $\chi_{\alpha\beta}$ and ζ_α are the membrane, bending and shear strains of the midsurface that are given by,

$$\gamma_{\alpha\beta}(u) = \frac{1}{2}(u_{\alpha|\beta} + u_{\beta|\alpha}) - b_{\alpha\beta} u_3 \qquad (10a)$$

$$\chi_{\alpha\beta}(u,\theta) = \frac{1}{2}(\theta_{\alpha|\beta} + \theta_{\beta|\alpha} - b_\beta^\lambda u_{\lambda|\alpha} - b_\alpha^\lambda u_{\lambda|\beta}) - c_{\alpha\beta} u_3 \qquad (10b)$$

$$\zeta_\alpha(u,\theta) = \frac{1}{2}(\theta_\alpha + u_{3,\alpha} + b_\alpha^\lambda u_\lambda). \qquad (10c)$$

Next, we write the variational formulation (8) to the lowest order terms for laminated shells of N layers. We follow [5] to consider the function space $\mathcal{V}$ defined by

$$\mathcal{V} = \{(u,\theta) \in [H^1(\omega;\mathbb{R}^3)]^2 | \theta \cdot a_3 = 0 \text{ in } \omega, \ u = \theta = 0 \text{ on } \partial\omega_0\} \qquad (11)$$

where $\partial\omega_0$ is the fixed part of the boundary $\partial\omega$ of ω. The space $H^1(\omega;\mathbb{R}^3)$ is the standard Sobolev space. We additionally make the assumption that the stiffness tensors are allowed to vary freely across the laminate thickness from layer to layer but not in a layer, that is, they depend of course on $(\xi_1,\xi_2) \in \omega$. The loads are assumed not to vary through the thickness. Under this assumption and substituting the strains in the variational formulation (8) by the strains in (9) we obtain the following variational formulation for the laminated shells. Find $(u,\theta) \in \mathcal{V}$ such that

$$\sum_{l=1}^{N} \int_\omega C_l^{\alpha\beta\lambda\mu} \Big(t_l \gamma_{\alpha\beta}(u) \gamma_{\lambda\mu}(v) + \tilde{t}_l(\gamma_{\alpha\beta}(u) \chi_{\lambda\mu}(v,\eta) +$$

$$\gamma_{\lambda\mu}(v) \chi_{\alpha\beta}(u,\theta)) + \tilde{\tilde{t}}_l \chi_{\alpha\beta}(u,\theta) \chi_{\lambda\mu}(v,\eta) \Big) dS \qquad (12)$$

$$+\kappa \sum_{l=1}^{N} \int_\omega t_l D_l^{\alpha\lambda} \zeta_\alpha(u,\theta) \zeta_\lambda(v,\eta) dS = \int_\omega t F \cdot v dS$$

for all $(v, \eta) \in \mathcal{V}$, where

$$t_l = t_{l,top} - t_{l,low}, \ \tilde{t}_l = \frac{1}{2}((t_{l,top})^2 - (t_{l,low})^2),$$

$$\tilde{\tilde{t}}_l = \frac{1}{3}((t_{l,top})^3 - (t_{l,low})^3). \tag{13}$$

The terms $t_{l,top}$ and $t_{l,low}$ denote the upper and lower transverse coordinate of the lth layer at the point (ξ^1, ξ^2) respectively. The coefficient $\kappa < 1$ multiplying the shear term is the shear correction factor introduced to consider the shell model which is used in application. The subscript l in the stiffness tensors C_l and D_l is implies that stiffnesses belong to the lth layer. Existence of a unique solution to the variational problem (12) is also shown under natural assumptions for shells in [5].

2.2 FMO problem formulations for layered plates and shells

In FMO the design variable is the elastic stiffness tensor, i.e., the tensors C and D for the case of laminated plates and shells. They are allowed vary freely at each point of the design domain but required to be physically attainable. Mathematically, they must be symmetric and positive semidefinite, i.e., $C = C^T$, $D = D^T$, $C \succeq 0$, and $D \succeq 0$, where $A \succeq B$ ($A \succ B$) means $A - B$ is positive semidefinite (positive definite). However, the measure of stiffness is not straight forward. We follow the stiffness measure used in most studies which is the trace of the stiffness tensors. Motivated by [9] and FMO models for solid structures we define the set of admissible materials $\mathcal{C}$ as

$$\mathcal{C} = \left\{ (C, D) \in [L^\infty(\Omega)]^{3 \times 3} \times [L^\infty(\Omega)]^{2 \times 2} \right|$$
$$C = C^T \succeq 0, D = D^T \succeq 0 \right\}. \quad (14)$$

The choice of the space of essentially bounded functions $L^\infty(\omega)$ to define the set of admissible material in (14) is standard in FMO to include the possibilities of material\no material in the optimal designs, see e.g. [2]. The requirement of the factor $\frac{1}{2}$ can be seen from the relation in (6). The traces are multiplied by the thickness t_l to conform the surface measure of the shell with the volume measure in three dimensional structures. The trace of the stiffness is locally bounded from above by $\bar{\rho}$ to avoid arbitrarily stiff material. We also introduce lower trace bounds to make restriction on softness. The bounds on the traces satisfy $0 \leq \underline{\rho} < \bar{\rho} < \infty$. The amount of resource material to distribute in the structure is also limited by

$$\sum_{l=1}^{N} \int_\omega t_l \left(\text{Tr}(C_l(x)) + \frac{1}{2} \text{Tr}(D_l(x)) \right) dS \leq \vartheta. \tag{15}$$

6

with the volume bound V satisfying $N|\omega|\underline{\rho} < \vartheta < N|\omega|\bar{\rho}$, where $|\omega|$ is the area of ω.

Given external loads $F_\ell, \ell \in L = \{1, \ldots, n_L\}$, we formulate the primal minimum compliance FMO problem as

$$
\begin{aligned}
&\underset{(u,\theta)_\ell \in \mathcal{V}, (C,D) \in \mathcal{C}}{\text{minimize}} && \sum_{\ell \in L} w_\ell \int_\omega t F_\ell \cdot u_\ell dS \\
&\text{subject to} && (u,\theta)_\ell \text{ satsifying (12) with } F = F_\ell, \ \forall \ell \in L, \\
& && \underline{\rho} \le t_l \left(\text{Tr}(C_l(x)) + \frac{1}{2}\text{Tr}(D_l(x)) \right) \le \bar{\rho}, \ \forall \ell \in L, \\
& && \sum_{l=1}^{N} \int_\omega t_l \left(\text{Tr}(C_l(x)) + \frac{1}{2}\text{Tr}(D_l(x)) \right) dS \le \vartheta,
\end{aligned}
\tag{16}
$$

where w_ℓ are given weights satisfying $\sum_\ell w_\ell = 1$, and $w_\ell > 0$ for each $\ell \in L$. Alternatively, we formulate the minimum weight FMO problem as

$$
\begin{aligned}
&\underset{(u,\theta)_\ell \in \mathcal{V}, (C,D) \in \mathcal{C}}{\text{minimize}} && \sum_{l=1}^{N} \int_\omega t_l \left(\text{Tr}(C_l(x)) + \frac{1}{2}\text{Tr}(D_l(x)) \right) dS \\
&\text{subject to} && (u,\theta)_\ell \text{ satsifying (12) with } F = F_\ell, \ \forall \ell \in L, \\
& && \underline{\rho} \le t_l \left(\text{Tr}(C_l(x)) + \frac{1}{2}\text{Tr}(D_l(x)) \right) \le \bar{\rho}, \ \forall \ell \in L, \\
& && \sum_{\ell \in L} w_\ell \int_\omega t F_\ell \cdot u_\ell dS \le \Upsilon.
\end{aligned}
\tag{17}
$$

Note that we do not claim that (16) and (17) are equivalent. The two problems are included since the method and the implementation can solve both. Existence of an optimal solution to FMO problems for *single* layer laminate is shown in [9] under natural assumptions. The problems (16) and (17) have similar mathematical structure to the problem formulation proposed in [9]. Due to the lack of sufficient theoretical results existence of an optimal solution it is *assumed* for now for the problems (16) and (17). The theoretical assumption of existence of solutions should be further investigated and clarified.

2.3 Discretization of the FMO problem formulations

We follow the discretization scheme used in [9] and [7]. The reference midsurface ω is partitioned in to m uniform quadrilateral finite elements ω_i for $i = 1, \ldots, m$. We approximate the displacement by a continuous bilinear function. The elastic stiffness tensors $C(x)$ and $D(x)$ are approximated by functions that are constant

on each element in each layer. We denote by C_{il} and D_{il} the constant approximation of the stiffness tensors C and D on the ith element and lth layer respectively constituting the vectors of block matrices

$$C = (C_{11}, \ldots, C_{1N}, \ldots, C_{m1} \ldots, C_{mN})^T$$

and

$$D = (D_{11}, \ldots, D_{1N}, \ldots, D_{m1} \ldots, D_{mN})^T.$$

Given external static nodal load vectors $f_\ell^h \in \mathbb{R}^{n_f}, \ell \in L$, where n_f is number of finite element degrees of freedom, the finite dimensional equilibrium equation of (12) is

$$K(C, D)(u^h, \theta^h)_\ell = f_\ell^h, \ \ell \in L \tag{18}$$

where $(u^h, \theta^h)_\ell$ is associated displacement and $K(C, D)$ is the stiffness matrix given by

$$K(C, D) = \sum_{i=1}^m (K_i^\gamma(C) + K_i^{\gamma\chi}(C) + (K_i^{\gamma\chi}(C))^T + K_i^\chi(C)$$
$$+ K_i^\zeta(D)). \tag{19}$$

In (19), the element stiffness matrices are given by

$$K_i^\gamma(C) = \sum_{l,(j,k)\in n_i} \int_{\omega_i} t_{il}(B_{jl}^\gamma)^T C_{il} B_{kl}^\gamma dS \tag{20a}$$

$$K_i^{\gamma\chi}(C) = \sum_{l,(j,k)\in n_i} \int_{\omega_i} \tilde{t}_{il}(B_{jl}^\gamma)^T C_{il} B_{kl}^\chi dS \tag{20b}$$

$$K_i^\chi(C) = \sum_{l,(j,k)\in n_i}^N \int_{\omega_i} \tilde{\tilde{t}}_{il}(B_{jl}^\chi)^T C_{il} B_{kl}^\chi dS \tag{20c}$$

$$K_i^\zeta(D) = \kappa \sum_{l,(j,k)\in n_i} \int_{\omega_i} t_{il}(B_{jl}^\zeta)^T D_{il} B_{kl}^\zeta dS, \tag{20d}$$

where n_i is the index set of nodes associated with the element ω_i, and the matrices B_{il}^γ, B_{il}^γ and $B_{i,l}^\zeta$ are the (scaled) strain-displacement matrices for membrane strains, for bending strains, and for shear strains, respectively. These are constructed from the derivatives of the shape functions. The factors t_{il}, $\tilde{t}_{il}$ and $\tilde{\tilde{t}}_{il}$ are computed as in (13) and evaluated at the center of the element ω_i.

The discrete primal minimum compliance FMO formulation approximating (16) is

$$\underset{(u^h,\theta^h)_\ell \in \mathbb{R}^{n_f}, (C,D) \in \tilde{\mathcal{C}}}{\text{minimize}} \quad \sum_{\ell \in L} w_\ell (f_\ell^h)^T (u^h, \theta^h)_\ell$$

$$\text{subject to} \quad K(C,D)(u^h,\theta^h)_\ell = f_\ell^h, \; \ell \in L,$$

$$\underline{\rho} \le t_{il} \left(\text{Tr}(C_{il}) + \frac{1}{2}\text{Tr}(D_{il}) \right) \le \bar{\rho}, \; i = 1, \dots, m, \quad (21)$$

$$\sum_{i=1}^{m} \sum_{l=1}^{N} t_{il} \left(Tr(C_{il}) + \frac{1}{2} Tr(D_{il}) \right) \le \bar{\vartheta},$$

where $\tilde{\mathcal{C}}$ denotes the set of admissible materials

$$\tilde{\mathcal{C}} = \left\{ (C, D) \in (\mathbb{R}^{3mN \times 3}) \times (\mathbb{R}^{2mN \times 2}) \right|$$

$$C_{il} = C_{il}^T \succeq 0, D_{il} = D_{il}^T \succeq 0 \}. \quad (22)$$

The discrete primal minimum weight FMO formulation approximating (17) is

$$\underset{(u^h,\theta^h)_\ell \in \mathbb{R}^{n_f}, (C,D) \in \tilde{\mathcal{C}}}{\text{minimize}} \quad \sum_{i=1}^{m} \sum_{l=1}^{N} t_{il} \left(Tr(C_{il}) + \frac{1}{2} Tr(D_{il}) \right)$$

$$\text{subject to} \quad K(C,D)(u^h,\theta^h)_\ell = f_\ell, \; \ell \in L,$$

$$\underline{\rho} \le t_{il} \left(\text{Tr}(C_{il}) + \frac{1}{2}\text{Tr}(D_{il}) \right) \le \bar{\rho}, \; i = 1, \dots, m, \quad (23)$$

$$\sum_{\ell \in L} w_\ell (f_\ell^h)^T (u^h, \theta^h)_\ell \le \bar{\Upsilon}.$$

The problems (21) and (23) are Simultaneous ANalysis and Design (SAND) formulations and belong to the class of non convex SDPs with many linear matrix inequalities. Assuming strict positive definiteness of the stiffens tensors C and D, the stiffness matrix $K(C,D)$ can be assumed to be non singular. Therefore, one can solve for the displacement in the elastic equilibrium equation (18) to eliminate it from the SAND formulations and obtain equivalent nested formulations. However, in [29] it is reported that there is no noticeable difference in the number of iterations the method requires in solving the SAND formulations or the equivalent nested formulations. Moreover, the elastic equilibrium equation needs to be solved at each iteration in the interior point method for the nested formulation. This is found to be an expensive task for large-scale problems. Furthermore, for all problem instances in [29] the non convex SAND formulations give the same optimal designs as the corresponding convex nested formulations. Therefore, we only consider the SAND formulations (21) and (23).

3   Outline of the primal-dual interior point method

For completeness and ease of readability we present the general outline of the primal-dual interior method developed in [29]. This entire section is almost identical to Section 3 of [29]. We describe the method for general nonlinear SDP suitable for representing FMO problems in the form

$$
\begin{aligned}
\underset{X \in \mathbb{S}, u \in \mathbb{R}^n}{\text{minimize}} \quad & f(X, u) \\
\text{subject to} \quad & g_j(X, u) \le 0, \quad j = 1, \dots, k, \\
& X_i \succeq 0, \qquad\ i = 1, \dots m,
\end{aligned}
\tag{24}
$$

with

$$
\mathbb{S} = \mathbb{S}^{d_1} \times \mathbb{S}^{d_2} \times \cdots \times \mathbb{S}^{d_m} \text{ and } (d_1, d_2, \dots, d_m) \in \mathbb{N}^m,
$$

and $\mathbb{S}^d$-space of symmetric $d \times d$ matrices. The functions $f, g_j : \mathbb{S} \times \mathbb{R}^n \to \mathbb{R}$, for $j = 1, \dots, k$ are assumed to be sufficiently smooth. We then formulate the associated barrier problem

$$
\begin{aligned}
\underset{X \in \mathbb{S}_+, u \in \mathbb{R}^n, s \in \mathbb{R}^k_+}{\text{minimize}} \quad & f(X, u) - \mu \sum_{i=1}^m \ln(\det(X_i)) - \mu \sum_{j=1}^k \ln(s_j) \\
\text{subject to} \quad & g_j(X, u) + s_j = 0, \quad j = 1, \dots, k.
\end{aligned}
\tag{25}
$$

where $s \in \mathbb{R}^k$ are slack variables and $\mu > 0$ is barrier parameter. We solve this barrier problem for a monotonically decreasing sequence of barrier parameter μ_k that approaches zero. In that case the barrier problem also approaches the original problem (24). The Lagrangian to problem (25) is

$$
\begin{aligned}
\mathcal{L}_\mu(X, u, s, \lambda) = f(X, u) - \mu \sum_{i=1}^m \ln(\det(X_i)) - \mu \sum_{j=1}^k \ln(s_j) \\
+ \lambda^T(g(X, u) + s), \quad (26)
\end{aligned}
$$

where $\lambda \in \mathbb{R}^k_+$ is Lagrangian multiplier. Problem (25) has the KKT conditions

$$
\nabla_X \mathcal{L}_\mu(X, u, s, \lambda) = \nabla_X f(X, u) - \mu X^{-1} + \nabla_X(g(X, u)^T \lambda)
$$
$$
= 0 \tag{27a}
$$
$$
\nabla_u \mathcal{L}_\mu(X, u, s, \lambda) = \nabla_u f(X, u) + \nabla_u g(X, u)^T \lambda = 0 \tag{27b}
$$
$$
\nabla_s \mathcal{L}_\mu(X, u, s, \lambda) = -\mu S^{-1} e + \lambda = 0 \tag{27c}
$$
$$
g(X, u) + s = 0 \tag{27d}
$$
$$
X \succ 0, s > 0, \lambda > 0 \tag{27e}
$$

where $S = \mathrm{diag}(s)$ and $e = (1, 1, \ldots, 1)^T$ is a vector of all ones of appropriate size. We modify the optimal conditions by making the substitution $Z := \mu X^{-1}$ in (27a) and including additional equation

$$XZ - \mu I = 0. \tag{28}$$

It is important that the product XZ in (28) has to be symmetric to get a square system. We use the linear operator $H_P : \mathbb{R}^{n \times n} \to \mathbb{S}^n$, introduced in [32] and defined by

$$H_P(Q) := \frac{1}{2} \left(PQP^{-1} + (PQP^{-1})^T \right)$$

where $P \in \mathbb{R}^{n \times n}$ is some non-singular matrix to achieve the symmetry. The complementarity condition (28) is then replaced by

$$H_P(XZ) - \mu I = 0. \tag{29}$$

The directions obtained by setting the matrices P are called members of the Monteiro-Zhang (MZ) family [32]. The most commonly used search directions are the AHO direction [1] obtained when $P = I$, the HRVW/KSH/M direction [11, 12, 18] when $P = Z^{1/2}$, the dual HRVW/KSH/M direction [12, 18] when $P = X^{-1/2}$, and the NT direction [19, 20] when $P = W^{-1/2}$ with $W = X^{1/2}(X^{1/2}ZX^{1/2})^{-1/2}X^{1/2}$. In this article the NT direction is used based on the recommendation in [29] for its robustness in solving FMO problems.

We apply Newton's method to solve the KKT system. We further use the operator $P \odot Q : \mathbb{S}^n \to \mathbb{S}^n$ defined by

$$(P \odot Q)K := \frac{1}{2}(PKQ^T + QKP^T).$$

to write the Newton system. In FMO the coefficient matrix in the Newton system has block diagonal matrices where each block matrix is small and relatively cheap to invert. Therefore, we only present the reduced saddle point system in $(\Delta u, \Delta \lambda) \in \mathbb{R}^n \times \mathbb{R}^k$ as

$$\begin{pmatrix} G & A \\ A^T & B \end{pmatrix} \begin{pmatrix} \Delta u \\ \Delta \lambda \end{pmatrix} = \begin{pmatrix} \tilde{r}_d \\ \tilde{r}_p \end{pmatrix} \tag{30}$$

where

$$\begin{aligned} G =& \nabla^2_{uu} \mathcal{L}_\mu(X, u, s, \lambda) \\ & - \nabla^2_{Xu} \mathcal{L}_\mu(X, u, s, \lambda) \tilde{H}^{-1} \nabla^2_{Xu} \mathcal{L}_\mu(X, u, s, \lambda)^T \\ A =& \nabla_u g(X, u)^T - \nabla^2_{Xu} \mathcal{L}_\mu(X, u, s, \lambda)^T \tilde{H}^{-1} \nabla_X g(X, u)^T \\ B =& -\Lambda^{-1}S - \nabla_X g(X, u) \tilde{H}^{-1} \nabla_X g(X, u)^T. \end{aligned}$$

The right hand sides in (30) are computed as

$$\tilde{r}_d = r_d - \nabla_{Xu}^2 \mathcal{L}_\mu(X, u, s, \lambda) \tilde{H}^{-1}(R_d + \mathcal{F}^{-1} R_C)$$

$$\tilde{r}_p = r_p - \Lambda^{-1} r_c - \nabla_X g(X, u) \tilde{H}^{-1}(R_d + \mathcal{F}^{-1} R_C)$$

with $(R_d, r_d, r_c, r_p, R_C)^T$ denoting the negative of left hand side of the systems (27) and (29). The other search directions $(\Delta X, \Delta s, \Delta Z) \in \mathbb{S} \times \mathbb{R}^k \times \mathbb{S}$ are then computed as

$$\Delta X = \tilde{H}^{-1}(R_d + \mathcal{F}^{-1} R_C - \nabla_{Xu}^2 \mathcal{L}_\mu(X, u, s, \lambda)^T \Delta u$$
$$- \nabla_X g(X, u)^T \Delta \lambda) \tag{31a}$$

$$\Delta Z = \mathcal{F}^{-1}(R_C - \mathcal{E} \Delta X) \tag{31b}$$

$$\Delta s = \Lambda^{-1}(r_c - S \Delta \lambda). \tag{31c}$$

For the complete details of the Newton system and the (tensor) products, see Section 3 and Appendix B of [29]. In (31) the block diagonal matrices $\mathcal{E} = \mathcal{E}(X, Z)$ and $\mathcal{F} = \mathcal{F}(X, Z)$ are the derivatives of $H_P(XZ)$ with respect to X and Z respectively and are given by

$$\mathcal{E} = P \odot P^{-T} Z \text{ and } \mathcal{F} = PX \odot P^{-1}. \tag{32}$$

Given a current iterate (X, u, s, λ, Z) and a search direction $(\Delta X, \Delta u, \Delta s, \Delta \lambda, \Delta Z)$ we perform the standard steps in interior point methods to determine the primal step length α_p and dual step length α_d. We first determine the maximum possible step to the boundary region

$$\bar{\alpha}_p = \max\{\alpha \in (0, 1] : X + \alpha \Delta X \succeq (1 - \tau)X,$$
$$s + \alpha \Delta s \geq (1 - \tau)s\} \tag{33a}$$

$$\bar{\alpha}_d = \max\{\alpha \in (0, 1] : Z + \alpha \Delta Z \succeq (1 - \tau)Z,$$
$$\lambda + \alpha \Delta \lambda \geq (1 - \tau)\lambda\} \tag{33b}$$

where $\tau \in (0, 1)$ is the fraction to the boundary parameter. Next follows a backtracking line-search to get sufficient decrease in the merit function ϕ_μ defined by

$$\phi_\mu(X, u, s, \lambda, Z) := \|\nabla_X f(X, u) - Z + \nabla_X(g(X, u)^T \lambda)\|_F^2$$
$$+ \|(S\Lambda - \mu I)e\|_2^2 + \|g(X, u) + s\|_2^2$$
$$+ \|\nabla_u f(X, u) + \nabla_u g(X, u)^T \lambda\|_2^2$$
$$+ \|H_P(XZ) - \mu I\|_F^2. \tag{34}$$

where $\|\cdot\|_F$ is Frobenius norm. A search direction decreases sufficiently the merit function if

$$\phi_\mu(X + \alpha_p\Delta X, u + \alpha_p\Delta u, s + \alpha_p\Delta_d s, \lambda + \alpha_d\Delta\lambda, Z + \alpha_d\Delta Z)$$
$$\leq (1 - \tau_0\eta)\phi_\mu(X, u, s, \lambda, Z) \quad (35)$$

for a parameter $\eta \in (0,1)$ and for a constant $\tau_0 \in (0,1)$. The final step lengths are then

$$\alpha_p \in (0, \bar{\alpha}_p], \text{ and } \alpha_d \in (0, \bar{\alpha}_d].$$

The new iterate $(X^+, u^+, s^+, \lambda^+, Z^+)$ is

$$(X^+, u^+, s^+) = (X, u, s) + \alpha_p(\Delta X, \Delta u, \Delta s) \quad (36a)$$

$$(\lambda^+, Z^+) = (\lambda, Z) + \alpha_d(\Delta\lambda, \Delta Z). \quad (36b)$$

The algorithm terminates when

$$\max\Big\{\max_i\|\nabla_{X_i}f(X,u) - Z_i + \nabla_{X_i}(g(X,u)^T\lambda)\|_F,$$
$$\|\nabla_u f(X,u) + \nabla_u g(X,u)^T\lambda\|_\infty\Big\} \leq \epsilon^o$$
$$\max\{\max_i\|H_P(X_iZ_i)\|_F, \|S\Lambda e\|_\infty\} \leq \epsilon^o$$
$$\|g(X,u)_+\|_\infty \leq \epsilon^f \quad (37)$$

where $g_j(X,u)_+ = \max\{0, g_j(X,u)\}$, and $\epsilon^o > 0$ and $\epsilon^f > 0$ are respectively given optimality and feasibility tolerances of the original problem (24). For the barrier problem (25) we determine the optimality tolerance ϵ_μ^o and feasibility tolerance ϵ_μ^f through

$$\epsilon_\mu^o = \max\{10\mu, \epsilon^o - \mu\}, \quad \text{and} \quad \epsilon_\mu^f = \max\{10\mu, \epsilon^f\}. \quad (38)$$

They thus become μ dependent such that the method performs few inner iterations in the first outer iterations. The inner iteration loop stops when

$$\max\Big\{\max_i\|\nabla_{X_i}f(X,u) - Z_i + \nabla_{X_i}(g(X,u)^T\lambda)\|_F,$$
$$\|\nabla_u f(X,u) + \nabla_u g(X,u)^T\lambda\|_\infty\Big\} \leq \epsilon_\mu^o$$
$$\max\{\max_i\|H_P(X_iZ_i) - \mu I\|_F, \|S\Lambda e - \mu e\|_\infty\Big\} \leq \epsilon_\mu^o$$
$$\|g(X,u) + S\|_\infty \leq \epsilon_\mu^f. \quad (39)$$

For each barrier problem we estimate the barrier parameter μ by

$$\mu = \sigma(\sum_i Tr(X_i^T Z_i)/d_i + s^T\lambda)/(m + k), \ \sigma < 1 \quad (40)$$

which is proportional to the gap between the objective functions of the primal and the dual problems.

The overall description of the interior point method is given in Algorithm 1. The algorithm is identical to the algorithm in [29].

Algorithm 1 A primal-dual interior point algorithm for nonlinear SDP problems (from [29]).

Choose $w_p^0 = (X^0, u^0, s^0)$, $w_d^0 = (\lambda, Z)$, and μ_0 as in (40).
Set the outer iteration counter $k \leftarrow 0$.
while stopping criteria (37) for problem (24) is not satisfied and $k < k_{max}$ **do**
    Set the inner iteration counter $i \leftarrow 0$
    while stopping criteria (39) for problem (25) is not satisfied and $i < i_{max}$) **do**
        Compute the search direction $\Delta w_p^{k,i}$ and $\Delta w_d^{k,i}$ by solving system (30) and (31).
        Compute $\bar{\alpha}_p$ and $\bar{\alpha}_d$ as in (33).
        Set the line search iteration counter $l \leftarrow 0$.
        Set `LineSearch` $\leftarrow$ `False`
        while `LineSearch = False` and $l < l_{max}$ **do**
            $\alpha_p \leftarrow \eta^l \bar{\alpha}_p$ and $\alpha_d \leftarrow \eta^l \bar{\alpha}_d$
            if $\phi_\mu(w_p^{k,i} + \alpha_p \Delta w_d^{k,i}, w_d^{k,i} + \alpha_d \Delta w_d^{k,i}) \leq (1 - \tau_0 \eta^l)\phi_\mu(w_p^{k,i}, w_d^{k,i})$ **then**
                Set the new iterate $(w_p^{k,i+1}, w_d^{k,i+1})$ as in (36).
                `LineSearch` $\leftarrow$ `True`
            else
                $l \leftarrow l + 1$.
            end if
        end while
        $i \leftarrow i + 1$.
    end while
    Update μ_{k+1} as in (40).
    $k \leftarrow k + 1$.
end while

---

4   Implementation, algorithmic parameters, and problem data

The code implemented and described in [29] to solve FMO problems for two- and three-dimensional FMO problems is generalized and used to solve the FMO problems for laminated plates and shells presented in section 2. The algorithm, the

Table 1: Algorithmic parameters and initial points used in the implementation of the primal-dual interior point method.

Parameters/ initial points	Values
Optimality tolerance ϵ^o	10^{-6}
Feasibility tolerance ϵ^f	10^{-7}
Minimum barrier parameter value $\mu_{\min}$	10^{-8}
Boundary to the fraction parameter τ	0.9
η - line-search parameter in (35)	0.5
τ_0 - line-search parameter in (35)	10^{-5}
Centrality constant σ	0.4
Initial stiffness tensors C_{il} and D_{il}	$0.1\bar{\rho}I$ for all i and l
Initial displacement vectors u_ℓ	0 for all ℓ
Initial slack variables	1
Initial Lagrange multipliers for equality constraints	0
Initial Lagrange multipliers for scalar (or matrix) inequality constraints	1 (or I)

parameters and choice of primal and dual initial points are kept unaltered except with minor changes to make the code suitable for the problems in this article. The interior point method and the finite element routines are implemented entirely in MATLAB Version 7.7. All numerical experiments are run on Intel Xeon X5650 six-core CPUs running at 2.66 GHz with 4GB of memory per core (only a single core is used per problem). The standard quadrangular CQUAD4 elements with six degrees of freedom per node are considered with full Gaussian integration layer wise and explicit integration over the thickness. The implementation of the finite element is exactly as described in [9].

The saddle point systems resulting from the application of Newton's method to solve the KKT conditions are solved using the LDL factorization routines which are built into MATLAB. We use the NT direction since numerical experiments in [29] show that the NT directions are more robust compared to the other AHO and HRVW/KSV/M directions.

The minimum compliance problems are, for all problem instances, solved with the total weight fraction set to 40% of the maximum possible weight. The algorithmic parameter values and choice of initial points used in the implementation are listed in Table 1. The local bounds on the box constraints are scaled such that $\bar{\rho}/\underline{\rho} = 10^5$.

Table 2: FMO problem instances.

Problems	No. of layers	No. of FEs	No. of linear matrix inequalities	No. of design variables	No. of non-fixed state variables
Michell beam	4	20000	160000	720000	121200
Plate	8	40000	640000	2880000	237606
Spherical cap	8	10000	160000	720000	60006
Cylindrical cap	1	80000	160000	720000	483486
Cylinder	1	40000	80000	360000	240000
Shell beam (two load cases)	1	12800	25600	115200	76320

5 Numerical experiments

In this section we report numerical results for six examples. To the best of our knowledge there are no other benchmark FMO problems for laminated plates and shells reported in literature with which we can compare our results. Nevertheless, for some of the examples we refer to results obtained by two-dimensional FMO problems or other structural optimization approaches such as DMO. However, these comparisons are only qualitative.

In all examples the normalized dimension of the spanned domain region is 1×1 if it is square and 1×2 if it is rectangular except for the shell beam in Example 5.6 where the dimensions are 1×8. The thickness is 0.01 times the length of the shortest dimension of spanned region. If the laminate has multiple layers then the thickness is divided evenly over the layers and numbering is from bottom layer to top layer. The problem instances are presented in Table 2. We refer the optimal density distribution to the trace of the optimal stiffness tensor and its plots scales to the color bar shown in Figure 1. The realization of solutions to FMO problems is in general difficult. There are some tools that have been developed to interpret FMO solutions, see e.g. [6]. Fiber reinforced composite structures could be one choice particularly for the results from this article. In that case the determination of fiber angle is important which is not however a design variable in FMO problems. Nevertheless, we report plots for the in-plane strain field computed via the eigenvectors of the strain tensors for some of the examples.

The computational time and number of iterations required to obtain solutions for the problem instances in Table 2 are reported in Table 3. The numerical figures in these tables show that the FMO problems are large-scale problems. The optimal designs are obtained within 50 and 60 iterations. This is modest for methods for nonlinear SDPs and so the efficiency of the method is implied.

Figure 1: Colorbar for the optimal density distribution.
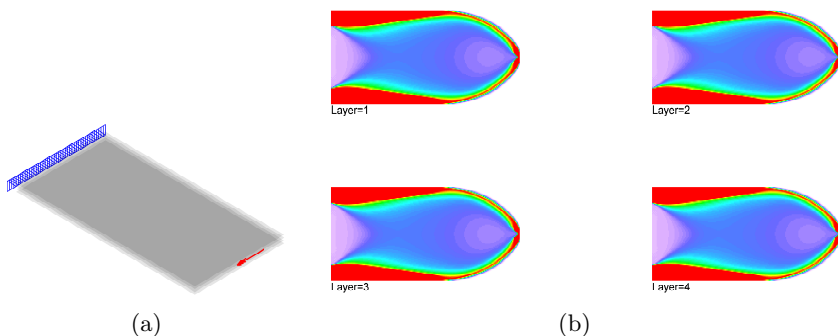
| (a) | (b) |

Figure 2: Design domain, boundary conditions, and external load (a), optimal density distribution (b) of the Michell beam consisting of four layers. The density distribution is identical in all layers as expected.

Studying the history of the iteration we also find that the direct solution of the saddle point system dominates the computation time of the method. This is also illustrated in Table 3 where the computational time in solving multiple load FMO problems dramatically increases.

Example 5.1. In the first example we consider a laminate of four plate layers clamped at one edge and subject to a pure in-plane load at the opposite edge as shown in Figure 2a. This example is included to show consistency of the models. The model gives results that are similar to solutions to two-dimensional FMO problem in [33] and Variable Thickness Sheet problem in [8]. Figure 2b shows that there is no distinction among the density distribution of the layers. The numerical values of the optimal solution also show that stiffness tensor C that accounts for membrane deformation dominates the tensor D (which is zero over the entire design domain). The traverse displacements are also zero. The in-plane strain field for the bottom layer is plotted in Figure 3. The other three layers have identical strain fields.

Example 5.2. In this example we consider a clamped laminate of eight plate layers subject to a uniformly distributed load, see Figure 4a. In the optimal

17
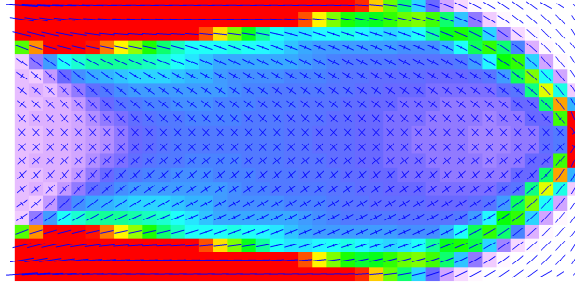
Figure 3: In-plane strain field of layer 1 for the Michell beam problem.

density distribution, shown in Figure 4b, the large interconnected reinforcement in the surface layers splits in to smaller edge and center reinforcements in the next inner layers and then ends up in soft material in the innermost layers. This property resembles the expected sandwich structures. The in-plane strain field of the lower left corners of the bottom four layers is plotted in Figure 5. These strain fields also correspond to that of the top four layers of equidistant from the midsurface. Therefore, the solution implies a symmetric laminate.

Example 5.3. We consider a hinged spherical cap of 8 layers subject to a single transversal load concentrated at the center as shown in the Figure 6a. The geometry of the shell is adapted from [24]. The plot for the optimal distribution of materials is shown Figure 6b. There are wider stiff regions in the surface layers than the inner layers with the center reinforcement appearing in all layers. However, the symmetry behavior of the density distribution with respect to the midsurface does not exist. We can also find the correspondence of the solution to a sandwich structure and the unsymmetrical behavior in a solution to a similar DMO problem in [24].

Example 5.4. The design domain is a corner hinged cylindrical cap loaded by a transversal load concentrated at the center as shown in Figure 7a. The plot for the optimal density distribution in Figure 7b shows the cross-like topology extending from the center to the corners which can be found in other structural optimization approaches, see e.g., [16].

Example 5.5. In this example a cylinder is clamped at one end and is subject to a load distributed on a small curve in the opposite end. All the nodal values of

(a)

Layer=1 Layer=2 Layer=3 Layer=4

Layer=5 Layer=6 Layer=7 Layer=8
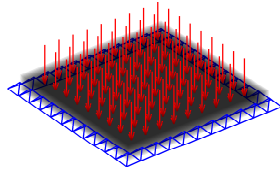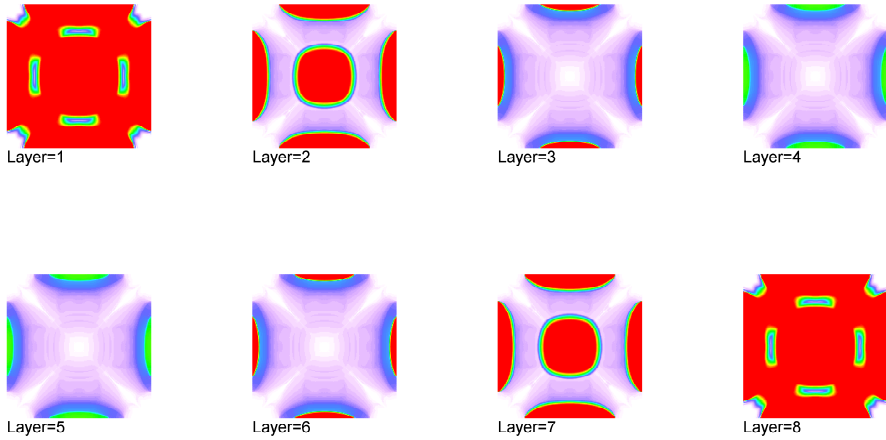
(b)

Figure 4: Design domain, boundary conditions, and external load (a), optimal density distribution (b) of the clamped plate consisting of eight layers.

(a)

(b)

(c)

(d)
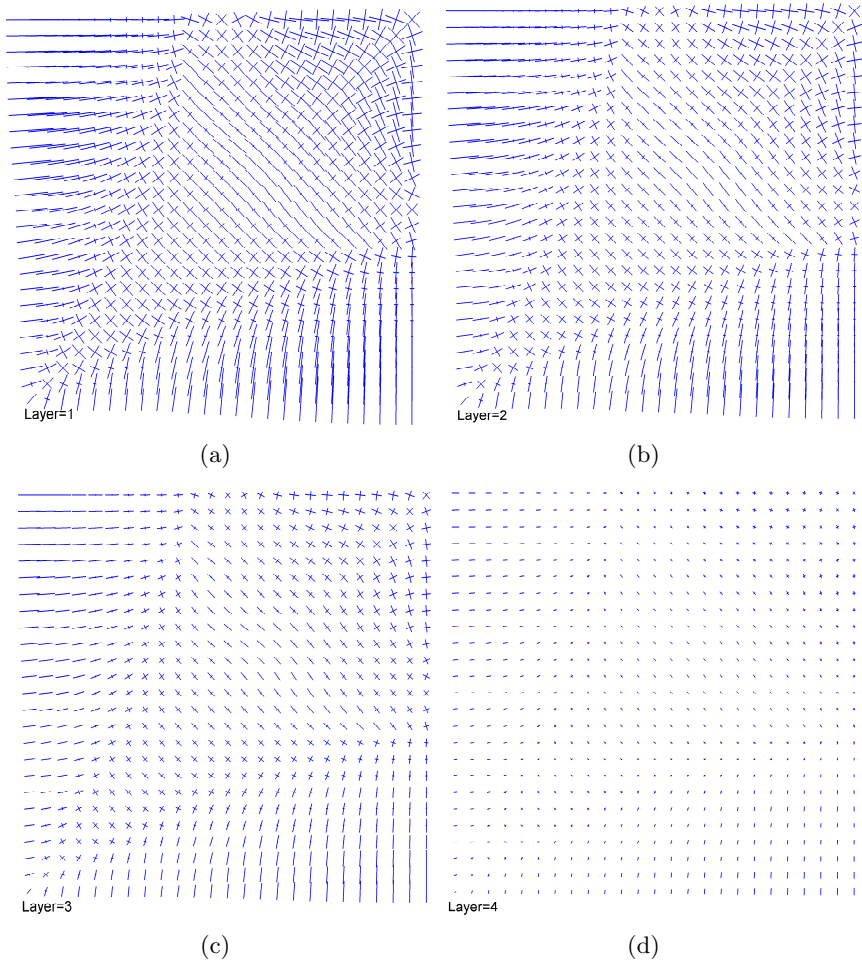
Figure 5: In-plane strain field of the bottom four layers of the lower left quarters for the plate problem.

20

(a)
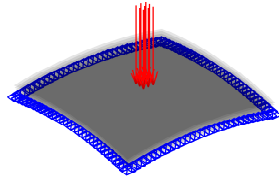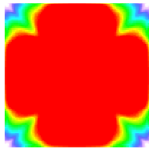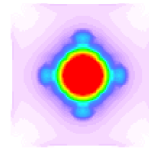
Layer=1   Layer=2   Layer=3   Layer=4
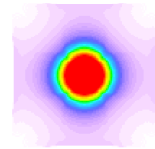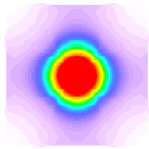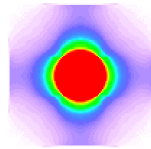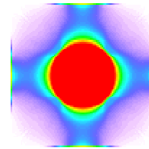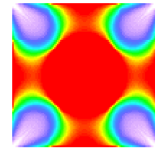
Layer=5   Layer=6   Layer=7   Layer=8

(b)

Figure 6: Design domain, boundary conditions, and external load (a), optimal density distribution (b) of the hinged spherical cap of eight layers.

(a)   (b)
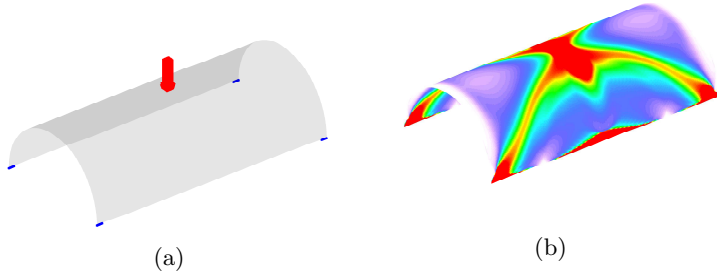
Figure 7: Design domain, boundary conditions, and external load (a), optimal density distribution (b) of the single layered cylindrical cap hinged at the four corners.

the load point in the same direction, see Figure 8a. The usual topology obtained when solving a two-dimensional cantilever beam problem, see e.g., [29], can be seen in Figure 8b spanning from the loading curve to the fixed base on both halves of the cylinder.

Example 5.6. We consider a shell beam clamped at both ends subject to two independent loads distributed over lines lying at the middle of opposite lateral surfaces as show in the Figure 9a. In the optimal design Figure 9b the stiff regions around the loading lines are extended and connected to the fixed regions forming a chain of diamond-like topology over the top and bottom surfaces. The response of the diamond like topology shows up in solutions to two-dimensional FMO problem on a rectangular design domain clamped at its two opposite edges and subject to two independent loads at the center of the other tow edges pointing in opposite directions, see [33]. Similar topology of the loaded surfaces can also be found in [31] while solving a single load problem over a three surface shell beam.

6   Conclusions

We extended existing FMO models and a primal-dual interior point method for plates and shells to laminated structures for the first time. The consistency of the model is shown first by solving a well-known Michell beam problem under
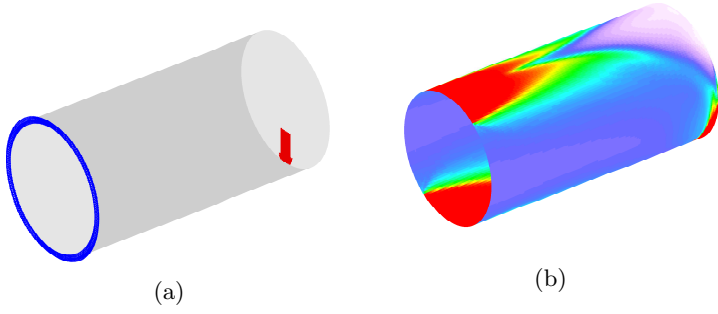
(a)

(b)

Figure 8: Design domain, boundary conditions, and external load (a), optimal density distribution (b) of the single layered cylinder clamped at one end.

(a)

(b)
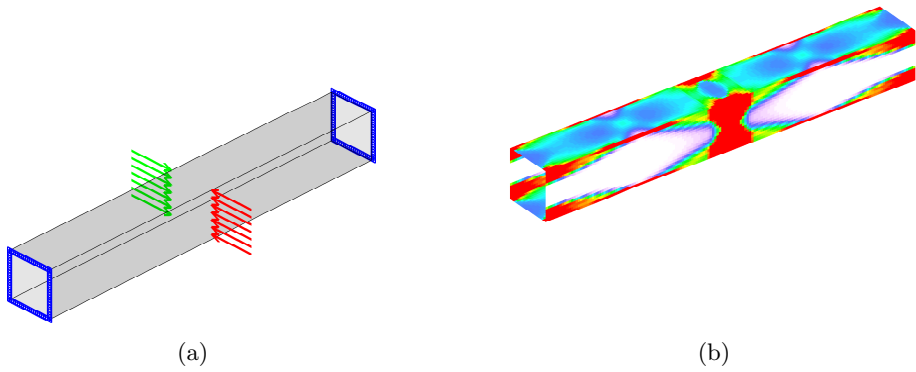
Figure 9: Design domain, boundary condition, and external loads (a), optimal density distribution (b) of the single layered rectangular pipe clamped at both ends.

Table 3: Numerical results for the problem instances in Table 2 and the minimum compliance problem (16).

Problems	No. of iterations	CPU time (hr:min:sec)
Michell beam	52	02:01:27
Plate	60	10:41:45
Spherical cap	54	02:06:44
Cylindrical cap	52	03:26:36
Cylinder	51	01:34:58
Shell beam	50	04:39:50
(two load cases)		

an in-plane load where the optimal designs of the layers are found to be identical. During transversal loading situations and multilayer laminate the obtained optimal designs correspond to sandwich structures. Similar designs have also been found by other structural optimization approaches such as Discrete Material Optimization and classical topology optimization. The authors are currently working on problem formulations including constrains on local properties such as stresses and strains.

The behaviour of the interior point method and its implementation initially introduced for FMO for two- and three-dimensional problems in [29] and now modified for FMO problems for plates and shells are not altered. In general the method is efficient, requires a modest number of iterations that increase very slowly with problem size, and gives high quality solutions.

Acknowledgements

References

[1] Alizadeh, F., Haeberly, J.A., Overton, M.L.: Primal-dual interior-point methods for semidefinite programming: convergence rates, stability and numerical results. SIAM Journal on Optimization **8**(3), 746–768 (2009)

[2] Ben-Tal, A., Nemirovski, A.: Robust truss topology design via semidefinite programming. SIAM Journal on Optimization **7**(4), 991–1016 (1997)

[3] Bendsøe, M.P., Díaz, A.R.: Optimization of material properties for Mindlin plate design. Structural Optimization **6**, 268–270 (1993)

[4] Bendsøe, M.P., Guedes, J.M., Haber, R.B., Pedersen, P., Taylor, J.E.: An analytical model to predict optimal material properties in the context of optimal structural design. Journal of Applied Mechanics **61**, 930–937 (1994)

[5] Blouza, A., Dret, H.L.: Nagdhi's shell model: Existence, uniqueness and continuous dependence on the midsurface. Journal of elasticity **64**, 199–216 (2001)

[6] Bodnár, G., Stadelmeyer, P., Bogomolny, M.: Methods for computer aided interpretation of FMO results. Tech. rep., PLATO-N Public Report PU-R-3-2008 (2008). Available from http://www.plato-n.org/

[7] Chapelle, D., Bathe, K.J.: The Finite Element Analysis of Shells - Fundamentals. Springer, Heidelberg (2003)

[8] Czarnecki, S., Lewiński, T.: On minimum compliance problems of thin elastic plates of varying thickness. Structural and Multidisciplinary Optimization **48**(1), 17–31 (2013)

[9] Gaile, S.: Free material optimization for shells and plates. Ph.D. thesis, Institute of Applied Mathematics II, Friedrich-Alexander University of Erlangen-Nuremberg (2011). Available from http://www.researchgate.net/

[10] Haslinger, J., Kočvara, M., Leugering, G., Stingl, M.: Multidisciplinary free material optimization. SIAM Journal on Applied Mathematics **70**(7), 2709–2728 (2010)

[11] Helmberg, C., Rendl, F., Vanderbei, R.J., Wolkowicz, H.: An interior-point method for semidefinite programming. SIAM Journal on Optimization **6**, 342–361 (1996)

[12] Kojima, M., Shindoh, S., Hara, S.: Interior-point methods for the monotone semidefinite linear complementarity problem in symmetric matrices. SIAM Journal on Optimization **7**(1), 86–125 (1997)

[13] Kočvara, M., Stingl, M.: A code for convex nonlinear and semidefinite programming. Optimization Methods and Software **18**(3), 317–333 (2003)

[14] Kočvara, M., Stingl, M.: Free material optimization for stress constraints. Structural and Multidisciplinary Optimization **33**, 323–355 (2007)

[15] Kočvara, M., Stingl, M., Zowe, J.: Free material optimization: recent progress. Optimization **57**(1), 79–100 (2008)

[16] Lee, S.J., Bae, J.E., Hinton, E.: Shell topology optimization using the layered artificial material model. International Journal for Numerical Methods in Engineering **47**, 843–867 (2000)

[17] Lund, E., Stegmann, J.: On structural optimization of composite shell structures using a discrete constitutive parametrization. Wind Energy **8**, 109–124 (2005)

[18] Monteiro, R.D.C.: Primal-dual path-following algorithms for semidefinite programming. SIAM Journal on Optimization **7**(3), 663–678 (1997)

[19] Nesterov, Y.E., Todd, M.J.: Self-scaled barriers and interior-point methods for convex programming. Mathematics of Operations Research **22**(1), 1–42 (1997)

[20] Nesterov, Y.E., Todd, M.J.: Primal-dual interior-point methods for self-scaled cones. SIAM Journal on Optimization **8**(2), 324–364 (1998)

[21] Reddy, J.: Mechanics of laminated composite plates and shells: theory and analysis, 2nd edn. London (2004)

[22] Ringertz, U.T.: On finding the optimal distribution of material properties. Structural Optimization **5**, 265–267 (1993)

[23] Stegmann, J.: Analysis and optimization of laminated composite shell structures. Ph.D. thesis, Institute of Mechanical Engineering, Aalborg University, Aalborg, Denmark (2004). Available from http://www.researchgate.net/

[24] Stegmann, J., Lund, E.: Discrete material optimization of general composite shell structures. International Journal for Numerical Methods in Engineering **62**, 2009–2007 (2005)

[25] Stingl, M.: On the solution of nonlinear semidefinite programs by augmented lagrangian method. Ph.D. thesis, Institute of Applied Mathematics II, Friedrich-Alexander University of Erlangen-Nuremberg (2006). Available from http://www2.am.uni-erlangen.de/

[26] Stingl, M., Kočvara, M., Leugering, G.: Free material optimization with fundamental eigenfrequency constraints. SIAM Journal on Optimization **20**(1), 524–547 (2009)

[27] Stingl, M., Kočvara, M., Leugering, G.: A new non-linear semidefinite programming algorithm with an application to multidisciplinary free material optimization. International Series of Numerical Mathematics **158**, 275–295 (2009)

[28] Stingl, M., Kočvara, M., Leugering, G.: A sequential convex semidefinite programming algorithm with an application to multiple-load free material optimization. SIAM Journal on Optimization **20**(1), 130–155 (2009)

[29] Weldeyesus, A.G., Stolpe, M.: A primal-dual interior point method for large-scale free material optimization. Computational Optimization and Applications (2014). DOI 10.1007/s10589-014-9720-6

[30] Werner, R.: Free material optimization-mathematical analysis and numerical solution. Ph.D. thesis, Institute of Applied Mathematics II, Friedrich-Alexander University of Erlangen-Nuremberg (2001)

[31] Yang, B.J., Chen, C.J.: Stress-based topology optimization. Structural Optimization **12**, 98–105 (1996)

[32] Zhang, Y.: On extending some primal-dual interior-point algorithms from linear programming to semidefinite programming. SIAM Journal on Optimization **8**(2), 365–386 (1998)

[33] Zowe, J., Kočvara, M., Bendsøe, M.P.: Free material optimization via mathematical programming. Mathematical Programming **79**, 445–466 (1997)

Chapter 7

Models and methods for Free Material Optimization with local stress constraints

Models and Methods for Free Material Optimization with Local Stress Constraints

Alemseged Gebrehiwot Weldeyesus*

Abstract

Free Material Optimization (FMO) is a powerful approach of structural optimization of composite structures leading to conceptual optimal designs. The design variable is the elastic material tensor which is allowed to change its values freely over the design domain giving optimal material properties and optimal material distribution. The only requirements are that the stiffness tensor is forced to be symmetric positive semidefinite as a necessary condition for its physical attainability. One of the goals of this article to introduce constraints on local stresses to existing FMO problems for laminated plates and shells and propose new stress constrained FMO problem formulations. The FMO problems are non convex semidefinite program with a special structure involving many small matrix inequalities. This structure is exploited by our special purpose optimization method. The second goal of this article is to extend primal-dual interior point method for classical FMO problems to stress constrained FMO problems. The numerical experiments show that the optimal solutions to the stress constrained problems can be achieved within a moderate number of iterations. The local stress constraints are satisfied with high accuracy. The method and models are supported by numerical examples.

Mathematics Subject Classification 2010: 90C22, 90C90, 74P05, 74P15

Keywords: Structural optimization, free material optimization, nonlinear semidefinite optimization, stress constraints

---

*DTU Wind Energy, Technical University of Denmark, Frederiksborgvej 399, 4000 Roskilde, Denmark. E-mail: alwel@dtu.dk

1 Introduction

Free Material Optimization (FMO) deals with obtaining a composite structure with optimal material properties and optimal material distribution that can sustain a given set of loads. Such optimal structures can be considered as ultimately best structures among all possible elastic continua [36]. These optimal designs can also be used as benchmarks with which other designs obtained by other approaches of structural optimization can be compared.

The basic concept of FMO can be traced back to the early 1990s in [2], [3], and [22]. Since then there are several research studies dealing with more advanced FMO models. FMO formulations have been extended to include a wide range of constraints such as constraints on local stresses, local strains, displacement and fundamental frequencies in e.g. [17], [15], [11], and [25]. Theoretical aspects of FMO problems including existence of optimal solutions are analyzed in different studies [11] and [34]. There are also numerical optimization methods proposed in several articles [36], [14], [24], [27], [26], and [33].

High stresses are one of the causes for engineering structures to fail. The scope of several studies in structural optimization are extended to control stresses within a certain limit in the optimal structures. However, addressing stresses in the optimization problem is not straight forward. The choice of optimization problem formulation with relevant stress criteria and the development of methods that can computationally handle the problems are some of the main challenges.

Topology optimization is one of the research fields that has been extensively studied. For stress-based topology optimization see [35], [23], [5], [7], [20], and [18] for continua, and [13], [10], [29], and [30] for trusses and the references therein. Stresses are addressed in topology optimization in several ways. One way is limiting the stresses by introducing stress constraints which can be local at element level or global by aggregating the stresses in the design. Adding such constraints however leads to optimization problems that are difficult to solve. Suitable mathematical properties such as convexity are lost. Moreover, the problems face the singularity phenomenon described in e.g. [13] and [1] among many others.

FMO problems with stress constraints are analyzed and solved in [17], [16], and [15] for two-dimensional and in [11] for three-dimensional structures. The constraints are introduced with a term of an integral of the norm of the stresses. One of the outcome of FMO models is that higher stresses are primarily removed by changing material properties. This is unlike to other approaches in structural optimization where the materials are fixed and higher stresses are avoided by other ways, for e.g., changing the geometry of the optimal structure. The result is supported by making a comparison between solutions to FMO problem and the classical Variable Thickness Sheet (VTS) problem in [15].

The stress constraints in FMO defined in e.g. [15] are highly nonlinear involving the design variable stiffness tensor. This makes the level of the difficulty to solve stress constrained FMO problems even worse. The stress constrained FMO problems in [15], [17], and [16] are solved with the method based on Augmented Lagrangian function in [14] and [24]. The problems in [11] are solved by one of the recent methods based on sequential convex programming developed in [27, 26]. The method in general requires large number of iterations. The original setting of the problems were approximated by problems where the stress constraints are removed and added to the objective function using a penalty term. The solutions to the new approximation problems are of high quality. However, the feasibility tolerance of the stress constraint is moderate.

The focus of this article is on FMO formulations with constraints on local stresses. As far as to our knowledge there are no analogous FMO formulations with stress constraints for laminated structures. In [32], FMO problems for laminated plates and shells are proposed based on the formulations in [9]. One of the objective of this article is to introduce constraints on local stresses to these formulations and propose FMO problem formulations with local stress constraints for laminates.

The necessary condition for physical attainability of the stiffness tensor results in matrix inequalities in the optimization problem. Therefore, FMO problems belong to a class of SemiDefinite Program (SDP). Recently, an efficient primal-dual interior point method with special purpose to FMO problems is developed in [33]. The method is generalized for FMO models for laminated plates and shells in [32]. It exploits the special structure that FMO problems have many but small matrix inequality constraints. Solutions are reported to the largest classical FMO problems solved to date. It requires a modest number of iterations that almost does not increase with problem size. The second objective of this article is to show that a slightly modified version of this method can successfully solve the stress constrained problems of this article. The stress constraints are treated in the algorithm keeping their original settings in the problem formulations. The numerical experiments show that the solutions are obtained in moderate number of iterations with higher accuracy.

The organization of the article is as follows. In Section 2 we formulate the finite dimensional FMO problems with stress constraints for both solid and laminated structures. In Section 3 we present the implementation of the algorithm and the slight modification introduced to the method described in detail in [33]. We report and explain the results of the performed numerical experiments in Section 4. The conclusions and possibly future research works are presented in Section 5.

2 Problem formulations

In this section we present FMO problem formulations with stress constraints for solid and laminated plate and shell structures. In both cases we start with the discrete version of the classical minimum compliance (maximum stiffness) and the minimum weight FMO formulations. For details on the problem formulations and finite element discretization, see [27] and [17] for solid structures, and [32], [9], and [4] for laminated structures.

It is pointed out in e.g. [15] that addressing stress constraints in structural optimization using FMO is a challenge. In the first place, there is no existing general failure criterion. The realization of the optimal structure is also important in using one of the several existing failure criteria, for example see [12] for different failure criteria in fiber reinforced composites. Moreover, in FMO material properties are also design variables giving conceptual optimal designs. Despite these challenges we follow the measure proposed in [15] which is the norm of the stresses integrated over the finite element in the discrete problems.

In FMO problem formulations the requirement of the physical attainability of the stiffness tensor is introduced by matrix inequality constraints. As a measure of stiffness the trace of the elastic stiffness tensor is used. It is locally bounded from above by $\bar{\rho}$ to avoid arbitrarily stiff materials and from below by $\underline{\rho}$ to limit the extent of softness. These bounds must satisfy the relation $0 \leq \underline{\rho} < \bar{\rho} < \infty$. We consider n_L given external static nodal load vectors $f_\ell \in \mathbb{R}^n$, where $\ell \in L = \{1, \ldots, n_L\}$ and n is the number of finite element degrees of freedom. We prescribe weights w_ℓ for the loads $\boldsymbol{f}_\ell$ satisfying $\sum_\ell w_\ell = 1$ and $w_\ell > 0$ for each $\ell \in L$.

Next, we present the FMO problems with local constraints for solids and laminated structures. In both cases we follow similar approach. We first formulate the problems without stress constraints. Then, we define the stress constraints and include in the unconstrained problems to formulate the stress constrained FMO problems.

2.1 FMO for solid structures

This section is essentially identical to the corresponding section in [33] and is included for completeness. We consider a design domain Ω partitioned in to m uniform finite elements Ω_i for $i = 1, \ldots, m$. The elastic stiffness tensor $E(x)$ is approximated by a function that is constant on each finite element with its element values making the vector of block matrices $E = (E_1, \ldots, E_m)^T$. For any given external static nodal load vectors f_ℓ, the associated displacement $\boldsymbol{u}_\ell$ must satisfy the linear elastic equilibrium equation

$$\boldsymbol{A}(\boldsymbol{E})\boldsymbol{u}_\ell = \boldsymbol{f}_\ell, \ \ell \in L, \tag{1}$$

where the stiffness matrix $\boldsymbol{A}(\boldsymbol{E})$ is given by

$$\boldsymbol{A}(\boldsymbol{E}) = \sum_{i=1}^{m} \boldsymbol{A}_i(\boldsymbol{E}), \quad \boldsymbol{A}_i(\boldsymbol{E}) = \sum_{k=1}^{n_G} \boldsymbol{B}_{i,k}^T \boldsymbol{E}_i \boldsymbol{B}_{i,k}. \tag{2}$$

The matrices $B_{i,k}$ are (scaled) strain-displacement matrices computed from the derivative of the shape functions and n_G is the number of Gaussian integration points, see e.g. [6].

We define the set of admissible materials $\tilde{\mathcal{E}}$ by

$$\tilde{\boldsymbol{E}} := \left\{ \boldsymbol{E} \in (\mathbb{S}_+^d)^m | \underline{\rho} \leq Tr(\boldsymbol{E}_i) \leq \bar{\rho}, i = 1, \ldots, m \right\} \tag{3}$$

where the space $\mathbb{S}_+^d$ is the cone of positive semidefinite matrices in the space $\mathbb{S}^d$ of symmetric $d \times d$ matrices, i.e., $\boldsymbol{E}_i \in \mathbb{S}_+^d$ if and only if $\boldsymbol{E}_i = \boldsymbol{E}_i^T$ and $\boldsymbol{E}_i \succeq 0$. The exponent d takes the value 3 for two-dimensional problems and 6 for three-dimensional problems.

Next, we formulate FMO problems for solids without stress constraints. The primal minimum compliance FMO problem is formulated as

$$\begin{aligned} \underset{\boldsymbol{u}_\ell \in \mathbb{R}^n, \boldsymbol{E} \in \tilde{\mathcal{E}}}{\text{minimize}} \quad & \sum_{\ell \in L} w_\ell \boldsymbol{f}_\ell^T \boldsymbol{u}_\ell \\ \text{subject to} \quad & \boldsymbol{A}(\boldsymbol{E})\boldsymbol{u}_\ell = \boldsymbol{f}_\ell, \ \ell \in L, \\ & \sum_{i=1}^{m} Tr(\boldsymbol{E}_i) \leq V. \end{aligned} \tag{4}$$

The constant $V > 0$ is an upper bound on the amount of resource material to distribute in the structure and satisfies the relation

$$\sum_{i=1}^{m} \underline{\rho} < V < \sum_{i=1}^{m} \overline{\rho}.$$

The primal minimum weight FMO problem is

$$\begin{aligned} \underset{\boldsymbol{u}_\ell \in \mathbb{R}^n, \boldsymbol{E} \in \tilde{\mathcal{E}}}{\text{minimize}} \quad & \sum_{i=1}^{m} Tr(\boldsymbol{E}_i) \\ \text{subject to} \quad & \boldsymbol{A}(\boldsymbol{E})\boldsymbol{u}_\ell = \boldsymbol{f}_\ell, \ \ell \in L, \\ & \sum_{\ell=1}^{L} w_\ell \boldsymbol{f}_\ell^T \boldsymbol{u}_\ell \leq \gamma. \end{aligned} \tag{5}$$

The weighted multiple load non convex FMO problems (4) and (5) are of Simultaneous ANalysis and Design (SAND) formulation without stress constraints.

Theories and methods for problems (4) and (5) and/or their minimax formulations have been extensively studied in several articles, see [28], [28], [34] and the references therein. By applying the Schur complement theorem the problems can be written as linear problems, but result in large matrix inequalities that can hardly be handled computationally [17]. Under the mild assumption $E \succ 0$ on the elastic stiffness tensor the stiffness matrix $\boldsymbol{A}(\boldsymbol{E})$ is nonsingular [28]. Therefore, by solving the displacement in the equilibrium equation (1), it can be eliminated from the problems (4) and (5) and then equivalent nested convex formulations can be derived. The SAND formulations are the preferred choices in this article. This is due to the numerical experiments in [33] and it is more convenient to track numerically the stress constraints in the SAND formulations than in the nested formulations for a second order method.

Now, we introduce the stress constraints. We determine the norm of the stress due to the load $\boldsymbol{f}_\ell$ integrated over ith element by

$$\|\boldsymbol{\sigma}_{i,\ell}\|^2 := \int_{\Omega_i} \|\boldsymbol{\sigma}_\ell\|^2 d\Omega = \sum_{k=1}^{n_G} \|\boldsymbol{E}_i \boldsymbol{B}_{ik} \boldsymbol{u}_\ell\|^2. \tag{6}$$

We then include in problems (4) and (5) the constraints on local stresses

$$\|\boldsymbol{\sigma}_{i,\ell}\|^2 \leq s_\ell, \ \text{ for each } \ell \in L \text{ and } \ i = 1, ..., m. \tag{7}$$

The upper bound s_ℓ is estimated first by solving the corresponding unconstrained problems (4) and (5) and scaling the maximum stress norm by a factor $k \in (0,1)$,i.e.,

$$s_\ell = k \max_i \{\|\boldsymbol{\sigma}_{i,\ell}\|^2\}. \tag{8}$$

The existence of optimal solution to the stress constrained FMO problems is shown in [11] under natural assumptions.

2.2 FMO for laminated pates and shells

This section is mostly adopted from Subsection 2.3 of [32] and is included for the completeness and ease of readability. In laminated structures mechanical properties are usually determined with respect to a reference midsurface, denoted by ω. In order to formulate the finite dimensional problem, ω is partitioned in to m uniform finite elements ω_i for $i = 1, \ldots, m$. As in the case of solid structures the plane-stress in-plane elastic stiffness tensor $\boldsymbol{C}$ and transverse tensor $\boldsymbol{D}$ are approximated by functions constant on each element in each layer. The ith element values of the stiffness tensors $\boldsymbol{C}$ and $\boldsymbol{D}$ on the lth layer are denoted by by $\boldsymbol{C}_{il}$ and $\boldsymbol{D}_{il}$ respectively.

Given external static nodal load vectors f_ℓ the resulting displacement $(\boldsymbol{u}, \boldsymbol{\theta})_\ell$ (translational and rotational) satisfies the elastic equilibrium equation

$$\boldsymbol{K}(\boldsymbol{C}, \boldsymbol{D})(\boldsymbol{u}, \boldsymbol{\theta})_\ell = \boldsymbol{f}_\ell, \ \ell \in L, \tag{9}$$

where $\boldsymbol{K}(\boldsymbol{C}, \boldsymbol{D})$ the stiffness matrix is given by

$$\boldsymbol{K}(\boldsymbol{C}, \boldsymbol{D}) = \sum_{i=1}^{m} (\boldsymbol{K}_i^\gamma(\boldsymbol{C}) + \boldsymbol{K}_i^{\gamma\chi}(\boldsymbol{C}) + (\boldsymbol{K}_i^{\gamma\chi}(\boldsymbol{C}))^T + \boldsymbol{K}_i^\chi(\boldsymbol{C}) + \boldsymbol{K}_i^\zeta(\boldsymbol{D})). \tag{10}$$

The element stiffness matrices in (10) are given by

$$\boldsymbol{K}_i^\gamma(\boldsymbol{C}) = \sum_{l,(j,k)\in n_i} \int_{\omega_i} t_{il}(\boldsymbol{B}_{jl}^\gamma)^T \boldsymbol{C}_{il} \boldsymbol{B}_{kl}^\gamma dS \tag{11a}$$

$$\boldsymbol{K}_i^{\gamma\chi}(\boldsymbol{C}) = \sum_{l,(j,k)\in n_i} \int_{\omega_i} \tilde{t}_{il}(\boldsymbol{B}_{jl}^\gamma)^T \boldsymbol{C}_{il} \boldsymbol{B}_{kl}^\chi dS \tag{11b}$$

$$\boldsymbol{K}_i^\chi(\boldsymbol{C}) = \sum_{l,(j,k)\in n_i}^{N} \int_{\omega_i} \tilde{\tilde{t}}_{il}(\boldsymbol{B}_{jl}^\chi)^T \boldsymbol{C}_{il} \boldsymbol{B}_{kl}^\chi dS \tag{11c}$$

$$\boldsymbol{K}_i^\zeta(\boldsymbol{D}) = \kappa \sum_{l,(j,k)\in n_i} \int_{\omega_i} t_{il}(\boldsymbol{B}_{jl}^\zeta)^T \boldsymbol{D}_{il} \boldsymbol{B}_{kl}^\zeta dS, \tag{11d}$$

where n_i is the index set of nodes associated with the element ω_i. The matrices B_{il}^γ, B_{il}^γ and $B_{i,l}^\zeta$ are the (scaled) strain-displacement matrices for membrane strains, for bending strains, and for shear strains, respectively. The factors t_{il}, $\tilde{t}_{il}$ and $\tilde{\tilde{t}}_{il}$ are computed as

$$t_{il} = t_{il}^b - t_{il}^a, \ \ \tilde{t}_{il} = \frac{1}{2}((t_{il}^b)^2 - (t_{il}^a)^2),$$
$$\tilde{\tilde{t}}_{il} = \frac{1}{3}((t_{il}^b)^3 - (t_{il}^a)^3), \tag{12}$$

where t_{il}^b and t_{il}^a the upper and lower transverse coordinates of the lth layer at the center of the element ω_i. The coefficient $\kappa < 1$ appearing in the shear term in (11d) is the shear correction factor. This is to take into account the shell model which is used in applications.

Given that the laminate has N number of layers we define the set of admissible

material $\tilde{\mathcal{E}}$ by

$$\tilde{\mathcal{E}} = \left\{ (\boldsymbol{C}, \boldsymbol{D}) \in (\mathbb{S}_+^3)^{mN} \times (\mathbb{S}_+^2)^{mN} \,\middle|\, \right.$$

$$\left. \underline{\rho} \leq t_{il} \left(\mathrm{Tr}(\boldsymbol{C}_{il}) + \tfrac{1}{2}\mathrm{Tr}(\boldsymbol{D}_{il}) \right) \leq \bar{\rho}, \quad i = 1, \ldots, m, l = 1, \ldots, N \right\}. \quad (13)$$

Now, we formulate the unconstrained problems. The primal minimum compliance FMO formulation is then stated as

$$\begin{aligned}
&\underset{(\boldsymbol{u},\boldsymbol{\theta})_\ell \in \mathbb{R}^n, (\boldsymbol{C},\boldsymbol{D}) \in \tilde{\mathcal{E}}}{\text{minimize}} \quad \sum_{\ell \in L} w_\ell(\boldsymbol{f}_\ell)^T(\boldsymbol{u},\boldsymbol{\theta})_\ell \\
&\text{subject to} \quad \boldsymbol{K}(\boldsymbol{C},\boldsymbol{D})(\boldsymbol{u},\boldsymbol{\theta})_\ell = \boldsymbol{f}_\ell, \ \ell \in L, \\
&\qquad\qquad \sum_{i=1}^m \sum_{l=1}^N t_{il} \left(Tr(\boldsymbol{C}_{il}) + \frac{1}{2}Tr(\boldsymbol{D}_{il}) \right) \leq V,
\end{aligned} \quad (14)$$

with the volume bound $V > 0$ satisfying

$$\sum_{l=1}^N \sum_{i=1}^m \underline{\rho} < V < \sum_{l=1}^N \sum_{i=1}^m \bar{\rho}.$$

The discrete primal minimum weight FMO formulation is

$$\begin{aligned}
&\underset{(\boldsymbol{u},\boldsymbol{\theta})_\ell \in \mathbb{R}^n, (\boldsymbol{C},\boldsymbol{D}) \in \tilde{\mathcal{E}}}{\text{minimize}} \quad \sum_{i=1}^m \sum_{l=1}^N t_{il} \left(Tr(\boldsymbol{C}_{il}) + \frac{1}{2}Tr(\boldsymbol{D}_{il}) \right) \\
&\text{subject to} \quad \boldsymbol{K}(\boldsymbol{C},\boldsymbol{D})(\boldsymbol{u},\boldsymbol{\theta})_\ell = \boldsymbol{f}_\ell, \ \ell \in L, \\
&\qquad\qquad \sum_{\ell \in L} w_\ell(\boldsymbol{f}_\ell)^T(\boldsymbol{u},\boldsymbol{\theta})_\ell \leq \gamma.
\end{aligned} \quad (15)$$

Next, we present our motivation for the type of stress constraints that we introduce to the problems (14) and (15).

It is known from mechanics of laminated structures that stresses vary across the thickness of the laminate with linear variation within a layer (we are talking about linear elasticity). Therefore, we make two stress evaluations in each layer over each element ω_i, at the top and lower transverse coordinates of the layer. This allows us to capture the stress extremities within each layer and each element. We follow similar approach proposed for solids and make these evaluations by the integral form of stresses, i.e., analogous to (6). The stress due to the load

$\boldsymbol{f}_\ell$ on the ith element at the bottom of the lth layer is

$$\|\boldsymbol{\sigma}_{il,\ell}^a\|^2 := \int_{\omega_i} \|\boldsymbol{\sigma}_{l,\ell}^a\|^2 d\omega =$$

$$\sum_{k=1}^{n_G} \left(\|\boldsymbol{C}_{il}(\boldsymbol{B}_{ikl}^\gamma(\boldsymbol{u},\boldsymbol{\theta})_\ell + t_{il}^a \boldsymbol{B}_{ikl}^\chi(\boldsymbol{u},\boldsymbol{\theta})_\ell)\|^2 + \|\boldsymbol{D}_{il}\boldsymbol{B}_{ikl}^\zeta(\boldsymbol{u},\boldsymbol{\theta})_\ell\|^2 \right).$$

and the top of the lth layer is

$$\|\boldsymbol{\sigma}_{il,\ell}^b\|^2 := \int_{\omega_i} \|\boldsymbol{\sigma}_{l,\ell}^b\|^2 d\omega =$$

$$\sum_{k=1}^{n_G} \left(\|\boldsymbol{C}_{il}(\boldsymbol{B}_{ikl}^\gamma(\boldsymbol{u},\boldsymbol{\theta})_\ell + t_{il}^b \boldsymbol{B}_{ikl}^\chi(\boldsymbol{u},\boldsymbol{\theta})_\ell)\|^2 + \|\boldsymbol{D}_{il}\boldsymbol{B}_{ikl}^\zeta(\boldsymbol{u},\boldsymbol{\theta})_\ell\|^2 \right).$$

Then, we propose the following stress constraints for laminated plates and shells

$$\begin{aligned} \|\boldsymbol{\sigma}_{il,\ell}^a\|^2 \le s_\ell, \quad \ell \in L, \quad i = 1,...,m, \text{ and } l = 1,...,N, \\ \|\boldsymbol{\sigma}_{il,\ell}^b\|^2 \le s_\ell, \quad \ell \in L, \quad i = 1,...,m, \text{ and } l = 1,...,N, \end{aligned} \tag{16}$$

with the value of s_ℓ is determined as in (8).

In [9], FMO problem formulations with similar structures to the problems (14) and (15) but for a *single* layer are studied and existence of optimal solution is proved. However, there is no sufficient theoretical background in the literature to guarantee the result for multilayer laminates. The case is even worse when the stress constraints in (16) are included to these problems. The theoretical aspect of these problems need to be further investigated. Any outcome of this article regarding the stress constrained FMO problems for laminates is only the result of numerical experiments.

3   Optimization method and implementation

The FMO problems (4), (5), (14), and (15) all have linear objective functions with matrix inequalities and nonlinear (and non convex) vector constraints. Therefore, they are classified as non convex SDPs. In general, FMO problems tend to be large-scale problems for a reasonable mesh size. This is because the design variable is the stiffness tensor at each point of the design domain. However, the special property that the matrix inequalities are small (but many) can be exploited with a special purpose optimization method. An efficient primal-dual method with special purpose to FMO is developed in [33]. The method has shown success in solving by far the largest FMO problems of formulations in (4) and (5)

and some other equivalent formulations. It is also generalized in [32] to solve the FMO problems for laminates of the formulation in (14).

Stress constrained structural optimization problems are in general difficult problems to solve and usually computationally expensive. The problems may not also satisfy constraint qualifications [1], stated as singularity phenomenon in [13]. The stress constraints for FMO problems in (7) and (16) are highly nonlinear in the stiffness tensor and displacement. Hence, the challenge in the handling of computations and finding accurate solutions rises to a complex issue in FMO problems with stress constraints.

In this article we slightly modify the primal-dual interior point method developed in [33] and [32] to solve the stress constrained problems. We employ a perturbation to the the coefficient matrix of the saddle point system that results during applying Newton's method to solve the optimality conditions. This is based on inertia controlling methods [19, 8, 31] to ensures that a search direction gives a decrease in the merit function chosen in the algorithm.

The stress constraints are treated in the algorithm directly keeping their original settings in (7) and (16). In other studies these are often moved to the objective function using a penalty term [27, 26]. The code is entirely implemented in MATLAB. The standard QUAD4 bilinear elements obtained by full Gaussian integration are considered for the two-dimensional problems. For the laminate problems we consider the standard quadrangular CQUAD4 elements with six degrees of freedom per node with full Gaussian integration layer wise and explicit integration over the thickness. The overview of algorithmic parameters are described in [33] and [32].

4 Numerical experiments

For the numerical experiments we consider the minimum compliance problems (4) together with stress constraints (7) for two-dimensional problems, and (14) together with the stress constraints (16) for problems on laminated structures. The total weight fraction is set to 40% of the maximum possible weight and the bounds on the traces of the stiffness tensors are scaled such that $\bar{\rho}/\underline{\rho} = 10^5$.

Through out this section we use the color scale with limits $\underline{\rho}$ and $\bar{\rho}$ given in Figure 1 for all plots of the optimal density distribution. We use own color scales for plots of optimal stress norms to easily show high stresses in the unconstrained problems and regions of active stress constraints in the constrained problems. Note that the labels of the color bar are the norm of the stresses, not the norm of the stresses squared, as used in Table 3. For the two-dimensional Examples 4.1 and 4.2 we also report the principal stress directions which are computed as principal eigenvectors associated to the Voigt-stress tensor.

Figure 1: Color bar for the plots of optimal density distribution.

There are five examples in this section. The first two examples are for two-dimensional problems and the last three examples are for laminated structures. In Example 4.1 we consider L-shaped design domain of dimension (normalized) 1×1 and a quarter removed from one of the corners. In Example 4.2 we consider a Michell beam problem on a rectangular design domain of dimension 2×1. For the examples on laminates we consider a laminate spanning a region of dimension 1×1 for the clamped plates in Examples 4.3 and 4.4, and 1×8 for the shell beam in Example 4.5. The ratio of the thickness to the shortest dimension is 0.01 and is distributed evenly for layered laminates. Layers are numbered in the thickness direction from bottom to top. The problem instances are presented in Tables 1 and 2.

The numerical results are reported in Table 3 listing some comparisons between solving the constrained and unconstrained problems. The optimality tolerances are the norm of the fist-order optimality conditions measured without perturbation on the complementarity conditions. By feasibility tolerances we also refer ot the feasibility of the stress constraints in the original problem settings (7) and (16). Looking at the numerical values the active stress constraints are feasible with high accuracy. The solutions to the unconstrained problems are obtained within 30 and 61 iterations where as within 85 and 142 for the constrained problems. This can be considered as modest taking in to account that the problems are nonlinear SDPs. Moreover, the number of iterations is modest compared to the results in other literatures, see for example [16] for two dimensional, and [11] for three-dimensional problems. The increase in the number of iterations in solving the constrained problems is expected since the stress constraints are nonlinear involving matrix variables. It is common practice in structural optimization that stresses are reduced at the cost of an increase in compliance. This is also shown in Table 3 for FMO problems. However, the surprising outcome from the numerical experiments is that compliances are worsened not significantly in FMO. In all examples the increase in compliance is less than 5% while stresses are reduced by more than 50%

In all cases, higher stresses near the fixed or loaded regions in the unconstrained problems are avoided in the constrained problems. For a physically meaningful chosen values of the scaling factor k in (8), the stress constraints are found to be active in wider stiff regions of the optimal designs in the constrained
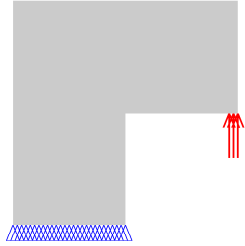
Figure 2: Design domain, boundary condition, and external load for the L-shape design domain.

problems. The similarity between the optimal density distributions for the constrained and unconstrained problems imply that stresses are primarily reduced in FMO by changing material properties. The case is different in other structural optimization approaches where material properties are fixed which and there is less freedom than in FMO. Therefore, the stresses are reduced by other means such us changing the geometry of the topology. Similar results can be found in, e.g., [15], [16], and [17].

Example 4.1. We consider the two-dimensional FMO problem on L-shaped design domain from [15], see Figure 2. When solving the problem without stress constraints, we can see the much higher stresses around the reentrant corner, Figure 4a. This is actually typical example giving stress singularity in the reentrant corner. For this case we can allow least value of the scaling factor k in (8) than in the rest of the examples of this article. It can be seen in Figure 4b the high stresses are avoided. However, looking at the optimal density distributions in Figure 3 the difference is not that big. The higher stress are reduced by reinforcing the reentrant corner with materials forming smooth-like arcs, see the zoom-in Figure 5b of the region. In general, these results closely agree with the results in [15].

Example 4.2. In this example we consider the classical two-dimensional Michell beam problem as shown in Figure 6. In the solution to the unconstrained problem there are higher stresses around the two ends of the fixed edge, see Figure 8a. These stresses are reduced in the constrained problem, Figure 8b. Similar to the previous example, there is no much difference in the optimal density distributions between the solutions to the constrained and unconstrained problems, see Figure 7. The reduction of the higher stresses is mainly accomplished by changing the material directions around these regions. The direction changing materials around these regions in Figure 9a in the unconstrained problem are replaced by unidirectional-like materials in Figure 9b in the constrained problem.

Table 1: FMO problem instances for the two-dimensional problems.

Problems	No. of FEs	No. of stress constraints	No. of linear matrix inequalities	No. of design variables	No. of non-fixed state variables
L-shape	7500	7500	7500	45000	15300
Michell beam	20000	20000	20000	120000	40400

Table 2: FMO problem instances for the laminate problems.

Problems	No. of layers	No. of FEs	No. stress constraints	No. of linear matrix inequalities	No. of design variables	No. of non-fixed state variables
Clamped plate (pressure load)	8	2500	40000	40000	180000	14406
Clamped plate (central load)	8	2500	40000	40000	180000	14406
Shell beam (two load cases)	1	12800	51200	25600	115200	76320

Table 3: Numerical results for the problem instances in Tables 1 and 2 and the minimum compliance problems (4) and (14) with the stress constraints (7) and (16) respectively. (Compliance and stress norms are scaled)

Problems	Without stress constraints				With stress constraints				
	Iter	Compl-iance	Max. stress norm	Opt/feas tolerances	k	Iter	Compl-iance	Max. stress norm	Opt/feas tolerances
L-shape	30	1.8951	1.3206	2.7e-08/4.0e-10	0.2	85	1.9281	0.2643	9.5e-08/8.9e-09
Michell Beam	47	2.4427	1.9372	8.1e-08/1.7e-11	0.4	102	2.4579	0.7749	8.5e-08/4.3e-10
Clamped plate (pressure load)	47	5.4771	2.1574	3.4e-07/6.9e-09	0.5	115	5.5624	1.0783	6.5e-06/8.8e-07
Clamped plate (central load)	54	7.1531	9.3224	3.5e-07/3.0e-08	0.5	138	7.1876	4.6612	3.7e-07/9.6e-09
Shell beam (two load cases)	61	6.5645	0.1370	7.6e-07/5.9e-09	0.4	142	6.7257	0.0548	3.4e-07/7.9e-10

(a)　　　　　　　　　　(b)
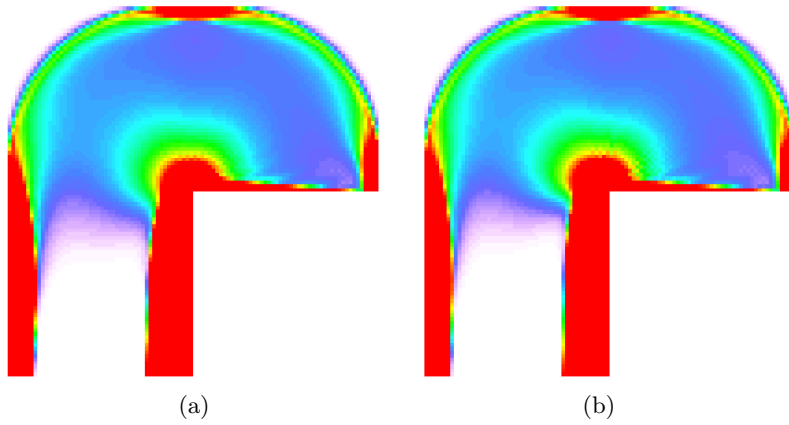
Figure 3: Optimal density distributions of the L-shape problem, (a) without stress constraints, (b) with stress constraints.

(a)　　　　　　　　　　(b)
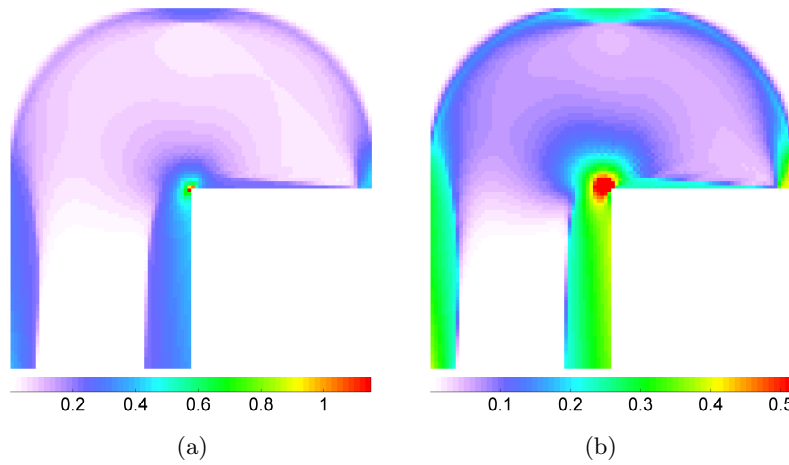
Figure 4: Optimal stress norms for the L-shape problem, (a) without stress constraints, (b) with stress constraints.

14
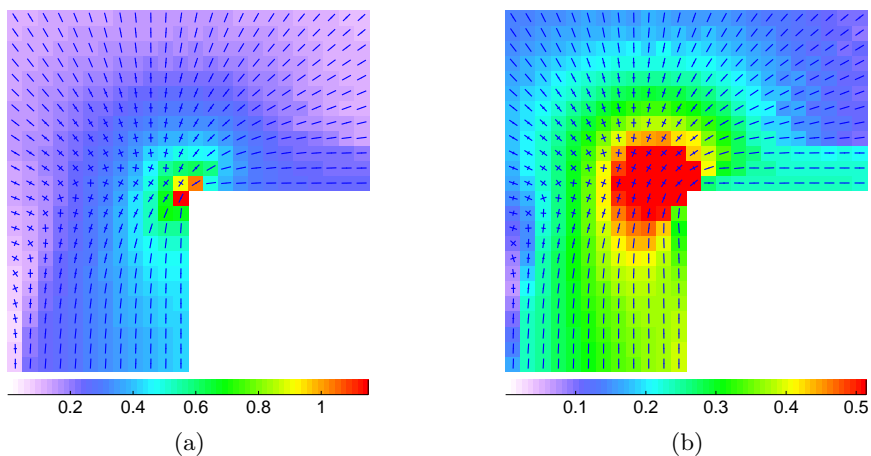
Figure 5: Optimal principal stresses around the reentrant corner for the L-shape problem, (a) without stress constraints, (b) with stress constraints.

Figure 6: Design domain, boundary condition, and external load for the Michell beam problem.
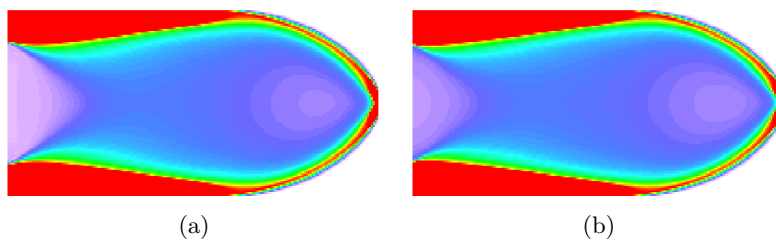
Figure 7: Optimal density distributions for the Michell beam problem, (a) without stress constraints, (b) with stress constraints.

15
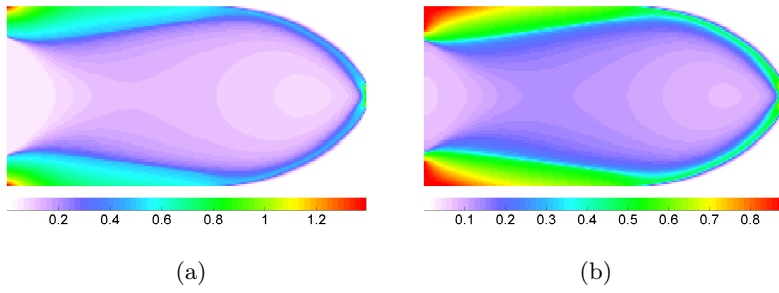
Figure 8: Optimal stress norms for the Michell beam problem, (a) without stress constraints, (b) with stress constraints.
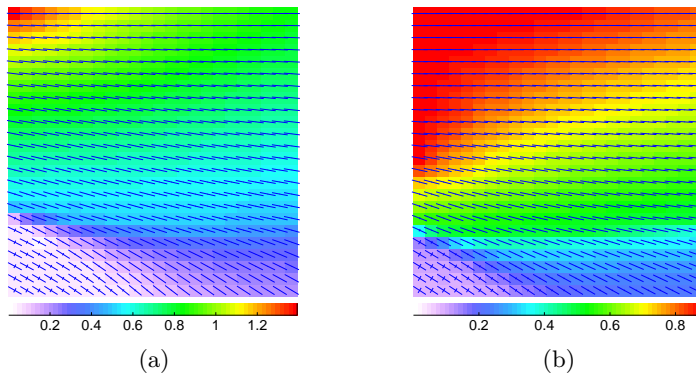
Figure 9: Optimal principal stresses around the upper left corner for the Michell beam problem, (a) without stress constraints, (b) with stress constraints.
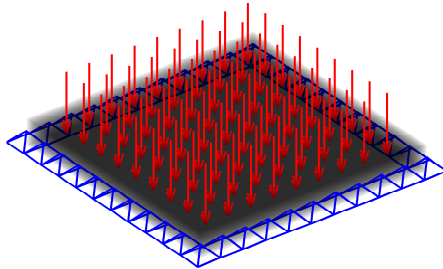
Figure 10: Design domain, boundary condition, and external load for the clamped plate with pressure load.

Example 4.3. We consider a clamped plate of eight layers loaded uniformly, see Figure 10. In this case the optimal solution corresponds to a sandwich-like symmetric laminate. Therefore, we report results only for the bottom four layers. Looking at the density distributions in Figure 11, we notice a slight visible difference in the middle four layers where some more materials are used around the fixed regions in the constrained problem than in the unconstrained problem. Figure 12 shows that there are higher stresses in the surface layers mainly concentrated around the fixed four edges of the plate. These are controlled to be within the limit in the constrained problem, Figure 13.

In our model we follow the First Order Deformation Theory (FSDT), see [21], in which the out-of-plane shear stresses are taken in to account. Unlike the two-dimensional problems, reporting the mechanism by which high stress are avoided is not straight forward for laminates. Hence, the realization of the solutions to FMO problems for laminates needs further investigation. This applies to examples 4.3, 4.4 and 4.5 of this article.

Example 4.4. We consider a similar case as example 4.3, a clamped laminate of eight plate layers but with the load concentrated at the center, see Figure 14. This is to consider a situation where local higher stresses are located around the loaded area. The solution again gives a sandwich-like symmetric laminate with the stiff area around the center appearing in all layers. The plots are for the first four layers. In the unconstrained problem we can see from Figure 16 that there are higher stresses in a small region around the center and mainly in the surface layers. These are avoided in the constrained problem 17 and all layers around

17

Layer=1   Layer=2   Layer=3   Layer=4

(a)

Layer=1   Layer=2   Layer=3   Layer=4
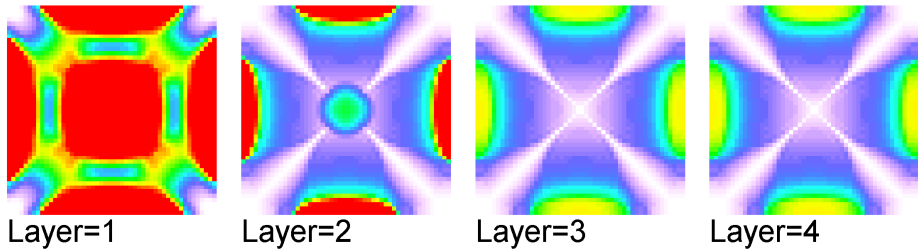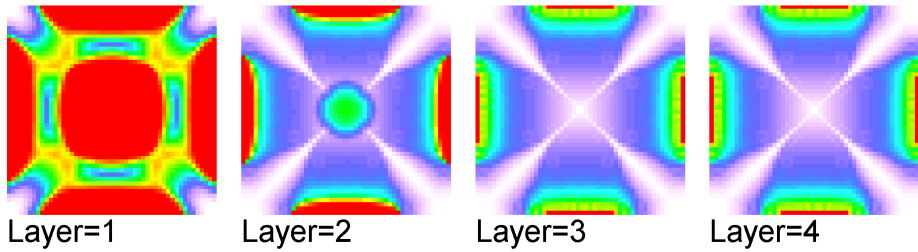
(b)

Figure 11: Optimal density distributions of the first four layers for the clamped plate with pressure load, (a) without stress constraints, (b) with stress constraints.
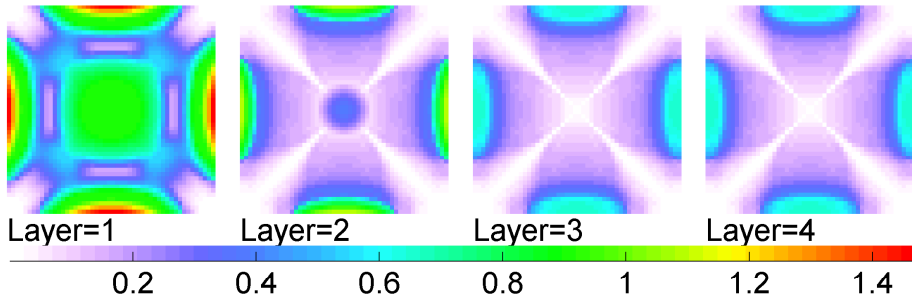
(a)
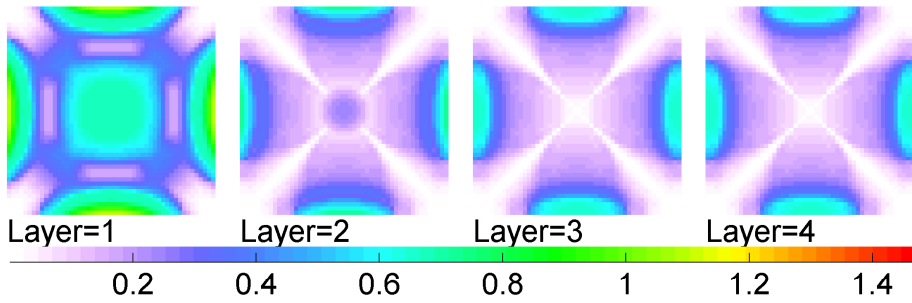
(b)

Figure 12: Optimal stress norms of the first four layers for the clamped plate with pressure load without stress constraints, (a) at the lower surfaces, (b) at the upper surfaces.
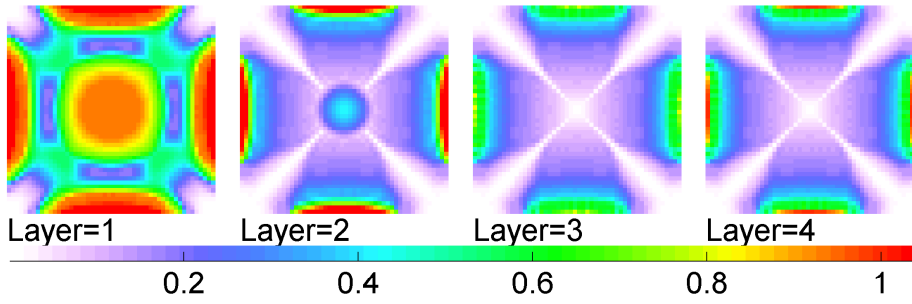
(a)
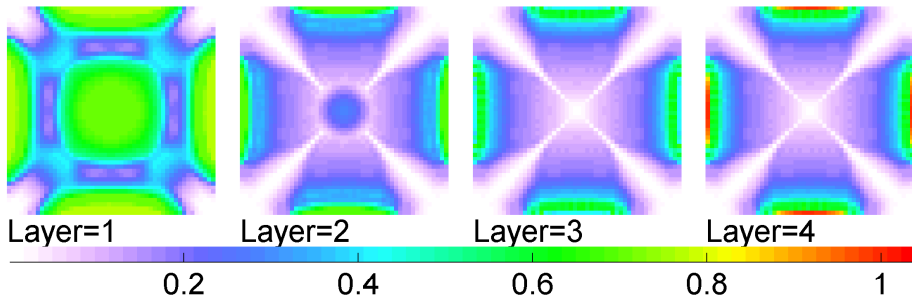
(b)

Figure 13: Optimal stress norms of the first four layers for the clamped plate with pressure load with stress constraints, (a) at the lower surfaces, (b) at the upper surfaces.
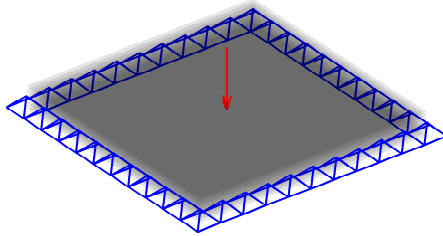
Figure 14: Design domain, boundary condition, and external load for the clamped plate with a point load at the center.

this region are involved in carrying the reduced stress. The density distributions are more or less similar, Figure 15.

Example 4.5. In this example we solve a two load case problem on a shell beam clamped at both ends loaded as in Figure 18. We report the plots for the optimal stress norms of the outer surface for one of the loads. The other cases can easily be determined from these plots. The higher stresses around the loaded region shown in Figure 20a in the unconstrained problem are avoided in the constrained problem, see Figure 20b. There is no clear difference in the topology of the optimal density distributions, Figure 19.

5   Conclusions

We introduce stress constraints to the FMO models proposed by the authors in [32] for laminated plates and shells for the first time. We extend the efficient primal-dual interior point method initially developed in [33] for solids and latter generalized in [32] for laminates to solve these stress constrained FMO problems. In the numerical experiments the high stresses in the unconstrained problems which occur mostly near the fixed or loaded areas are reduced in the constrained problems. The feasibility of the stress constraints is higher than we find in other articles (literatures are available only for solids). The number of iterations required to obtain solution to the problems of this article is between 85 and 142. This is modest considering the highly nonlinearity of the stress constraints and non-convexity of the problems. The efficiency of the method is implied indeed.

Layer=1   Layer=2   Layer=3   Layer=4

(a)

Layer=1   Layer=2   Layer=3   Layer=4
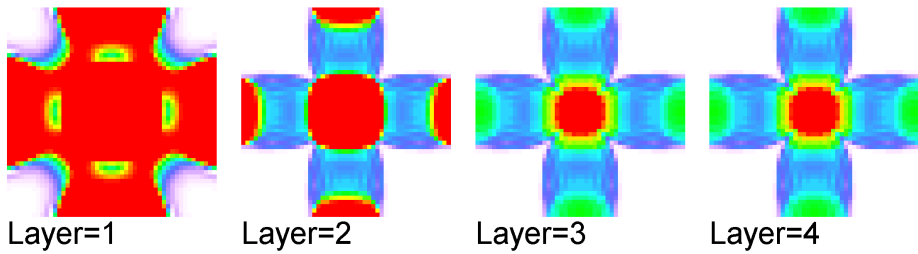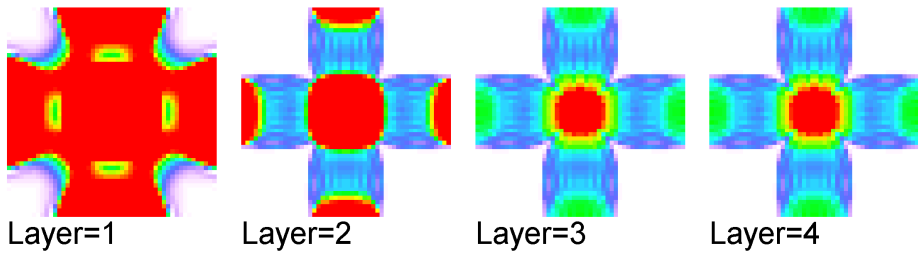
(b)

Figure 15: Optimal density distributions of the first four layers for the clamped plate with load at the center, (a) without stress constraints, (b) with stress constraints.
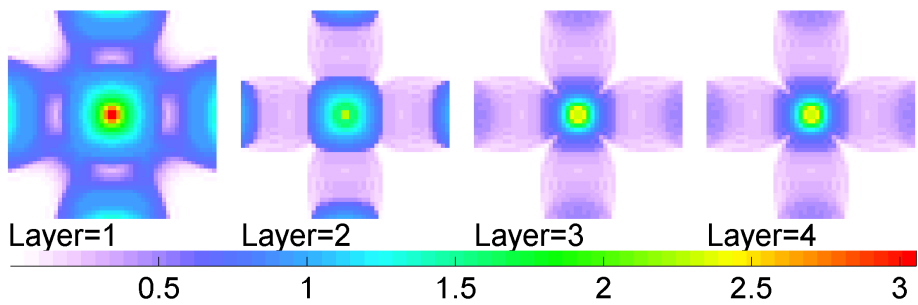
(a)
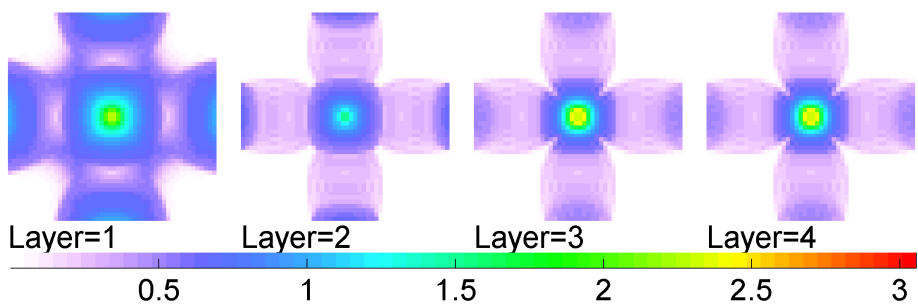
(b)

Figure 16: Optimal stress norms of the first four layers for the clamped plate with load at the center without stress constraints, (a) at the lower surfaces, (b) at the upper surfaces.
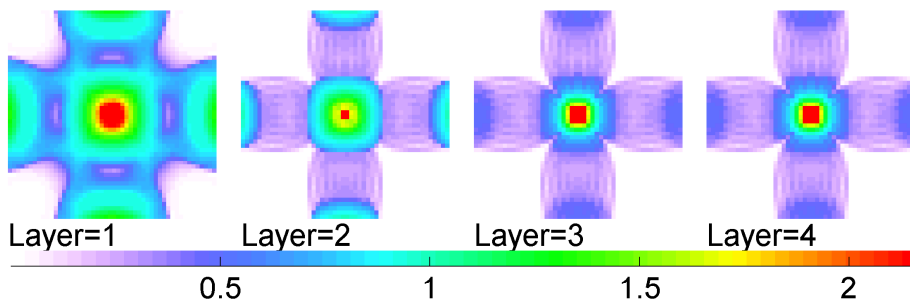
(a)
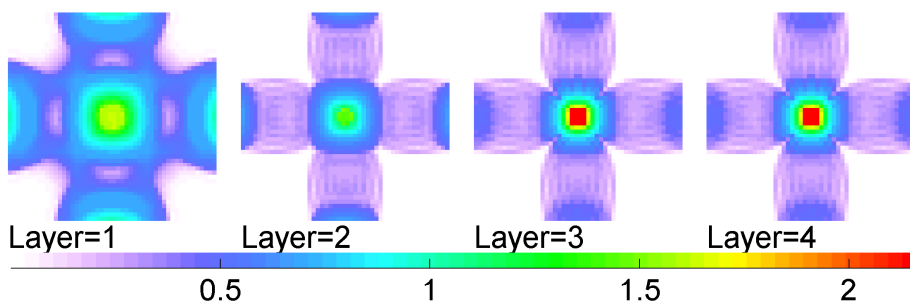
(b)

Figure 17: Optimal stress norms of the first four layers for the clamped plate with load at the center with stress constraints, (a) at the lower surfaces, (b) at the upper surfaces.
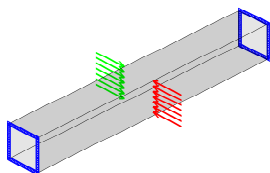
Figure 18: Design domain, boundary condition, and external load for the shell beam.
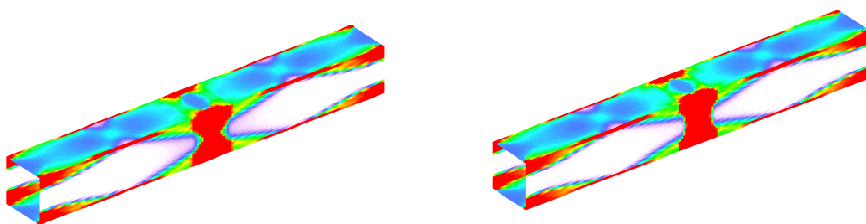
(a)   (b)

Figure 19: Optimal density distributions for the shell beam, (a) without stress constraints, (b) with stress constraints.

(a) (b)
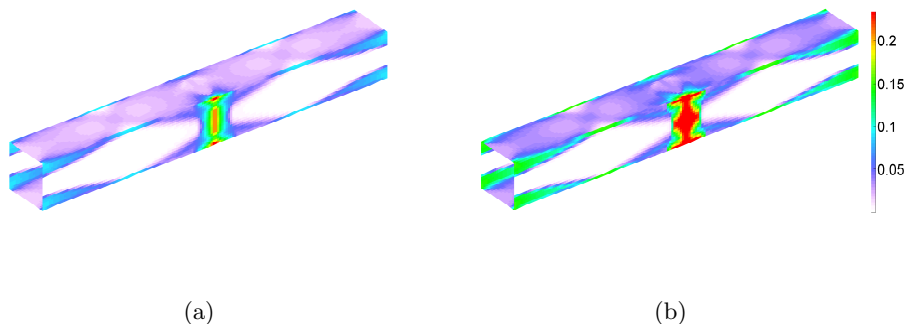
Figure 20: Optimal stress norms for the shell beam, (a) without stress constraints, (b) with stress constraints.

There are two special behaviors that we observed from the numerical experiments. There are (usually) only small differences in the density distributions of the solutions to the constrained an unconstrained FMO problems. This is because in FMO there is more freedom that it is possible to change material properties to avoid the high stresses. This actually contradicts to the practice in classical topology optimization with isotropic materials where the materials are fixed. The second behavior is that we see different practice regarding the compliance in FMO than in other structural optimizations. The values of compliances are only a little relaxed with less than 5% in the constrained problems even when the norm of the stresses are reduced by more than 50%.

We point out two future research areas. The first one is to analyze solutions to FMO problems on laminates. This will give a direction to identify the way stresses are reduced in FMO approach to laminates. The second future research work is on improving the computational efficiency of the algorithm. Stress constraints are in most cases active only in a certain regions in the design domain. Therefore, treating these constraints over the entire design domain in the algorithm is not numerically efficient. The algorithm can be improved by introducing active set technique where inactive stress constraints are removed during the optimization process.

Acknowledgments

My special thanks also go to my colleagues José Pedro Blasques and Robert Bitsche for many and fruitful discussions on laminated composite structures.

References

[1] Achtziger, W., Kanzow, C.: Mathematical programs with vanishing constraints. Mathematical Programming **114**(1), 69–99 (2008)

[2] Bendsøe, M.P., Díaz, A.R.: Optimization of material properties for Mindlin plate design. Structural Optimization **6**, 268–270 (1993)

[3] Bendsøe, M.P., Guedes, J.M., Haber, R.B., Pedersen, P., Taylor, J.E.: An analytical model to predict optimal material properties in the context of optimal structural design. Journal of Applied Mechanics **61**, 930–937 (1994)

[4] Chapelle, D., Bathe, K.J.: The Finite Element Analysis of Shells - Fundamentals. Springer, Heidelberg (2003)

[5] Cheng, G.D., Guo, X.: ε-relaxed approach in structural topology optimization. Structural Optimization **13**, 258–266 (1997)

[6] Cook, R.D., Malkus, D.S., Plesha, M.E., Witt, R.J.: Concepts and Applications of Finite Element Analysis, 4th edn. John Wiley and Sons (2002)

[7] Duysinx, P., Bendsøe, M.P.: Topology optimization of continuum structures with local stress constraints. International Journal for Numerical Methods in Engineering **43**, 1453–1478 (1998)

[8] Forsgren, A.: Inertia-controlling factorizations for optimization algorithms. Applied Numerical Mathematics **43**, 91–107 (2002)

[9] Gaile, S.: Free material optimization for shells and plates. Ph.D. thesis, Institute of Applied Mathematics II, Friedrich-Alexander University of Erlangen-Nuremberg (2011)

[10] Guo, X., Cheng, G., Yamazaki, K.: A new approach for the solution of singular optima in truss topology optimization with stress and local buckling constraints. Structural and Multidisciplinary Optimization **22**, 364–372 (2001)

[11] Haslinger, J., Kočvara, M., Leugering, G., Stingl, M.: Multidisciplinary free material optimization. SIAM Journal on Applied Mathematics **70**(7), 2709–2728 (2010)

[12] Hinton, M.J., Kaddour, A.S., Soden, P.D.: Failure criteria in fibre reinforced polymer composites: The world-wide failure exercise. Elsevier, Oxford, UK (2004)

[13] Kirsch, U.: On singular topologies in optimum structural design. Structural Optimization **2**, 133–142 (1990)

[14] Kočvara, M., Stingl, M.: A code for convex nonlinear and semidefinite programming. Optimization Methods and Software **18**(3), 317–333 (2003)

[15] Kočvara, M., Stingl, M.: Free material optimization for stress constraints. Structural and Multidisciplinary Optimization **33**, 323–355 (2007)

[16] Kočvara, M., Stingl, M.: Mathematical models of FMO with stress constraints FMO. Tech. rep., PLATO-N Public Report PU-R-1-2008 (2009). Available from http://www.plato-n.org/

[17] Kočvara, M., Stingl, M., Zowe, J.: Free material optimization: recent progress. Optimization **57**(1), 79–100 (2008)

[18] Le, C., Norato, J., Bruns, T., Ha, C., Tortorelli, D.: Stress-based topology optimization for continua. Structural and Multidisciplinary Optimization **41**, 605–620 (2010)

[19] Nocedal, J., Wright, S.J.: Numerical Optimization. Springer, NewYork, NY, USA (1999)

[20] París., J., Navarrina, F., Colominas, I., Casteleiro, M.: Topology optimization of continuum structures with local and global stress constraints. Structural and Multidisciplinary Optimization **39**(4), 419–437 (2009)

[21] Reddy, J.: Mechanics of laminated composite plates and shells: theory and analysis, 2nd edn. London (2004)

[22] Ringertz, U.T.: On finding the optimal distribution of material properties. Structural Optimization **5**, 265–267 (1993)

[23] Rozvany, G.I.N.: Difficulties in truss topology optimization with stress, local buckling and system stability constraints. Structural Optimization **11**, 213–217 (1996)

[24] Stingl, M.: On the solution of nonlinear semidefinite programs by augmented lagrangian method. Ph.D. thesis, Institute of Applied Mathematics II, Friedrich-Alexander University of Erlangen-Nuremberg (2006)

[25] Stingl, M., Kočvara, M., Leugering, G.: Free material optimization with fundamental eigenfrequency constraints. SIAM Journal on Optimization **20**(1), 524–547 (2009)

[26] Stingl, M., Kočvara, M., Leugering, G.: A new non-linear semidefinite programming algorithm with an application to multidisciplinary free material optimization. International Series of Numerical Mathematics **158**, 275–295 (2009)

[27] Stingl, M., Kočvara, M., Leugering, G.: A sequential convex semidefinite programming algorithm with an application to multiple-load free material optimization. SIAM Journal on Optimization **20**(1), 130–155 (2009)

[28] Stingl, M., Kočvara, M., Leugering, G.: A sequential convex semidefinite programming algorithm with an application to multiple-load free material optimization. SIAM Journal on Optimization **20**(1), 130–155 (2009)

[29] Stolpe, M., Svanberg, K.: On the trajectories of the epsilon-relation relaxation approach for stress-constrained truss topology optimization. Structural and Multidisciplinary Optimization **21**, 140–151 (2001)

[30] Stolpe, M., Svanberg, K.: A note on tress-based truss topology optimization. Structural and Multidisciplinary Optimization **25**, 62–64 (2003)

[31] Wächter, A., Biegler, L.T.: On the implementation of an interior-point filter line-search algorithm for large-scale nonlinear programming. Mathematical Programming **106**, 25–57 (2006)

[32] Weldeyesus, A.G., Stolpe, M.: Free material optimization for laminated plates and shells. Tech. rep., DTU Wind Energy (2014). Submitted

[33] Weldeyesus, A.G., Stolpe, M.: A primal-dual interior point method for large-scale free material optimization. Computational Optimization and Applications (2014). DOI 10.1007/s10589-014-9720-6

[34] Werner, R.: Free material optimization-mathematical analysis and numerical solution. Ph.D. thesis, Institute of Applied Mathematics II, Friedrich-Alexander University of Erlangen-Nuremberg (2001)

[35] Yang, B.J., Chen, C.J.: Stress-based topology optimization. Structural Optimization **12**, 98–105 (1996)

[36] Zowe, J., Kočvara, M., Bendsøe, M.P.: Free material optimization via mathematical programming. Mathematical Programming **79**, 445–466 (1997)

Chapter 8

On solving Free Material Optimization problems using iterative methods

On solving Free Material Optimization problems using iterative methods

Mathias Stolpe[*] and Alemseged Gebrehiwot Weldeyesus[†]

Abstract

Free Material Optimization (FMO) is concerned with obtaining the optimal material distribution and the optimal local material properties of a load bearing structures. The problems are formulated with the stiffness tensor taken as design variable. These formulations lead to large scale nonlinear semidefinite programming problems for which specialized and efficient methods are usually preferred. The authors have developed a primal-dual interior point method in which the saddle point systems for obtaining the search directions are solved using direct solvers. This requires large memory and restricts the size of the problems that can solved. The goal of this article is to introduce iterative solvers to the method. Two different preconditioners are proposed and they are evaluated by solving several large-sclae 3D problems.

Mathematics Subject Classification 2010: 90C22, 90C90, 74P05, 74P15

Keywords: Structural optimization, free material optimization, semidefinite optimization, iterative methods

1   Introduction

Free Material Optimization (FMO) is branch of structural optimization in which we search for the optimal material distribution and the optimal local material

[*]DTU Wind Energy, Technical University of Denmark, Frederiksborgvej 399, 4000 Roskilde, Denmark. E-mail: matst@dtu.dk

[†]DTU Wind Energy, Technical University of Denmark, Frederiksborgvej 399, 4000 Roskilde, Denmark. E-mail: alwel@dtu.dk

properties. The basic formulations were studied in the early 1990s in [2], [3], and [20]. Throughout the last two decades FMO has been studied in several articles. Current FMO models have been extended to treat a wide range of constraints such as limits on stresses, strains, displacement, and fundamental frequencies in e.g. [16], [14], [12], and [23]. The models are further extended to problems on curved thin-wall structures in [9] and to laminated structures in [29]. FMO theories focusing on existence of optimal solutions have been analyses in several article, see e.g. [12] and [31].

The design variable in FMO is the stiffness tensor which is allowed to vary at each point of the design domain but forced to be symmetric and positive semidefinite. Hence, the problems are classified as nonlinear semidefinite programs. Various methods have been proposed for solving FMO problems. These include a method based on penalty/barrier multipliers (PBM) in [34] and a method based on augmented Lagrangian function in [13] and [22], a method based on a sequential convex programming concept [25, 24], and a method based on interior point methods [30]. Second-order methods, such as interior point methods, for solving large-scale FMO problems demand typically large memory. In order to cope with this challenge it is important that iterative solvers are employed to the methods. In none of the methods and articles listed above the use of iterative solvers is explicitly described.

The main challenge in using iterative solvers is the development of an efficient preconditioners. The extent of the challenge is even worse in optimization methods since the saddle-point system that needs to be solved becomes more and more ill-conditioned as the iterates are closing in on the optimal solution. Various preconditioners have been proposed for linear and convex quadratic programming, see [1] and [19], and for nonlinear optimization problems, see [7] and [5] and the references therein. The optimization problems arising form FMO belong to a class optimization called (nonlinear) SemiDefinite Programming (SDP). In [8], [27], [28], and [33] iterative solvers have been used for solving linear SDP problems. For the method based on augmented Lagrangian function in [13] iterative solvers are introduced in [15]. The method has solved a set of SDP problems. It is claimed in [22], [14], and [16] that it has been also used to solve FMO problems with no report on related numerical statistics. However, in [25] it is pointed out that the success is moderate.

The objective of this article is to introduce iterative solvers to the saddle-point system in the primal-dual interior point method in [30]. The method in [30] has appealing numerical behavior. It efficiently utilizes the problem structure that each of the matrix inequalities involves small size matrix. It has obtained high quality solutions to large two-dimensional FMO problems within modest number of iterations that is almost independent to problem size.

Notation: For $(d_1, d_2, \ldots, d_m) \in \mathbb{N}^m$ let $\mathbb{S} = \mathbb{S}^{d_1} \times \mathbb{S}^{d_2} \times \cdots \times \mathbb{S}^{d_m}$ where

$\mathbb{S}^{d_i}$ be the space of symmetric $d_i \times d_i$ matrices. We denote by $\mathbb{S}^{d_i}_+$ the cone of positive semidefinite matrices $\mathbb{S}^{d_i}$, i.e., $E_i \in \mathbb{S}^N_+$ if and only if $E_i = E_i^T$ and $E_i \succeq 0$. We define the operator $\mathcal{T}_1 : \mathbb{S} \to \mathbb{R}^m$ by $(\mathcal{T}_1 E)_i = Tr(E_i)$ and the operator $\mathcal{T}_2 : \mathbb{S} \to \mathbb{R}$ by $\mathcal{T}_2 E = \sum_i Tr(E_i)$ for every $E = (E_1, \ldots, E_m)^T \in \mathbb{S}$. The adjoints of these operators are $\mathcal{T}_1^* : \mathbb{R}^m \to \mathbb{S}$ defined by $(\mathcal{T}_1^* y)_i = y_i I$ for every $y \in \mathbb{R}^m$ and $\mathcal{T}_2^* : \mathbb{R} \to \mathbb{S}$ defined by $(\mathcal{T}_2^* \alpha)_i = \alpha I$ for every $\alpha \in \mathbb{R}$ where the identity matrix I in both cases has the same size as E_i. For some non-singular matrix $P \in \mathbb{R}^{n \times n}$ is the linear operator H_P[1] $: \mathbb{R}^{n \times n} \to \mathbb{S}^n$ is defined by $H_P(Q) := \frac{1}{2} \left(PQP^{-1} + (PQP^{-1})^T \right)$. The operator $P \odot Q : \mathbb{S}^n \to \mathbb{S}^n$ is defined by $(P \odot Q)K := \frac{1}{2}(PKQ^T + QKP^T)$.

2 Problem formulations

We consider the discrete version of the minimum compliance (maximum stiffness) FMO problem formulation described in most of todays articles. For the problem formulation in function space and related mathematical treatments such as existence of solution, see the recent article [12] and the references there in.

We consider a design domain Ω which is partitioned into m uniform elements. The stiffness tensor $E(x)$ is function constant on each element such that the element values constituting the vector of block matrices $E = (E_1, \ldots, E_m)^T$. For a given static load vector $f \in \mathbb{R}^n$ the associated displacement satisfies the linear elastic equilibrium equation

$$A(E)u = f \tag{1}$$

where $A(E) \in \mathbb{R}^{n \times n}$ is the global stiffness matrix.

The most common quantity used in FMO to measure stiffness is the trace of the stiffness tensor. Arbitrary local stiffness and extreme softness are controlled by introducing a local upper bound $\bar{\rho}$ and a lower bound $\underline{\rho}$ on the trace of the stiffness tensor. These bounds are assumed to satisfy $0 \leq \underline{\rho} < \bar{\rho} < \infty$. For the requirement of the physical attainability of the stiffness tensor is introduced by matrix inequality constraints. We then define the set of admissible materials by

$$\mathbb{E} := \left\{ E \in (\mathbb{S}^d_+)^m \mid \underline{\rho}e \leq \mathcal{T}_1 E \leq \bar{\rho}e \right\} \tag{2}$$

where $e = (1, 1, \ldots, 1)^T$ is a vector of all ones of appropriate size and $d = 3$ for two-dimensional problems and $d = 6$ for three-dimensional problems. The amount of available resource material is described by $\mathcal{T}_2 E$ and this should not

---

[1] This was introduced in [32]. Moreover, it is shown that $H_P(Q) = \mu I \Leftrightarrow Q = \mu I$ for a scalar μ.

exceed the volume fraction V satisfying the relation

$$\sum_{i=1}^{m} \underline{\rho} < V < \sum_{i=1}^{m} \bar{\rho}.$$

The basic single load minimum compliance FMO problem is the formulated as

$$\begin{aligned}
\underset{u\in\mathbb{R}^n, E\in\mathbb{E}}{\text{minimize}} \quad & f^T u \\
\text{subject to} \quad & A(E)u = f \\
& \mathcal{T}_2 E \le V.
\end{aligned} \tag{3}$$

The problem formulation (3) has a linear objective function, linear matrix inequalities and nonlinear (and nonconvex) vector constraints. Hence, it is classified as nonconvex SDP problems.

3 The barrier problem and optimality condition

This section, which presents parts of the interior point method, is essentially identical to Section 4 of [30] and is included for completeness. We introduce the slack variables $(\bar{r}, \underline{r}, s) \in \mathbb{R}_+^m \times \mathbb{R}_+^m \times \mathbb{R}_+$ and barrier parameter $\mu > 0$ to problem (3) and formulate the associated barrier problem as

$$\begin{aligned}
\underset{u\in\mathbb{R}^n, E\in\mathbb{E}, \bar{r}, \underline{r}, s}{\text{minimize}} \quad & f^T u - \mu \sum_{i=1}^{m} \ln(\det(E_i)) - \mu \sum_{i=1}^{m} \ln(\bar{r}_i) - \mu \sum_{i=1}^{m} \ln(\underline{r}_i) - \mu \ln(s) \\
\text{subject to} \quad & A(E)u - f = 0, \\
& \mathcal{T}_1 E + \bar{r} - \bar{\rho} e = 0, \\
& \underline{\rho} e - \mathcal{T}_1 E + \underline{r} = 0, \\
& \mathcal{T}_2 E + s - V = 0.
\end{aligned} \tag{4}$$

The strict positivity of the slack variables is implicitly understood in the logarithmic functions. The barrier problem (4) has the following Lagrange function

$$\begin{aligned}
\mathcal{L}(x) = & f^T u - \mu \sum_{i=1}^{m} \ln(\det(E_i)) - \mu \sum_{i=1}^{m} \ln(\bar{r}_i) - \mu \sum_{i=1}^{m} \ln(\underline{r}_i) - \mu \ln(s) \\
& + \lambda^T (A(E)u - f) + \bar{\beta}^T (\mathcal{T}_1 E + \bar{r} - \bar{\rho} e) \\
& + \underline{\beta}^T (\underline{\rho} e - \mathcal{T}_1 E + \underline{r}) + \alpha(\mathcal{T}_2 E + s - V),
\end{aligned} \tag{5}$$

4

where $x = (E, u, \bar{r}, \underline{r}, s, \lambda, \bar{\beta}, \underline{\beta}, \alpha)$ and $(\lambda, \bar{\beta}, \underline{\beta}, \alpha) \in \mathbb{R}^n \times \mathbb{R}^m_+ \times \mathbb{R}^m_+ \times \mathbb{R}_+$ are Lagrange multipliers. The first-order optimality conditions to problem (4) are

$$\lambda^T F(u) - Z + \mathcal{T}_1^* \bar{\beta} - \mathcal{T}_1^* \underline{\beta} + \mathcal{T}_2^* \alpha = 0 \tag{6a}$$

$$A(E)\lambda + f = 0 \tag{6b}$$

$$A(E)u - f = 0 \tag{6c}$$

$$\mathcal{T}_1 E + \bar{r} - \bar{\rho}e = 0 \tag{6d}$$

$$\underline{\rho}e - \mathcal{T}_1 E + \underline{r} = 0 \tag{6e}$$

$$\mathcal{T}_2 E + s - V = 0 \tag{6f}$$

$$\bar{R}\bar{B} - \mu e = 0 \tag{6g}$$

$$\underline{R}\,\underline{B} - \mu e = 0 \tag{6h}$$

$$s\alpha - \mu = 0 \tag{6i}$$

$$H_P(EZ) - \mu I = 0 \tag{6j}$$

where

$$\bar{B} = \operatorname{diag}(\bar{\beta}), \ \underline{B} = \operatorname{diag}(\underline{\beta}), \ \bar{R} = \operatorname{diag}(\bar{r}), \ \underline{R} = \operatorname{diag}(\underline{r}),$$

and $F(u) = (A_1(E)^{j,k}u, \ldots, A_m(E)^{j,k}u)$ with $A_i(E)^{j,k} = \frac{\partial A_i(E)}{\partial (E_i)_{j,k}}$ and the multiplication $\lambda^T F(u)$ defined such that $(\lambda^T F(u))_i = \lambda^T A_i(E)^{j,k}u$ for each j and k in the set of indices of E_i. The complementarity equation (6j) appearing in the optimality conditions is the result of setting $Z := \mu E^{-1}$ in equation (6a). The application of the operator H_p is to ensure symmetry of the product EZ. The directions obtained by various choices of P are of the Monteiro-Zhang (MZ) family [32]. We follow the recommendation made in [30] and use the NT direction [17, 18] obtained when $P = W^{-1/2}$ with $W = E^{1/2}(E^{1/2}ZE^{1/2})^{-1/2}E^{1/2}$ for its robustness in solving FMO problems.

Under the assumption that $E \succ 0$ the matrix $A(E)$ is positive definite [25]. The Lagrange multiplier λ is then uniquely determined is then adjoint equation $A(E)\lambda + f = 0$. This allows us to make the substitution $\lambda = -u$ in (6a) and reduce the optimality conditions to the the primal residuals (6c)-(6f), the perturbed complementary conditions (6g)-(6j) and

$$-u^T F(u) - Z + \mathcal{T}_1^* \bar{\beta} - \mathcal{T}_1^* \underline{\beta} + \mathcal{T}_2^* \alpha = 0. \tag{7}$$

Let R_d, $(r_{p_1}, \ldots, r_{p_4})$, and $(r_{c_1}, \ldots, r_{c_3}, R_{c_4})$ be the negative of the left hand sides of (7), the negative of the primal residuals, and the negative of the perturbed complementary residuals respectively. We apply Newton's method to the reduced system to compute the search directions. After making reductions by eliminating

$\Delta\bar{\beta}$, $\Delta\underline{\beta}$, $\Delta\bar{r}$, $\Delta\underline{r}$, and Δs as in (13) we obtain a reduced primal-dual system

$$\begin{pmatrix} -\frac{1}{2}A(E) & F(u) & 0 \\ F(u)^T & D & \mathcal{T}_2^* \\ 0 & \mathcal{T}_2 & -s/\alpha \end{pmatrix} \begin{pmatrix} \Delta\tilde{u} \\ \Delta E \\ \Delta\alpha \end{pmatrix} = \begin{pmatrix} f - A(E)u \\ R_1 \\ r_1 \end{pmatrix} \qquad (8)$$

where D is a block diagonal matrix given by

$$D = \mathcal{F}^{-1}\mathcal{E} + \mathcal{T}_1^*(\bar{R}^{-1}\bar{B} + \underline{R}^{-1}\underline{B})\mathcal{T}_1, \qquad (9)$$

and R_1 and r_1 are given by

$$R_1 = R_d + \mathcal{F}^{-1}R_{c_4} - \mathcal{T}_1^*\bar{R}^{-1}(r_{c_1} - \bar{B}r_{p_2}) + \mathcal{T}_1^*\underline{R}^{-1}(r_{c_2} - \underline{B}r_{p_3}) \qquad (10)$$

$$r_1 = r_{p_4} - \frac{1}{\alpha}r_{c_3}. \qquad (11)$$

Note that $F(u)\Delta E = \sum_i \sum_{j,k}(A_i(E)^{j,k}u)(\Delta E_i)_{j,k}$ with j and k in the set of indices of E_i.
The block diagonal matrices $\mathcal{E} = \mathcal{E}(E,Z)$ and $\mathcal{F} = \mathcal{F}(E,Z)$ in (9) are the derivatives of $H_P(EZ)$ with respect to E and Z respectively and are determined by

$$\mathcal{E} = P \odot P^{-T}Z \text{ and } \mathcal{F} = PE \odot P^{-1} \qquad (12)$$

The search directions $\Delta\bar{\beta}$, $\Delta\underline{\beta}$, $\Delta\bar{r}$, $\Delta\underline{r}$, and Δs are computed as

$$\Delta u = -2\Delta\tilde{u} \qquad (13a)$$

$$\Delta Z = \mathcal{F}^{-1}(R_{c_4} - \Delta E) \qquad (13b)$$

$$\Delta\bar{r} = r_{p_2} - \mathcal{T}_1\Delta E \qquad (13c)$$

$$\Delta\underline{r} = r_{p_3} + \mathcal{T}_1\Delta E \qquad (13d)$$

$$\Delta\bar{\beta} = \bar{R}^{-1}(r_{c_1} + \bar{B}(-r_{p_2} + \mathcal{T}_1\Delta E)) \qquad (13e)$$

$$\Delta\underline{\beta} = \underline{R}^{-1}(r_{c_2} + \underline{B}(-r_{p_3} - \mathcal{T}_1\Delta E)) \qquad (13f)$$

$$\Delta s = \frac{1}{\alpha}(r_{c_3} - s\Delta\alpha). \qquad (13g)$$

where $\tilde{u}$ in (13a) is introduced to make the coefficient matrix in (8) symmetric.

4 Preconditioners

The preconditioners proposed in this section are motivated by those proposed in [26] for solving large-scale variable thickness sheet problems. We start first with

constructing the preconditioner for the stiffness matrix $A(E)$ based on the Separate Displacement Component (SDC), see e.g. [11]. This is done by reordering of the stiffness matrix $A(E)$ as

$$A(E) = \begin{pmatrix} A_{xx}(E) & A_{xy}(E) & A_{xz}(E) \\ A_{yx}(E) & A_{yy}(E) & A_{yz}(E) \\ A_{zx}(E) & A_{zy}(E) & A_{zz}(E) \end{pmatrix} \tag{14}$$

and taking the taking the decoupling terms to define the SDC preconditioner $P(E)$ by

$$P(E) = \text{blkdiag}(A_{xx}(E), A_{yy}(E), A_{zz}(E)). \tag{15}$$

Based on the general theory in [4], we propose the block triangular preconditioner

$$P_S = \begin{pmatrix} -\frac{1}{2}P(E) & F(u) & 0 \\ 0 & \hat{S} & \mathcal{T}_2^* \\ 0 & \mathcal{T}_2 & -s/\alpha \end{pmatrix} \tag{16}$$

where

$$\hat{S} = D + 2\text{diag}(F(u)^T \text{diag}(P(E))^{-1} F(u)) \tag{17}$$

is an approximation of the Schur complement for the primal-dual system (8) and for relatively large μ values, say $\mu > 10^{-4}$.

The preconditioner P_s in (16) is not effective when μ values are small and the interior-point iterates approach an optimal solution. This is because the the saddle-point system (8) becomes severely ill-conditioned at this point. For this case we go for a rather expensive approach that overcomes the ill-conditioning by employing perturbation in the block diagonal matrix D. This is done by introducing the matrix

$$G = C + D \tag{18}$$

where C is a given positive semidefinite (block) diagonal matrix. In the system (8) we multiply the second row by $-F(u)G^{-1}$ and add it to the first row and by $-\mathcal{T}_2 G^{-1}$ and add it to the third row. Moreover, we make the change of variable

$$\Delta\tilde{E} = G^{-1}C\Delta E \tag{19}$$

and rewrite the system (8) as

$$\begin{pmatrix} H & F(u) & b \\ F(u)^T & DC^{-1}G & \mathcal{T}_2^* \\ b^T & \mathcal{T}_2 & q \end{pmatrix} \begin{pmatrix} \Delta\tilde{u} \\ \Delta\tilde{E} \\ \Delta\alpha \end{pmatrix} = \begin{pmatrix} f - A(E)u - F(u)G^{-1}R_1 \\ R_1 \\ r_1 - \mathcal{T}_2 G^{-1} R_1 \end{pmatrix} \tag{20}$$

where

$$H = -\left(\frac{1}{2}A(E) + F(u)G^{-1}F(u)^T\right), \ b = -F(u)G^{-1}\mathcal{T}_2^*, \ q = -(s/\alpha + \mathcal{T}_2 G^{-1}\mathcal{T}_2^*) \tag{21}$$

7

For the system (20) we propose the block triangular preconditioner

$$Q_s = \begin{pmatrix} \tilde{H} & F(u) & b \\ 0 & \tilde{S}_{11} & \tilde{S}_{12} \\ 0 & \tilde{S}_{21} & \tilde{S}_{22} \end{pmatrix} \tag{22}$$

where

$$\tilde{H} = -\left(\frac{1}{2}P(E) + F(u)G^{-1}F(u)^T\right), \ \tilde{S}_{11} = DE^{-1}G - \text{diag}(F(u)^T\text{diag}(\tilde{H})^{-1}F(u))$$

$$\tilde{S}_{12} = \mathcal{T}_2^* - F(u)^T\text{diag}(\tilde{H})^{-1}b, \ \tilde{S}_{22} = q - b^T\text{diag}(\tilde{H})^{-1}b$$

For solving with $\hat{H}$ we expand the system to

$$\begin{pmatrix} -\frac{1}{2}P(E) & F(u) \\ F(u)^T & G \end{pmatrix} \tag{23}$$

and from numerical experiment point of view we suggest the preconditioner

$$\begin{pmatrix} -\frac{1}{2}P(E) - \text{diag}(F(u)^T G^{-1}F(u)) & F(u) \\ 0 & G \end{pmatrix}. \tag{24}$$

We use preconditioned conjugate gradient method with incomplete Cholesky factorization for solving with the preconditioner $P(E)$. We apply flexible GMRES to solve the systems (8), (20) and (23) where low tolerance is set for the last system. For details on the Krylov subspace methods, see e.g. [21]. We employ the Sherman-Morrison formula [10] for solving with the blocks in the second and third rows and columns of the preconditioners P_s and Q_s.

5 The algorithm

In the primal-dual interior point method developed in [30] the barrier problem (4) needs to be solved for a sequence of barrier parameter μ_k monotonically converging to zero. The solution of the barrier problem for sufficiently small μ value corresponds to the solution of the original problem (3). The detail of method is described in [30]. We present an overview of the method in Algorithm 1 for compelteness.

6 Implementation and numerical experiments

The interior point method and the finite element routines are implemented in MATLAB. The standard eight-node hexahedral elements are considered with full

Algorithm 1 The primal-dual interior point algorithm described in [30]

Choose x^0 and μ_0.
while stopping criteria for problem (3) is not satisfied **do**
    while stopping criteria for problem (4) is not satisfied **do**
        Compute the search direction Δx^k by solving system (8) and (13).
        Compute step length α in two steps.
            1. Compute the maximum possible step using fraction to the boundary rule.
            2. Perform a backtracking line search using the norm of the KKT system as merit function.
        Set the new iterate as $x^{k+1} = x^k + \alpha\Delta x^k$.
    end while
    Update μ_{k+1}.
end while

Gaussian integration, see e.g. [6]. The optimality measure for solving the barrier problem (4) is the norm of the optimality conditions. The optimality measure for solving the original problem (4) is the norm of the optimality conditions measured without perturbation on the complementarity conditions. The optimality and feasibility tolerances are both set to 10^{-6} in the implementation. For starting point in the algorithm the design variable is set to $E = 0.1\bar{\rho}I$. The displacement and Lagrange multiplies for the equality constraints are set to zero. is set to $u = 0$. The slack variables and Lagrange multiplies for the inequality constraints are set to ones or identity. The volume fraction is set to 40% of the maximum possible weight. The local volume bounds are set to $\bar{\rho} = 1$ and $\underline{\rho} = 10^{-5}$. The matrix C in (18) is set to $0.01I$.

If the number flexible GMRES iterations exceeds 70 for solving the system (8) with the preconditioner (16) then the algorithm is set to switch to solving the system (20) with the preconditioner (22). After making this switch the maximum number of flexible GMRES iterations for the first inner interior point iterations is set to 70 and for the next inner iterations to 20. This approach is not particularly efficient (or pretty) and will be improved in the future.

For the numerical experiments we consider the three-dimensional problems shown in Figure 1. The first problem is the classical Michell beam problem with dimensions $1 \times 2 \times 4$ with lower side fixed and shear load at the top, see Figure 1a. The second problem is the cantilever beam problem of dimensions $1 \times 1 \times 1.5$ fixed at the four corners of the lower side subjected to a tip load, see Figure 1b. In the third example the design domain is a bar stool of dimensions $1 \times 1 \times 1$ and is fixed at the four corners of the lower side and loaded at the middle of the upper side, see Figure 1c. There are three levels of finite element discretizations
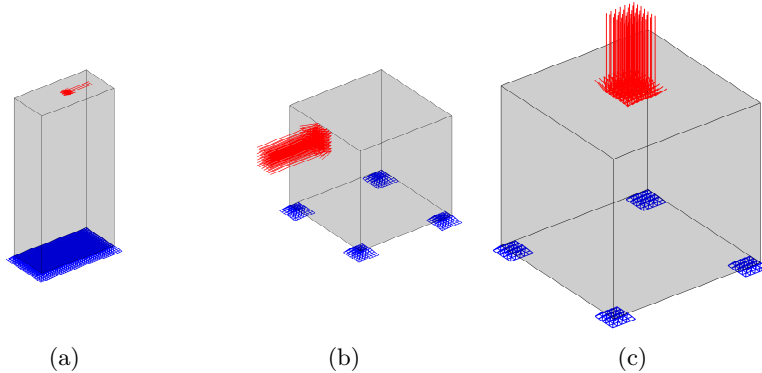
Figure 1: Design domains, boundary conditions and loads for the Michell beam problem (a), the Cantilever beam problem (b), the Bar stool problem (c).

for each of the design domains. In all cases the loads are applied over an area of size 0.2×0.2. The problem instances are reported in Table 1.

We report the numerical results in Table 2 for the problems in Table 1. The method has obtained the optimal solutions for all problem instances satisfying the prescribed tolerances. The optimal density distributions are shown in Figure 2. The behavior of the method is rather promising but not fully satisfactory. This can be seen from Figure 3 relating flexible GMRES iterations to interior point iterations for the Michell beam problem. The plot shows that after certain interior point iterations the method requires almost the maximum allowed number of iterations for each first inner interior point iterations that is followed by multiple inner interior point iterations. The switching μ values from using the preconditioner (16) to using the preconditioner (22) for the problems Michell I, Michell II, and Michell III are $3.3e - 04$, $1.3e - 06$, and $1.1e - 03$, respectively.

7   Conclusions

We introduce iterative solvers to the primal-dual interior point method in [30] and achieve preliminary numerical success. It was possible to obtain solution for a set of large-scale problems. However, the preconditioners proposed for solving the barrier problem that corresponds to small barrier parameter are expensive and are not powerful enough. The research is an ongoing study and is in its early

(a)

(b)

(c)
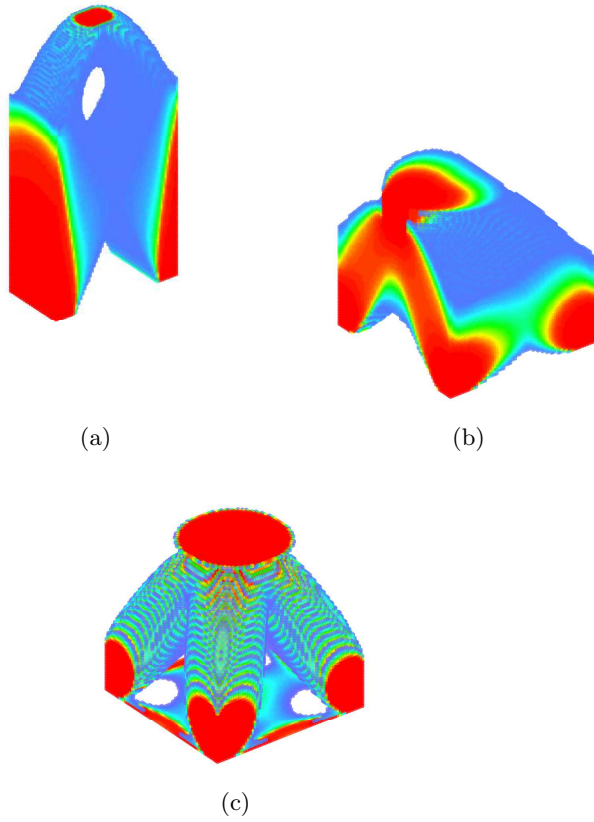
Figure 2: Optimal density distribution for the Michell beam problem (a), the Cantilever beam problem (b), the Bar stool problem (c).
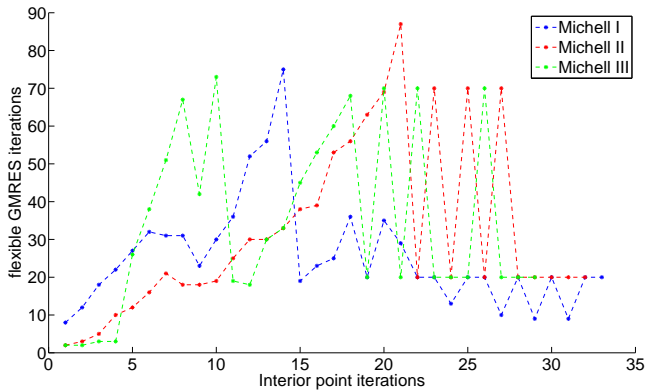
Figure 3: Flexible GMRES iterations versus interior point iterations for the Michell beam problems.

Table 1: Problem instances.

Problem	No. of finite elements in each direction $(N_x \times N_y \times N_z)$	Total No. of of finite elements	No. of design variables	No. of non-fixed state variables
Michell I	$8 \times 16 \times 32$	4096	86016	14688
Michell II	$16 \times 32 \times 64$	32768	688128	107712
Michell III	$32 \times 64 \times 128$	262144	5505024	823680
Cantilever I	$16 \times 16 \times 16$	4096	86016	14691
Cantilever II	$32 \times 32 \times 32$	32768	688128	107619
Cantilever III	$64 \times 64 \times 64$	262144	5505024	823443
Bar stool I	$16 \times 16 \times 16$	4096	86016	14691
Bar stool II	$32 \times 32 \times 32$	32768	688128	107619
Bar stool III	$64 \times 64 \times 64$	262144	5505024	823443

stages. The main topics to work on will be the development of more efficient preconditioners, theoretical explanations, and improved algorithmic strategies.

References

[1] Al-Jeiroudi, G., Gondzio, J., Hall, J.: Preconditioning indefinite systems in interior point methods for large scale linear optimisation. Optimization

Table 2: Numerical results.

Problem	Itn	FGMRES itn. large μ	FGMRES itn. small μ	feas/opt tolerances
Michell I	38	453	389	$1.2e-07/2.4e-07$
Michell II	30	647	370	$2.6e-07/8.8e-07$
Michell III	29	307	696	$5.1e-07/6.6e-07$
Cantilever I	26	410	378	$3.9e-07/1.8e-07$
Cantilever II	39	490	643	$4.6e-07/9.1e-07$
Cantilever III	33	561	370	$3.0e-07/5.4e-07$
Bar stool I	28	487	478	$2.3e-07/7.4e-07$
Bar stool II	43	467	961	$1.7e-07/8.7e-07$
Bar stool III	40	394	746	$2.4e-07/8.0e-07$

Methods and Software **23**, 345–363 (2008)

[2] Bendsøe, M.P., Díaz, A.R.: Optimization of material properties for Mindlin plate design. Structural Optimization **6**, 268–270 (1993)

[3] Bendsøe, M.P., Guedes, J.M., Haber, R.B., Pedersen, P., Taylor, J.E.: An analytical model to predict optimal material properties in the context of optimal structural design. Journal of Applied Mechanics **61**, 930–937 (1994)

[4] Benzi, M., Golub, G.H., Liesen, J.: Numerical solution of saddle point problems. Acta Numerica **14**, 1–137 (2005)

[5] Bergamaschi, L., Gondzio, J., Zilli, G.: Preconditioning indefinite systems in interior point methods for optimization. Computational Optimization and Applications **28**, 149–171 (2004)

[6] Cook, R.D., Malkus, D.S., Plesha, M.E., Witt, R.J.: Concepts and Applications of Finite Element Analysis, 4th edn. John Wiley and Sons (2002)

[7] Forsgren, A., Gill, P.E., Griffin, D.J.: Iterative Solution of Augmented Systems Arising in Interior Methods. SIAM Journal on Optimization **18**, 666–690 (2007)

[8] Fukuda, M., Kojima, M., Shida, M.: Lagrangian dual interior-point methods for semidefinite programs. SIAM Journal on Optimization **12**, 10071031 (2002)

[9] Gaile, S.: Free material optimization for shells and plates. Ph.D. thesis, Institute of Applied Mathematics II, Friedrich-Alexander University of Erlangen-Nuremberg (2011). Available from http://www.researchgate.net/

[10] Golub, G.H., van Loan, C.F.: Matrix Computations, 3rd edn. Johns Hopkins University Press (1996)

[11] Gustafsson, I., Lindskog, G.: On parallel solution of linear elasticity problems: Part I: theory. Numerical Linear Algebra with Applications **5**(2), 123–139 (1998)

[12] Haslinger, J., Kočvara, M., Leugering, G., Stingl, M.: Multidisciplinary free material optimization. SIAM Journal on Applied Mathematics **70**(7), 2709–2728 (2010)

[13] Kočvara, M., Stingl, M.: A code for convex nonlinear and semidefinite programming. Optimization Methods and Software **18**(3), 317–333 (2003)

[14] Kočvara, M., Stingl, M.: Free material optimization for stress constraints. Structural and Multidisciplinary Optimization **33**, 323–355 (2007)

[15] Kočvara, M., Stingl, M.: On the solution of large-scale SDP problems by the modified barrier method using iterative solvers. Mathematical Programming **120**(1), 285–287 (2009)

[16] Kočvara, M., Stingl, M., Zowe, J.: Free material optimization: recent progress. Optimization **57**(1), 79–100 (2008)

[17] Nesterov, Y.E., Todd, M.J.: Self-scaled barriers and interior-point methods for convex programming. Mathematics of Operations Research **22**(1), 1–42 (1997)

[18] Nesterov, Y.E., Todd, M.J.: Primal-dual interior-point methods for self-scaled cones. SIAM Journal on Optimization **8**(2), 324–364 (1998)

[19] Oliveira, A.R.L., Sorensen, D.: A new class of preconditioners for large-scale linear systems from interior point methods for linear programming. Linear Algebra and Its Applications **394**, 1–24 (2005)

[20] Ringertz, U.T.: On finding the optimal distribution of material properties. Structural Optimization **5**, 265–267 (1993)

[21] Saad, Y.: Iterative Methods for Sparse Linear Systems, Second Edition (2003)

[22] Stingl, M.: On the solution of nonlinear semidefinite programs by augmented lagrangian method. Ph.D. thesis, Institute of Applied Mathematics II, Friedrich-Alexander University of Erlangen-Nuremberg (2006). Available from http://www2.am.uni-erlangen.de/

[23] Stingl, M., Kočvara, M., Leugering, G.: Free material optimization with fundamental eigenfrequency constraints. SIAM Journal on Optimization **20**(1), 524–547 (2009)

[24] Stingl, M., Kočvara, M., Leugering, G.: A new non-linear semidefinite programming algorithm with an application to multidisciplinary free material optimization. International Series of Numerical Mathematics **158**, 275–295 (2009)

[25] Stingl, M., Kočvara, M., Leugering, G.: A sequential convex semidefinite programming algorithm with an application to multiple-load free material optimization. SIAM Journal on Optimization **20**(1), 130–155 (2009)

[26] Stolpe, M., Weldeyesus, A.G.: On solving large-scale variable thickness sheet problems. Tech. rep., DTU Wind Energy (2014). Submitted

[27] Toh, K.C.: Solving large scale semidefinite programs via an iterative solver on the augmented systems. SIAM Journal on Optimization **14**(3), 670–698 (2004)

[28] Toh, K.C., Kojima, M.: Solving some large scale semidefinite programs via the conjugate residual method. SIAM Journal on Optimization **12**, 669691 (2002)

[29] Weldeyesus, A.G., Stolpe, M.: Free material optimization for laminated plates and shells. Tech. rep., DTU Wind Energy (2014). Submitted

[30] Weldeyesus, A.G., Stolpe, M.: A primal-dual interior point method for large-scale free material optimization. Computational Optimization and Applications (2014). DOI 10.1007/s10589-014-9720-6

[31] Werner, R.: Free material optimization-mathematical analysis and numerical solution. Ph.D. thesis, Institute of Applied Mathematics II, Friedrich-Alexander University of Erlangen-Nuremberg (2001)

[32] Zhang, Y.: On extending some primal-dual interior-point algorithms from linear programming to semidefinite programming. SIAM Journal on Optimization **8**(2), 365–386 (1998)

[33] Zhao, X., D.Sun, Toh, K.C.: A Newton-CG augmented lagrangian method for semidefinite programming. SIAM Journal on Optimization **20**(4), 1737–1765 (2010)

[34] Zowe, J., Kočvara, M., Bendsøe, M.P.: Free material optimization via mathematical programming. Mathematical Programming **79**, 445–466 (1997)